Turun yliopisto
University of Turku

DISCONTINUOUS FIBER-REINFORCED COMPOSITE FOR DENTAL APPLICATIONS

Studies of the fracture resistance and the mechanical properties of the material used for extensive direct restorations

Jasmina Bijelic-Donova

TURUN YLIOPISTON JULKAISUJA – ANNALES UNIVERSITATIS TURKUENSIS
Sarja - ser. D osa - tom. 1261 | Medica - Odontologica | Turku 2016

University of Turku

Faculty of Medicine
Institute of Dentistry
Department of Biomaterials Science
Finnish Doctoral Program in Oral Sciences (FINDOS-Turku)
Turku Clinical Biomaterials Centre (TCBC)

Supervised by

Professor Pekka K. Vallittu
Department of Biomaterials Science
Institute of Dentistry
University of Turku
Turku, Finland

Adjunct Professor Sufyan Garoushi
Department of Biomaterials Science
Institute of Dentistry
University of Turku
Turku, Finland

Reviewed by

Professor Alison Qualtrough
School of Dentistry
University of Manchester
Dental School
Manchester, UK

Professor Ivo Krejci
Division of Cariology and
Endodontology
University of Geneva
Geneva, Switzerland

Opponent

Professor Cees M. Kreulen
Department of Preventive and Restorative Dentistry
Radboud University Medical Center
Nijmegen, The Netherlands

The originality of this thesis has been checked in accordance with the University of Turku quality assurance system using the Turnitin OriginalityCheck service.

ISBN 978-951-29-6651-6 (PRINT)
ISBN 978-951-29-6652-3 (PDF)
ISSN 0355-9483 (Print)
ISSN 2343-3213 (Online)
Painosalama Oy - Turku, Finland 2016

If you can't explain it simple enough, you don't understand it well enough

Albert Einstein

To my mentors for opening me the door of science and upholding my curiosity,

To all colleagues, students and scientists, to whom it might help, and

To Dime, for his endless support and faith

ABSTRACT

Jasmina Bijelic-Donova

Discontinuous fiber-reinforced composite for dental reconstructions - Studies of the fracture resistance and the mechanical properties of the material used for extensive direct restorations.

University of Turku, Faculty of Medicine, Institute of Dentistry, Department of Biomaterials Science, Finnish Doctoral Program in Oral Sciences (FINDOS-Turku) and Turku Clinical Biomaterials Centre (TCBC), Annales Universitatis Turkuensis, Turku, Suomi, 2016

Earlier developed low aspect ratio dental discontinuous-fiber-reinforced composites (discontinuous-FRCs) are micrometer-scale discontinuous-FRCs, which lack sufficient strength and fracture toughness to reinforce structures. The aim of this thesis was to evaluate the fracture resistance, bonding properties and some mechanical properties of newly developed millimeter-scale discontinuous-FRC.

Four studies were designed to evaluate the fracture resistance and the failure mode of anterior restorations reinforced with millimeter-scale discontinuous-FRC, assess the shear bonding strength between incrementally placed layers of this fibrous composite, measure the thickness and the effect of the oxygen inhibition layer (OIL) on the interlayer bonding characteristics, and determine various physicomechanical properties. In addition, fiber related properties (fiber volume fraction, fiber length, critical fiber length, fiber diameter) and matrix related properties (fiber orientation) were computed.

The results of these studies showed that the use of a millimeter-scale discontinuous-FRC post-core-crown structure was advantageous in terms of both providing reinforcement and preventing catastrophic fractures. Furthermore, it was found that presence of an OIL improved the interlayer connection. The protruding fiber ends at the interface between the fibrous composite layers and the semi-IPN were considered to promote durable adhesion upon OIL removal. Millimeter-scale fibers substantially improved fracture toughness due to the fibers ability to bridge the crack, blunt the crack tip and carry the load, accompanied with the semi-IPN aided plasticity. However, the results also showed that fibers shorter than 0.4 mm most likely behave as reinforcing filler particles instead of reinforcing fibers. Furthermore, fiber orientation was found to be important for impeding crack progression.

These studies suggest that millimeter-scale discontinuous-FRC should accompany the individually made FRC post insertion and should fill the pulp chamber and extend coronally as core material, in order to provide retention and strengthen the cervical portion of the tooth. Alternatively, it could be used as a post-core structure. In both cases a homogenous unit is assumed, due to the identical composition of the materials. Upon curing, the OIL should be left on the surface of the composite and should not be contaminated. This could improve the bonding and improve the inherent fracture resistance of the material. This was observed also in the ability of the material to resist fracture propagation, which approached the toughness value of dentin. These studies indicate that some of the benefits of using millimeter-scale discontinuous-FRC particularly include improved fracture toughness and resistance to fracture, as well as improved interlayer bonding compared to conventional composites. Moreover, using millimeter-scale discontinuous-FRC changes the fracture pattern and more reparable fractures were found for this material.

Keywords: fiber-reinforced composite, short fiber-reinforced composite, fiber post, bonding, air inhibited layer, mechanical properties, fiber aspect ratio, fiber length, fiber orientation.

TIIVISTELMÄ

Jasmina Bijelic-Donova

Lyhytkuitulujitteinen komposiitti vaurioituneiden hampaiden korjaamisessa – materiaalin sidosominaisuudet, mekaaniset ominaisuudet ja kuormankantokyky

Turun Yliopisto, Lääketieteellinen tiedekunta, Hammaslääketieteen laitos, Biomateriaalitieteen oppiaine, Kansallinen suun terveystieteiden tohtoriohjelma (FINDOS-Turku) ja Turun Kliininen Biomateriaalikeskus (TCBC), Annales Universitatis Turkuensis, Turku, Suomi, 2016

Paikkaamalla korjattujen hampaiden lujuus ei ole aina riittävä hampaiston alueilla, joilla purentakuormitus on suuri. Perinteisen yhdistelmämuovin lujuutta ja rakenteellista kuormankantokykyä on aikaisemmin parannettu lisäämällä kuituvahvisteinen kerrosrakenne osaksi yhdistelmämuovipaikkaa. On havaittu, että yhdistelmämuovin mekaanisia ominaisuuksia on mahdollista parantaa käyttämällä lyhytkuitulujitetta osana hammaspaikkaa. Hammaspaikkojen lisäksi kuitulujitteisia yhdistelmämuoveja käytetään muun muassa kruunujen juurikanava-ankkuroinnissa. Aikaisemmin on todettu, että yksilöllisesti muotoilulla kuitunastalla saavutetaan suurempi kruunun rakenteellinen lujuus kuin käyttämällä tehdasvalmisteisia kuitunastoja.

Tässä tutkimuksessa lyhytkuitukomposiittia (lasikuitu) testattiin *in vitro* kuormitus-olosuhteissa ja koemalleina käytettiin kruunu ja nasta-pillari-kruunu -tyyppisiä rakenteita. Tutkimuksen erityistavoitteena oli testata lyhytkuitukomposiitin ominaisuuksia mm. staattisilla sidoslujuus-, puristus- ja taivutustesteillä käyttämällä eri pituisia ja eri tavoin suunnattuja lasikuituja. Materiaalin pitkäaikaiskestävyyttä testattiin dynaamisilla väsytystesteillä. Materiaalia käytettiin kerrosrakenteina, joissa kerrosten välillä on oltava riittävän luja sidos. Kerrosrakenteiden valmistuksessa materiaalin pintaan muodostuu hapen vaikutuksesta kovettumaton ns. happi-inhibitiokerros. Tavoitteena oli mitata inhibitiokerroksen paksuutta sekä tutkia sen vaikutusta lyhytkuitukomposiitin sidosominaisuuksiin osana kerrosrakennetta.

Tutkimustulosten perusteella voidaan todeta, että juurikanava-ankkuroinnissa käytettävä lyhytkuitukomposiittinastapilari lujittaa yhdistelmämuovikruunuja merkittävästi. Mekaanisilta ominaisuuksiltaan lyhytkuitulujitettu yhdistelmämuovi oli erityisesti murtositkeydeltään parempi kuin tavanomaiset yhdistelmämuovit. Lujuusominaisuudet tulivat esille sekä staattisissa että dynaamisissa kuormitustesteissä. Lyhytkuitukomposiitin isotrooppinen (suunnasta riippumaton) lujitevaikutus ja kuidun toimiminen ns. crack-stopperinä selittävät lujuutta ja murtumismekanismia. Happi-inhibitiokerros paransi kerroksittain kovetettujen yhdistelmämuovirakenteiden lujuutta.

Yhteenvetona voidaan todeta, että lyhytkuitukomposiitin käytöllä voidaan vahvistaa rakenteellisesti vaurioituneita hampaita. Tämä tarkoittaa sitä, että lyhytkuitukomposiitilla korjatut hampaat eivät lohkea herkästi voimakkaassa purentarasituksessa ja mikäli murtuma pääsee muodostumaan, on murtuma helpommin korjattavissa kuin muita materiaaleja käytettäessä.

Avainsanat: lyhytkuitukomposiitti, yksilöllisesti muotoiltu nasta, happi-inhibitio kerros, sidostaminen, vaurioitunut hammas, kuitupituus, kuitu-orientaatio, murtumasitkeys.

TABLE OF CONTENTS

ABBREVIATIONS

ANOVA	Analysis of variance
AHSS	Apparent horizontal shear strength
Bis-GMA	Bisphenol A glycidil dimethacrylate
Bis-EMA	Bisphenol A ethoxylated Bis-GMA
°C	Degree celsius
CFL	Compressive fatigue limit
CS	Compressive strength
d_f	Fiber diameter
Discontinuous-FRC	Discontinuous fiber-reinforced composite
DTS	Diametral tensile strength
2D	Two-dimensional
3D	Three-dimensional
ECHCPMS	Epoxycyclohexylcyclo-polymethylsiloxane
EGDMA	Ethylene glycol dimethacrylate
E-glass	Electrical glass
ETT	Endodontically treated teeth
ETI	Endodontically treated incisors
FF	Final failure
FM	Flexural modulus
FOD	Fiber orientation distribution
FS	Flexural strength
FT, K_{IC}	Fracture toughness
FRC	Fiber-reinforced composite
GPa	Gigapascal
HEMA	Hydroxyethylmethacrylate
Hz	Hertz
IF	Initial failure
ISO	International organization for standardization
l/d	Aspect ratio
l_f	Fiber length
l_{fc}	Critical fiber length
l_{fo}	Optimal fiber length
Millimeter-scale discontinuous-FRC	Millimeter-scale discontinuous fiber reinforced composite
min	Minute
mm	Millimeter
MMA	Methylmethacrylate
MPa	Megapascal
µm	Micrometer
N	Newton
n	Number of specimens per group (group size)
OIL	Oxygen inhibition layer

PF	Post-fatigue failure
PFC	Particulate filler-reinforced composite
PMMA	Polymethylmethacrylate
ρ	Density
ρ_f	Fiber density
s	Second
S	Standard deviation
SEM	Scanning electron microscopy
Semi-IPN	Semi-interpenetrating network
SENB	Single edge-notched-beam specimens
TC	Thermocycling
TEGDMA	triethylene glycol dimethacrylate
UDMA	Urethane dimethacrylate
Vf%	fiber volume fraction
Vol%	Volume percent
Wf	work of fracture
Wt_f	Fiber weight fraction
Wt%	Weight percent

LIST OF ORIGINAL PUBLICATIONS

This thesis is based on the following original publications, which are referred to in the thesis by the Roman numerals I-IV.

I. Bijelic J., Garoushi S., Vallittu PK., Lassila LV. Short fiber reinforced composite in restoring severly damaged incisors. Acta Odontol Scand. 2013; 71(5): 1221-1231.

II. Bijelic-Donova J., Garoushi S., Lassila LV., Vallittu PK. Oxygen inhibition of resin composites: the effects of layer thickness and the surface layer treatment on the interlayer bond strength. Eur J Oral Sci. 2015; 123(1): 53-60.

III. Bijelic-Donova J., Garoushi S., Vallittu PK., Lassila LV. Mechanical properties, fracture resistance, and fatigue limits of short fiber reinforced dental composite resin. J Prosthet Dent. 2016; 115(1): 95-102.

IV. Bijelic-Donova J., Garoushi S., Lassila LV., Keulemans F., Vallittu PK. Mechanical and structural characterization of discontinuous fiber-reinforced dental resin composite. J Dent. 2016; 52: 70-78.

1. INTRODUCTION

The growing need for durable and esthetically pleasing tooth-colored restorative materials has spurred the search for a biologically suitable restorative material that has physicomechanical characteristics similar to natural teeth. As a result, diversity of dental composite resins is available for dentists today. However, since the natural hard tooth structures are being replaced, it should be defined as to whether these restorative materials are suitable substitutes for them. Biological structures such as bone and teeth, are natural composites with mechanical properties essentially meeting the requirements for their optimal performance in service. Teeth are composed of hard inorganic hydroxyapatite in a tough organic matrix encompassing type I collagen fibers. As a composite material teeth are distinctly anisotropic. Although dentinal tubules with their peritubular dentin cuffs act like fibers and account to aligned composite, it is the collagen fibers aligned perpendicular to the dentinal tubules, which define the dentin's anisotropic nature (Kinney et al, 2003; Nalla et al, 2003a). Owing to this orthogonal arrangement of the dentin tubules and collagen fibrils, there is some concern that dentin is somehow an isotropic material (Kinney 1999; Kinney et al, 2003), however. From a biomechanical perspective, the collagen fibers with high aspect ratios account for the high tensile strength and the toughness of the teeth, whereas the hydroxyapatite composed of mineral calcium phosphate provides their enhanced compressive strength (Vallittu, 2015).

On the other hand, the anisotropicity in man-made dental composite materials, must be controlled and adjusted for according to the design of the restoration used to replace the missing structure. This has been successfully achieved by the use of fiber-reinforced composites (FRCs) (Brown, 2000; Vallittu et al, 2000; van Heumen et al, 2009). The strength predictions related to the fiber direction are explained by appropriate factor known as Krenchel factor (Murphy, 1998). If, however, the loads encountering the structure are unpredictable, then the isotropic properties must be designed so, that the structure withstands the applied forces from all directions. A solution to the isotropicity related weakness of the composite resins has been offered with the introduction of millimetre-scale discontinuous fiber-reinforced composite (millimetre-scale discontinuous-FRC) (Garoushi et al, 2007a). However, there have also been previous attempts made to enhance the mechanical properties of composite resins by incorporating short fibers into them. Owing to the difficulty to maintain the high aspect ratio (l/d) of the discontinuous fibers, which is important for the high strength performance of the composite (Lee,

1993) and keeping the fiber length above its critical value (Vallittu PK, 2015), those earlier efforts were unsuccessful. Indeed, the micrometer–scale fibers fillers (60-120μm) (Drummond et al, 2004; Manhart et al, 2000) used in earlier discontinuous-FRCs, were well below the critical fiber length (0.5-1.6mm) (Vallittu, 2015).

Restorative materials must fulfill certain requirements in terms of physicomechanical properties (Ferracane, 2005) as well as applicability. The application technique is important, because defects induced during placement, such as voids, may lead to early failure of the restoration. In order to ideally mimic the structure of the replacing tissue, it is desirable that a restorative material would have a fibrous structure and properties close to dentin. Due to the fiber related properties and their orientation, the millimeter-scale discontinuous-FRC could be the material of choice for the mentioned purpose.

Studies carried out within this research series are focused on evaluating selected mechanical properties of millimeter-scale discontinuous-FRC, which is attempted to be used as direct dentin replacing restorative material for extensive restorations. The fracture resistance of the material was also evaluated by means of static and fatigue load.

2. REVIEW OF LITERATURE

2.1 Loss of sound tooth substance and management of tooth loss

The primary cause of tooth damage is dental caries. Conservatively, the treatment of primary or secondary caries involves direct composite restorations, known as particulate filler composite (PFC) restorations. Other therapeutic options include a combination of prostho-restodontics or resto-endodontics solutions such as indirect composite, ceramic or metal cast inlays, onlays and overlays (Polesel, 2014), and endocrowns (Biacchi et al, 2013; Rocca et al, 2013). Therapeutic decision is determined by the amount of affected tooth substance and pulp tissue involvement. Some of the therapeutic procedures require tooth preparation, which leads to additional tooth tissue loss. As tooth tissue loss is an irreversible process, the least invasive technique should be considered as the first therapeutic choice. However, this approach should be effective in preventing repetitive replacements and repairs, as they cause additional hard tissue alterations.

Direct restorations are indicated for other purposes as well such as treatment of traumatic tooth injuries (Flores et al, 2007; Eden et al, 2015), various wear processes (Smales et al, 2007), closing diastemas (Frese et al, 2013), esthetic discomfort (Demarco et al, 2015), correcting tooth form and position (Peumans et al, 1997) and cracked tooth syndrome (Banerji et al, 2010). Moreover, direct replacement of failed or defective restorations is also a common operative procedure (Hickel et al, 2013).

2.2 Longevity of restored teeth

The life span of a restoration, known as service life or length of service, defines the longevity of the restored tooth unit, and is multifactorial. It depends on the patient, operator (dentist) and material related properties (Donovan, 2004; Sarrett, 2005; Hickel et al, 2001; Bernardo et al, 2007). The amount of residual tooth tissue is also of paramount importance (Bernardo et al, 2007; Demarco et al, 2012; Beck et al, 2015).

The caries risk of the patient is the main factor that determines the service life of dental restorations. Patient compliance, oral hygiene, cooperation during the restorative procedure, age, diet, bite force and bruxism are some patient

related factors affecting the longevity of restorations (Kubo et al, 2011; Hickel et al, 2001).

The other group of factors are comprised of determinants such as the initial treatment indication, which from the “operator’s” point of view means having the correct indication, then size and type of the restoration, properties of both restorative material and adhesive system used, restorative technique, curing mode, occlusion, vitality of the tooth (Hickel et al, 2001) and material choice (Sarrett, 2005; Hickel et al, 2001; Ferracane, 2005). Operators’ skills have also been mentioned as having an effect on the longevity of the restoration (Donovan, 2004; Kubo et al, 2011).

Regarding the material used to restore the lost tooth structure, there is a trend towards hybrid composite materials in the literature. Hybrid composite materials are considered to be “gold standard” and three-step or two-step agents are recommended as “gold standard” adhesives (Demarco et al, 2012). The academy of operative dentistry - European section (AODES) also suggests the use of microhybrid or nanohybrid composites with minimum 60% filler load by volume (Lynch et al, 2014). Follow-up studies are consistent with these recommendations and have showed that both nanohybrid and conventional hybrid composite materials have comparable clinical performance (van Dijken et al, 2013; van Dijken et al, 2014; Frankenbergen et al, 2014; Beck et al, 2015). On other hand, such findings have been susceptible to critics, because clinical trials have mostly evaluated and compared hybrid composites. Although the controlled clinical studies are not focused on evaluating the properties of composite materials covered in them, some studies have documented that filler size (Brunthaler et al, 2003; Hickel et al, 2001) and filler load fraction (Demarco et al, 2012) have an effect on the clinically observed failure mode. Hence, it seems that the properties of the material are important for the long-term behavior of anterior and posterior composite restorations (Baldissera et al, 2013; DaRosa Rodolpho et al, 2011).

A material that has been increasingly used in restorative dentistry is the FRC. The indications complemented with recommendations for the clinical use of FRCs in dentistry have been presented to dentists on few occasions (Brown 2000; Butterworth et al, 2003; Tayab et al, 2015). FRCs have extended the indications for use of composite materials in the field of restorative dentistry, enabling direct, semi-direct or indirect prostho-restodontic and resto-endodontic solutions. This material group is heterogenic and includes different types of fibers, various fiber architectures and resin matrix types. FRCs are

used as a fiber bundle placed as a substructure with the unique role of reinforcing the structure by acting as a crack stopping layer (Butterworth et al, 2003). One limitation of fiber bundles and fiber nets could be the restoration size, as it would restrict the use of uni- and bidirectional FRCs due to difficult or unfeasible placement. Alternatively, discontinuous-FRC could be utilized here. However, this type of FRC material has only had moderate use in dentistry thus far. Fibers in the discontinuous-FRC system are embedded within the resin matrix; this type of composite material is designed to serve as a reinforcing base for conventional PFC restorations. Some characteristics of this material are discussed in the forthcoming paragraphs.

Literature is consistent in saying that the amount of residual tooth tissue is crucial and directly related to the longevity of the restored tooth unit (Bernardo et al, 2007; Demarco et al, 2012; Beck et al, 2015). The size of the restorations is decay-orientated or defect-orientated, often determined by the cause leading to tooth damage (disease, traumatic injury, replacement or pulp pathology). Hence, the primary treatment indication determines the amount of lost tooth tissue and thus the cavity size. This fact defines the number of surfaces to be restored and affects the longevity of the restored tooth.

2.3 Properties of restored teeth: biomechanics perspective

Biomechanics assesses stresses and deformations appearing in biologic complexes. The biomechanics of the tooth-restoration complex takes into account several factors such as loads occurring in the dentition, tooth structure and shape, the action of the tooth-supporting structures as well as the physicomechanical properties of tooth components versus the properties of the restorative materials, including their interface (Bayne, 2013).

Intact teeth accept and dissipate the occlusal load from enamel to dentin in the form of compression throughout large area with almost nonexistent localized stresses. Teeth deform slightly under normal biting load, causing tooth flexure, that is lateral or axial bending (Bayne, 2013). The restored tooth unit *i.e.* tooth-restoration complex, on the other hand, behaves differently because enamel continuity or enamel itself is completely lost. As a consequence, the resistance to fracture significantly decreases and the stresses encountered by the restoration are not purely compressive, but are a combination of compressive, tensile and shear stresses. Nevertheless, when stresses come upon dentin, they transfer thereafter in a similar way as is in the intact tooth unit. Hence, it is

favorable to design the restorations to allocate stresses against sound dentin (Bayne, 2013). The most critical structure in the restored tooth unit is the tooth-restoration interface. The size of the restoration determining both the length and the location of the interface (occlusal, gingival) plays a significant role. Possible interactions of stresses applied to different size restorations versus intact tooth are presented in Figure 1 and some laboratory tests for their assessment are presented in paragraph 2.5. The possible correlation between them is schematically presented in Figure 6.

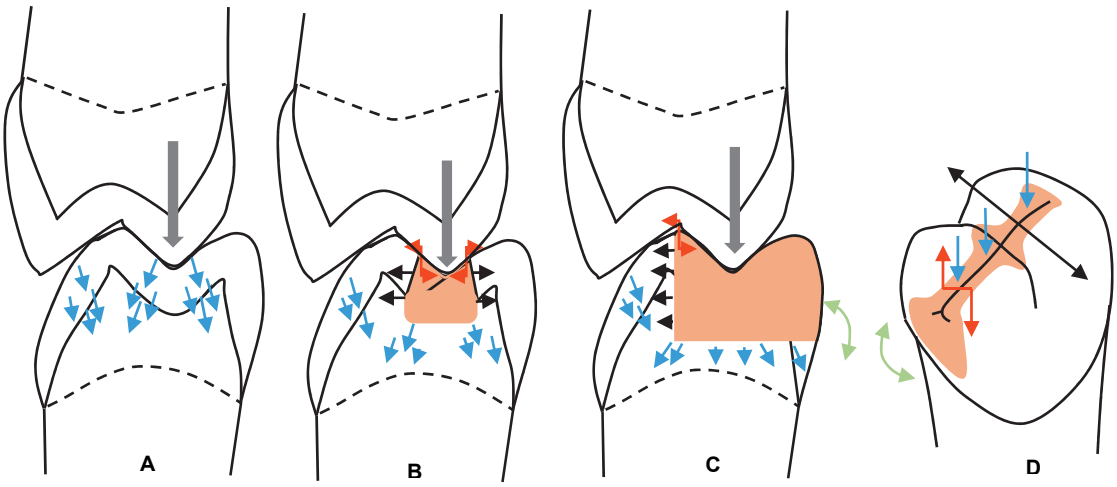

Figure 1. Schematically presented cases of occlusal load applied to **A:** intact tooth; **B:** Class I - small intracoronal composite restoration; **C:** Class I - cusp replacing composite restoration and **D:** Class II composite restoration. Blue arrows: compression; Black arrows: tension; Red arrows: shear; Green arrows: Flexure and Gray arrows: load direction. (Modified from Bayne, 2013 pp. e8, e12).

2.4 Materials for direct restorations

2.4.1 Particulate filler composites (PFCs)

2.4.1.1 Composition and classification

Composites are blends of ceramics, metals or polymers. The purpose of producing composites is to utilize the best properties of each constituent participating in the blend. Thus, the composite will have intermediate properties of the parts formulating the mixture. The traditional composite blend for dental restorations comprise dispersed phase of ceramic particles within a continuous phase of the resin matrix. It can also be described as a reinforced resin

system. Technically the proper term is dental composite, but these materials have been commonly referred to as *resin composites, composite resins, resin-based composites, composite restorative materials, filled resins and filled composites* (Bayne et al, 2013). However, the correct scientific term is *polymer matrix composite* or *particulate-reinforced polymer matrix composite* (Sakaguchi et al, 2012). The latter term is commonly modified and particulate filler composite (PFC) is usually used instead. This thesis will use the correct scientific term (PFC) when referring to the material.

Dental composites are typically composed of inorganic filler particles (inorganic phase) bonded to the dimethacrylate resin matrix (organic phase) via a coupling agent, usually silane. Additives such as photoinitiators, co-initiators, pigments and stabilizers are added to the organic matrix. Classically, monomers are dimethacrylates, Bis-GMA (bisphenol A glycidil dimethacrylate), Bis-EMA (bisphenol A ethoxylated Bis-GMA) and UDMA (urethane dimethacrylate) monomers diluted with TEGDMA (triethylene glycol dimethacrylate) or EGDMA (ethylene glycol dimethacrylate). The presence of double bonds at both ends of the dimethacrylates enables a free-radical initiated, addition reaction of polymerization. Another class of monomer which has been used in some dental composites is silorane. It encompasses siloxane and oxirane, the latter with epoxy groups as functional groups at the ends, allowing cationic polymerization (Weinmann et al, 2005; Sakaguchi et al, 2012). Despite the efforts to change or modify the continuous phase of the dental composites, the monomer system has generally remained unchanged, however. The reinforcing phase principally contains silica-based fillers, but the inorganic composition is often modified with other ions in order to achieve desirable properties. For example, lithium and aluminum are used to generate small particles, because they are easier to crush and thus suitable as pre-polymerized particles for microfill composites, whereas barium, boron, zirconium, yttrium and zinc ions give better radiopacity. An essential part of the composite blend is the silane, which is a difunctional coupling agent able to condense with the hydroxyl groups on the surface of the silica particles with its methoxy groups and co-polymerize with the double bonds of matrix monomers with its double bond end (Bayne et al, 2013). Consequently, a siloxane bridge is formed with filler particles and covalent bond with the resin matrix. Silane is known to enhance surface wettability, bind filler particles to the matrix, and intermediate stress distribution between the two phases (Sakaguchi et al, 2012).

Composites are classified in various ways based on the filler size (midifiller, minifiller, macrofiller, microfiller, nanofiller) or filler load (percent of weight or volume), consistency (packable, flowable), placement technique (incremental, bulk), monomer system used (Bis-GMA, UDMA or Silorane-based) or polymerization method (light-curing, self-curing or dual-curing). The most common is the classification established on filler size or filler load. It is worth noting that the reported volume percent is always lower than the weigh percent, which is due to the density of the filler being higher than the resin's (2.5 g/cm^3 and 1.23 g/cm^3 for filler and resin, respectively) (Söderholm et al, 1984; Kim et al, 2002). For example, 75 wt% is approximately equivalent to 50 vol% (Bayne et al, 2013). Comprehensive classifications of dental composites are made by several authors (Willems et al 1992; Willems et al, 1993; Ferracane, 2011; Bayne et al, 2013)

2.4.1.2 Characterization

The properties of the dental composite may be tailored by selectively combining the components of the monomer phase (Peutzfeldt, 1997; Asmussen et al, 1998). The monomer type and chemistry are important, because the monomer system controls and governs the final viscosity of the resin (Conçalves et al, 2009), determines the rates of water sorption (Söderholm et al, 1984; Miettinen et al, 1999), degree of conversion and polymerization contraction, and also influences the flexural properties of the composite material (Conçalves et al, 2009). However, the reinforcing phase is of primary importance in the materials response to the stressing conditions. Indeed, the addition of fillers imparts substantial endurance to the composites, and filler content, size and shape endow specific properties.

2.4.1.3 Filler load

Filler load is expressed either as volume percent (vol%) or weight percent (wt%). Although higher filler loads are associated with improved properties, there is a critical filler level above which any addition of the filler would have an inverse effect. This level is between 50 and 60 vol% (55, 57, 60 vol%) (Ilie et al, 2009a; Ilie et al, 2012; Kim et al, 2002). The filler load is considered as a more relevant factor compared to filler size or morphology (Masouras et al, 2008). Filler particles dissipate the nominal forces encountered into the components, causing energetically unfavorable conditions for crack growth. Hence, when the number of filled particles is increased, the number of obstacles that can dissipate the components of the nominal force between particles and allow the crack front to curve also increase (Lien et al, 2010). In

other words, higher filler load increases the possibility for crack deflection and for energy loss. The manufacturers' data regarding the filler load should be taken with caution, because there is no standard for determining the wt% of fillers. Namely, it has been observed that some manufacturers weight fillers before and others after the silanization process. Consequently, the differences in the manufacturing processes have been perceived to change the final weight by 2.8 to 9 wt% (Sabbagh et al, 2004).

2.4.1.4 Filler size and shape

Filler load has been given prior importance in determining the mechanical properties of the composite material (Masouras et al, 2008; Rodrigues et al, 2008). Filler size (Miyasaka, 1996) and shape (Kim et al, 2002; Leprince et al, 2010) define the filler load, however. Namely, filler shape influences the total filler load and the filler distribution within the composite material (Willems et al, 1992; Kim et al, 2002; Beun et al, 2007). Thus, they indirectly affect the mechanical properties of the material. Furthermore, filler size is important because it determines the interparticle space and the filler surface area to volume ratio. The interparticle space is also known as interfiller space or critical spacing and is the distance between the two closest filler particles. Mechanical properties will weaken if particles are too close or in contact with each other (Htang et al, 1995). This is due to the friction and the interaction at the matrix-filler interface (Wagner et al, 2004). However, the noteworthy importance of the interparticle space is its contribution to the toughening mechanisms of the composite materials (Ferracane et al, 1987; Johnson et al, 1993), which is discussed in the subsequent paragraph.

Decreasing filler size, on other hand, has been considered to increase the interface area between the filler and the organic matrix because of the enlarged filler surfaces and enlarged boundary areas with the matrix. This can influence a variety of the composite's properties (Ilie et al, 2009b; Ilie et al, 2011; Ilie et al, 2012).

There are two basic filler shapes, spheroidal and irregular. Irregular shaped filler particles have either sharp or round edges. Sharp edges might function as defects, which favor crack initiation instead of impeding crack development. For example, certain angles and protuberances could act as sharp edges (Sabbagh et al, 2004; Beun et al, 2007). Furthermore, spheroidal particles and round edges improve the packing of the fillers into the resin matrix and provide composites with higher filler load (Rodrigues et al, 2008). Moreover, spheroidal particles diminish stress concentration in comparison to irregular fillers with

sharp edges (Söderholm et al, 1984; Sabbagh et al, 2004). The shape of the fillers also affects the reinforcing properties of the composite. Indeed, spherical fillers possess better properties than irregular shaped fillers with same load (Leprince et al, 2010).

2.4.1.5 Toughening mechanism of PFCs

The basis of the toughening mechanism is to provide efficient stress transfer from the matrix to the filler particles. This necessitates optimum filler content and good filer-matrix coupling. Mechanisms by which fillers provides enhanced fracture toughness are known as crack pinning, crack branching, microcrack induced toughening mechanism and crack-deflection induced toughening effect, all of which have been summarized in several studies (Lloyd et al, 1982; Ferracane et al, 1987; Johnson et al, 1993; Kim et al, 1994; Kim et al, 2000; Kim, 2002).

When a crack tip affronts filler, it curves. The interparticle space has the utmost role in this process, because closely packed filler particles with minimal interparticle space might change the pattern of crack propagation as more filler particles are in the way of the crack path. If critical spacing has been reached, an optional mechanism for passing a particle filler is initiated. This alternative mechanism is the filler particle decohesion at the crack tip or ahead of it. Subsequently, the interparticle space, defined by the filler size and the filler volume load, is responsible for this *crack pinning effect*. However, the pinning effect could be weakened if crack fronts are overlapping, which happens when the critical filler load level has been surpassed. A main crack leading to failure does not occur instantaneously and there is usually a microcrack starting from a small flaw first, which releases the stress and enhances fracture toughness. This is known as the *microcrack induced toughening effect*. If the main crack is surrounded by a number of microcracks, a *crack-deflection induced toughening effect* would likely take place due to the coalescence of the propagating main crack with broadly distributed microcracks. In other words, cracks are joined together. High filled composite materials would undergo *crack branching induced toughening mechanisms*, because filler addition allows disintegration *i.e.* branching of the propagating crack between particles, and increases the fracture (crack) surface area, which increases the fracture energy. *Matrix-filler interface* also provides a toughening mechanism, owing to the plastic deformation of the resin matrix around the fillers.

2.4.1.6 Physicomechanical properties

Properties such as flexural, compressive or diametral strength, flexural modulus, fracture toughness and fatigue resistance generally improve with increasing filler load. Nevertheless, all filler related properties (size, shape, load) are important for the overall properties of the PFCs. Most sensitive to the filler content is the flexural modulus (Ilie et al, 2009a), which increases linearly with the filler content. However, further addition of filler will add more defects into the resin matrix. It will not enhance the mechanical properties, but may actually have an inverse effect. Hence, typically the maximum filler load limit is 80 wt% (Htang et al,1995; Ilie et al, 2009a). Reports on the properties of currently used PFCs are thoroughly documented by several authors (Beun et al, 2007; Rodrigues et al, 2008; Ilie et al, 2009a; Illie et al, 2009b; Lien et al, 2010; Leprince et al, 2010; Ilie et al, 2011; Ilie et al, 2012). In general, the fracture toughness of PFCs is below 2 MPa•$m^{1/2}$, moduli are below or around 10 GPa and flexural strength is below 150 MPa (Table 1).

Table 1. Some mechanical properties of different direct restorative composite materials.

Material	Type	FM (GPa)	FS (MPa)	CS (MPa)	DTS (MPa)	FT (MPa $m^{1/2}$)
Z250	Microhybrid	8.2*	135*	390*	57*	1.5^
Supreme XTE	Nanofill	6.7#	115*	360*	52*	1.3^
Silorane	Microhybrid	9.2*/ 6.3#	121*/ 96#	121*	49*	1.6†
Grandio	Nanohybrid	9.2#	116#	181.8Ø	32.4œ	1.2√
Tetric Evo Ceram	Nanohybrid	6.5#	89#	220†	36†	1.7¨

* Lien et al, 2010 (specimen stored in water at 37°C for 24h).
\# Leprince et al, 2010 (specimen stored dry at room temperature for 24 h).
† Illie et al 2009a (specimen stored in water at 37°C for 24h).
^Rodrigues et al, 2008 (specimen stored in water at 37°C for 24h).
œ Marchan S, White D, Smith W, Coldero L, Dhuru V. (2009) Comparison of the mechanical properties of two nano-filled composite materials. Rev Clin Pesq Odontol 5(3): 241-246. (tested immediately after preparation).
Ø Rosa RS, Balbinot CE, Blando E, Mota EG, Oshima HM, Hirakata L, Pires LA, Hubler R. (2012) Evaluation of mechanical properties on three nanofilled composites. Stomatologija 14(4): 126-130. (tested immediately after preparation).
√ Schultz S, Rosentritt M, Behr M, Handel G. (2010) Mechanical properties and three-body wear of dental restoratives and their comparative flowable materials. Quintessence Int 41(1): e1-10. (specimen stored in water at 37°C for 7d).
¨ manufacturer's online data.

Water has predominantly deteriorating effect on the mechanical properties of the composites, although some composite material related dependency has been observed (Ilie et al, 2009b). Water enters the resin network in the PFCs

resin matrix via porosities and the degradation processes happens through several mechanisms (Söderholm et al, 1984; Ferracane et al, 1998; Söderholm et al, 1990; Curtis et al, 2008): 1. water uptake by the resin matrix inducing plasticization and swelling (hydroscopic expansion) of the cross-linked network; 2. hydrolysis of the bonds between the matrix and the fillers leading to filler leaching and interface cracking, and 3. degradation of the silane coupling agent via hydrolysis of the siloxane bonds to silanol groups, accelerating the filler debonding at the interface. Plasticization, however, has a positive toughening effect, known as *crack blunting* by plastic deformation, which releases stress accumulation at the crack tip and disintegrates the crack, or hinders or even retards the crack propagation (Ferracane et al, 1998; Takeshige et al, 2007).

2.4.1.7 Clinical failures of PFC restorations

One of the major concerns in dental practice is the failure of restorations. Numerous studies, however, report mutual reasons for this problem. Fracture of the bulk of the restoration or fracture of the tooth and secondary caries are stated as the most common reasons for restoration failure (Hickel et al, 2001; Demarco et al, 2012; Brunthaler et al, 2003; Pallesen et al, 2003; van Dijken et al, 2000; van Nieuwenhuysen et al, 2003; Bernardo et al, 2007; Opdam et al, 2010). Less frequently cited reasons for failure are marginal deterioration (Hickel et al, 2001) and marginal defects (Brunthaler et al, 2003), loss of proximal contact (Pallesen et al, 2003), isthmus fracture (van Dijken et al, 2000), cusp fracture (van Nieuwenhuysen et al, 2003, Frankenbergen et al, 2014; van Dijken et al, 2013; van Dijken et al, 2014) and decreased integrity of the restoration due to wear traces, chipping and voids (Frankenbergen et al, 2014). Early failures of restorations are correlated with inadequate manipulation of the material (Hickel et al, 2001) and common early failure is fracture of the restoration (Demarco et al, 2012). Late failures are mostly caries related (Demarco et al, 2012) or are caused by deterioration of the material (Hickel et al, 2001). At this stage fracture of the restoration and/or tooth usually occurs (Hickel et al, 2001).

The amount of residual hard tooth tissue is of crucial importance also here. Indeed, the quantity of residual tooth structure versus lost tooth structure affects not only the longevity, but also the type of failure. Multiple cusp replacing restorations, indirect restorations and endodontically treated teeth (ETT) have a higher susceptibility for severe tooth fracture leading to tooth loss. Complications of crowned vital or ETT teeth are crown fracture, loss of

retention, root fracture, secondary caries (Goodacre et al, 2003; Ohlmann et al, 2014) and endodontic complications of vital crowned teeth.

Another classification divides the restoration failures into mechanical, including fracture of the cusp, restoration or veneering material, as well as wear and retention loss, and biological which encompasses secondary caries, pulp inflammation and alteration of the periodontal tissue. Mechanical failures are induced by fatigue and material sensitivity to it, whereas the biological failures are initially controlled by the dentist, but then controlled and caused by the patient (Donovan, 2004). Secondary caries might cause restoration fracture, but also, cuspal fracture might lead to recurrent caries. The vice versa relationship between the mechanical and biological failures is obvious.

2.4.2 Bilayered composite structures: material combination of PFC and FRC

Bilayered composite structures are types of restorations which encompass both PFC and FRC. They are aimed to improve the brittleness and low fracture resistance of PFCs when used in large restorations encountering high occlusal stresses, such as direct cusp replacing posterior restorations or indirect inlay and onlay restorations. In other words, the FRC in these types of restorations is used as a substructure and its purpose is to reinforce the PFC. Two types of bilayered composite structures are schematically presented in Figure 2. The first is the hypothesized use of a discontinuous-FRC bilayered structure, whereas the second is the most commonly used type of uni- or bidirectional FRC-PFC combination. Figure 2 is utilized to show the orientation of dentinal tubules (yellow lines in the coronal part of the schematic tooth) and collagen fibrils (gray lines) oriented perpendicularly to dentinal tubules. This is further discussed in paragraph 2.6.

Bilayered composite structures have been evaluated in several *in vitro* investigations. The effect of the thickness of the FRC substructure versus the thickness of the overlaying PFC (Garoushi et al, 2006a; Monaco et al, 2015), the effect of fiber orientation, short random FRC versus continuous bidirectional and unidirectional FRC (Garoushi et al, 2006a; Garoushi et al, 2007b; Fennis et al, 2005), the effect of fiber type, polyethylene versus glass fiber (Behr et al, 2003a) and the bond strength to the tooth structure (Tezvergil, et al, 2005) are among the important factors affecting the strength of bilayered structures. These studies showed that the FRC substructure supports the PFC layer and serves as a crack prevention layer. The FRC substructure's thickness has prior importance, as it influences the failure mode and the crack

arresting mechanism. Furthermore, the type of the FRC substructure also plays a significant role. Indeed, continuous bidirectional-FRC was found to arrest the propagating crack better than the discontinuous-FRC (Garoushi et al, 2006a) or unidirectional-FRC (Garoushi et al, 2007b; Fennis et al, 2005), which could be owned to its lower stiffness (Dyer et al, 2004; Fennis et al, 2005). As a result, delamination of PFC from the underlaying FRC is typical for bidirectional-FRC, whereas variations of total, partial fractures and delamination are characteristics for discontinuous-FRC (Garoushi et al, 2006a; Garoushi et al, 2007b). If multilayers of bidirectional-FRC are used, failure between the fiber layers typically occurs (Fennis et al, 2005). These findings suggest that fiber orientation plays a significant role not only for the missing-tooth replacing FRC constructions (such as fixed partial fiber-reinforced prostheses), but also in reinforcing bilayered, single-tooth restorative applications (such as dental fillings).

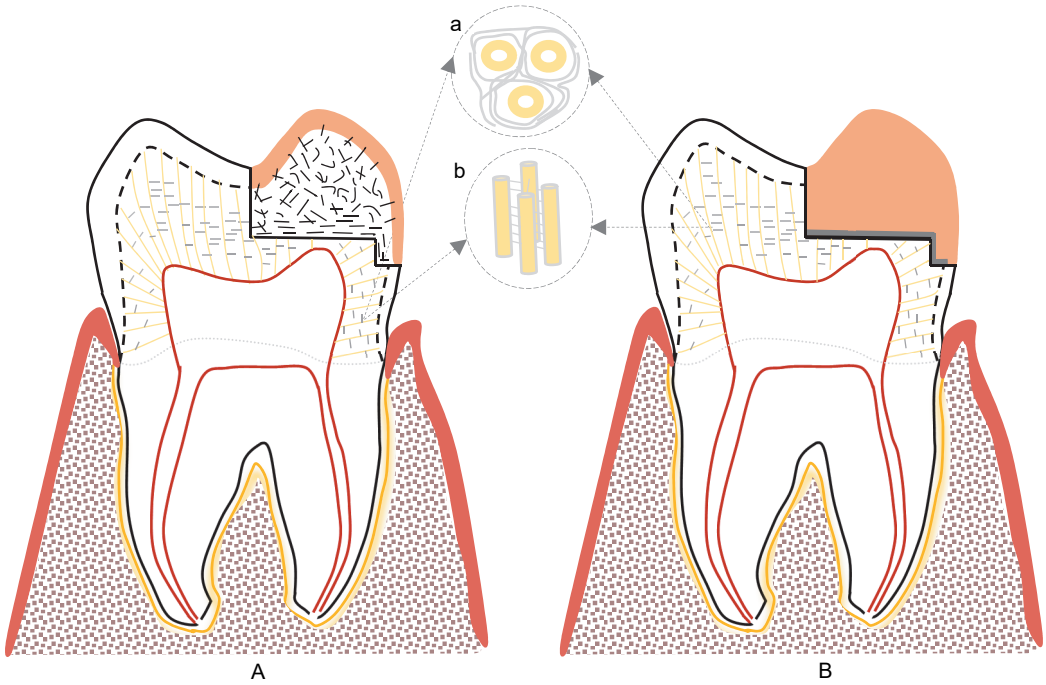

Figure 2. Schematically presented two types of bilayered structures. **A:** Discontinuous-FRC base veneered with PFC, and **B:** bidirectional-FRC placed on the cavity bottom and cavity filled with PFC. Yellow lines in the coronal part of the schematic tooth represent some of the dentinal tubules, whereas the gray lines that are oriented perpendicular to them, represent some of the collagen fibrils. The enlarged sections represent their internal orientation in relation to each other in **a:** cross-section (perpendicular to dentinal tubules) and **b:** longitudinal section (parallel to dentinal tubules). *(***a** and **b** Modified from Söderholm, 2012).

Furthermore, the reinforcing efficiency of continuous FRC inserts containing glass ionomer particles has also been investigated. Likewise, these kind of fiber preforms gained successful reinforcement to the direct composite resin restorations *in vitro* (Xu et al, 2003).

The mechanisms of arresting crack propagation is greatly influenced by the distance between the FRC substructure and the surface where the stress initiates. In other words, it is highly important how many FRC layers are embedded into the restoration and how they are shaped (Monaco et al, 2015). *In vitro* it was observed that the optimal thickness of the veneering composite over the discontinuous-FRC substructure is 1.5 mm and 1.5-2.0 mm over the bidirectional-FRC substructure (Garoushi et al, 2006a). In addition to these laboratory studies, there are also clinical reports on the use of various bilayered restorations (Deliperi, 2008; Garoushi et al, 2009; Garoushi et al, 2012; Rocca e tal, 2013).

2.4.3 Discontinuous fiber-reinforced composite

Composites reinforced with short fibers, orientated in plane or randomly, are known as discontinuous fiber-reinforced composites (discontinuous-FRCs). Generally, most dental discontinuous-FRCs materials are comprised of short E-glass fibers and inorganic particulate fillers as a reinforcing phase and a dimethacrylate-based resin matrix. Commonly, the short fibers are multidirectionally orientated. Discontinuous-FRCs are developed to enhance the properties of conventional PFCs; the attempt is to offer a stronger restorative material than conventional PFCs, however, with possibility to be used in a composite-like way. Despite the efforts and some successful outcomes, discontinuous-FRCs are still relatively uncommon material choice clinically.

The group of fiber-related properties has substantial influence on the mechanical properties of the discontinuous-FRCs. Aspect ratio, critical fiber length, fiber loading and fiber orientation are the main factors that could either improve or impair the mechanical properties of discontinuous-FRCs (Murphy, 1998).

2.4.3.1 Fiber-related properties

2.4.3.1.1 Aspect ratio

Aspect ratio is the fiber length to fiber diameter ratio (l/d). It affects the tensile strength, flexural modulus and the reinforcing efficiency of the FRC (Lee, 1993).

The fiber diameter is controlled by adjusting the diameter of the holes, the draw (winding) speed, the temperature, melt viscosity and cooling rate during the manufacturing process of the fibers (Hull et al, 1996). The diameter of the E-glass falls between 8 and 20 μm, with an average diameter of 15-17 μm (Hull et al, 1996; Harris, 1999). Fiber length (l_f) is important, because although the length of the fibers embedded into the composite is usually known, the processing operations can cause fiber fracture and consequently could alter the mechanical properties of the final composite mixture. The length can be calculated either indirectly, by utilizing properties which depend on the fiber length (such as strength or modulus) or directly, by separating the fibers from the matrix. The direct technique includes few steps. First, the matrix has to be dissolved away in order to get suspension of the fibers. Next, the fibers are deposited onto a suitable substrate and are examined with either an optical or SEM microscope. Nonetheless, the fiber length must surpass the critical fiber length in order to provide actual reinforcement to the system wherein included. For numerous glass systems, the critical fiber length is between 20 and 150 times the diameter of the fiber, which is on a scale of 1 mm (Callister et al, 2011).

2.4.3.1.2 Critical fiber length (l_{fc})

Critical fiber length (l_{fc}) is the minimum fiber length that will allow tensile failure of the fiber and attenuate the shear failure of the interface or the matrix. (Hull et al, 1996). It is also defined as a "*fiber length that is twice the length over which the transfer of load from the matrix is sufficient for the peak tensile stress in the fiber to reach the ultimate tensile strength*" (Norman et al, 2003). In other words, it is the minimum length ($\boldsymbol{l_f = l_{fc}}$) that will permit maximal stress concentration and fiber failure at the fiber's midpoint. The shear-lag model is an analytical model employed to estimate the critical fiber length. It describes the tensile and interfacial shear stress distribution along the length of the fiber, which is aligned parallel in the direction of the load of the matrix (Hull et al, 1996; Harris 1999; Callister et al, 2011). The model assumes that the shear stress at the fiber-matrix interphase is constant. A typical glass-FRC has a shear stress of 20 MPa (Hull et al, 1996), although variations between 17.6 MPa and 33.8 MPa are possible depending on the fiber surface treatment method and the testing protocol (McDonough et al, 2001).

In order to achieve effective reinforcement, the fiber length ($\boldsymbol{l_f}$) must be sufficiently greater than the critical fiber length ($\boldsymbol{l_{fc}}$). If $\boldsymbol{l_f < l_{fc}}$, then failure will occur either at the matrix-fiber interface or in the matrix (fiber reinforcement will not be attained). If $\boldsymbol{l_f > l_{fc}}$, then the ultimate tensile strength of the fiber will be

fully achieved. If $l_f = l_{fc,}$ the stress will be concentrated in the middle of the fiber and the fiber reinforcement achieved only in the middle of the fiber *i.e.* at the fiber's axial center (Harris 1999; Callister et al, 2011). Basically, the critical fiber length is affected by the interfacial (adhesional) fracture energy between the fibers and the matrix against the fiber's ultimate tensile strength (Vallittu, 2015). Only the fibers equal to or exceeding the critical fiber length would be able to withstand fiber debonding under tensile stress and only longer fibers would be able to exhibit the similar strength of the continuous fiber reinforcement (Vallittu, 2015).

To express it in another way, decreasing fiber length decreases the reinforcing efficiency. The changes arising at the fiber end are crucial in such cases. Namely, the ends of the short fiber with a subcritical length have ineffective length, which consequently reduces the reinforcement capacity of the composite reinforced with such short fibers (Hull et al, 1996; Harris, 1999; Callister et al, 2011). These fibers cannot reach the maximum failure stress and undergo mainly matrix deformation, with little shear stress transfer. Consequently, they behave as particulate fillers (Callister et al, 2011). As a result, the role of mixture cannot be applied to this type of composite without considering the fiber-end effect expressed by the efficiency factor (stress transfer aspect ratio) for the aligned discontinuous-FRCs and both, the efficiency parameter and the Krenchel factor for the random discontinuous-FRCs (Harris, 1999; Callister et al, 2011). The efficiency factor varies from 0.1 to 0.6 and depends on the fiber volume fraction (Vf) and the ratio of the moduli of elasticity of the fiber and the matrix (Ef/Em) (Callister et al, 2011). The Krenchel factor for discontinuos-FRCs is nearly 0.2 (0.167) or 0.38 (0.375) for multidirectional (3D) and aligned (2D) short fiber orientation, respectively (Murphy, 1998; Harris,1999). Isotropic reinforcement is achieved with the 3D orientation and anisotropic with the 2D orientation.

2.4.3.1.3 Fiber loading

Fiber loading is a measure of the quantity of the fibers. Although embedding more fibers will improve the fracture resistance of the FRC restoration, clinically the quantity of the fibers versus the space for the veneering composite should be balanced (Butterworth et al, 2003). The addition of fibers into the inorganic filler particle filled or unfilled resin increases the viscosity of the composite and limits further fiber incorporation. Excessive inclusion of fibers not only increases the risk of poor wetting of the fibers with resin (Fonseca et al, 2014), but would also hamper the handling properties and workability of the composite. This could lead to clustering of the fibers and

entrapment of air (Shouha et al, 2014). However, inhomogeneous fiber distribution due to low fiber quantity might lead to the formation of air bubbles and the development of matrix-reach parts. Both situations provide potential downsides because of the role of the bubbles as an oxygen reservoir and as paths for facilitated water infiltration (Fonseca et al, 2016). The quantity of the fibers can be expressed either by the weight (wt_f%) or volume (v_f%) fraction using generally accepted equations, described elsewhere (Hull et al, 1996).

2.4.3.1.4 Fiber orientation distribution (FOD)

The orientation of the short fibers within the discontinuous-FRC is crucially important because of the isotropic versus the anisotropic reinforcement they provide, as presented earlier (Paragraph 2.4.3.1.2). Determining the orientation distribution of discontinuous fibers is more challenging than it is for unidirectional fibers, particularly if the discontinuous fibers are oriented in a multidirectional fashion. There are some methods for measuring the FOD, however. One of the methods proposes a geometrical model with two basic assumptions; first that all fibers are straight cylinders and second, that in a cross-section, each fiber is viewed as an ellipse (Hull et al, 1996; Zhy et al, 1997; Christensen et al, 1972). Another group of methods encompasses imaging techniques, such as optical microscope and scanning-electron microscope (SEM) techniques (Norman et al, 2003). A limitation of the imaging methods is the two-dimensional projection of the discontinuous fibers aligned in one plane. One possible solution to this could be to provide sections of the same sample cut in orthogonal planes and analyzing each of them (Lee, 1993).

2.4.3.1.5 Fiber toughening mechanisms

The toughening mechanisms provided by the fibers are result of their ability to stretch, deflect crack propagation, bridge, and resist the opening and propagation of the crack, consequently inducing a closure force on the crack (Kim et al, 2004). The stretching capacity of fibers may enable *crack bridging* and *crack blunting mechanisms* to occur. During crack-bridging, the short fibers would stretch between the edges of the propagating crack. The stretching of the short fibers in the vicinity of the crack tip, during the crack propagation, would decrease the notch sensitivity and cause blunting of the initially sharp crack (Faber et al, 1983; Wetherhold RC, 1989). This would lower the stress concentration at the crack tip and possibly slow down or retard the crack progression. Furthermore, as the crack front deflects and bridges the microcracks around the crack tip, the fracture surface increases and toughness improves, since the resin matrix is still able to carry the load, even though the

crack continues to extend. This mechanism of improving the toughness is known as *crack-deflection-induced toughening mechanism*.

2.4.3.2 Dental discontinuous fiber-reinforced (discontinuous-FRC) composites

Dental discontinuous-FRCs are commonly low aspect ratio composites, with lengths varying between 60 μm and 200 μm and diameters from 6 μm to 15 μm (Table 2).

To the author's knowledge, there have been three low aspect ratio dental discontinuous-FRCs available on the market so far. These are Alert, Nulite F and Restolux (Table 2). Van Dijken clinically evaluated two of them (Alert and Nulite F) and observed that both are associated with surface roughness causing progressive wear and fiber exposure, and non-uniform fiber distribution. In addition to secondary caries, the main reasons for failure were material fracture and cusp fracture. A significantly higher failure rate was detected for Nulite F, which did not fulfill the ADA (American Dental Association) requirements, than for Alert, which complied with the ADA directives. The author suggested that the differences between the materials are correlated to the quantity and size of glass fibers, fiber geometry and the fiber-matrix bond (van Dijken et al, 2006).

At present Restolux has been withdrawn from the market, but few studies have succeeded to analyze its behavior *in vitro*. The presence of a fiber filler enabled good fatigue resistance, but the fiber length was not sufficiently long enough to improve its mechanical properties (Al-Turki et al, 2007; Drummond et al, 2009). Micrometer – scale discontinuous-FRCs are good examples in showing that the simple addition of fibers to resin formulations does not improve their mechanical properties.

Fiber length and the aspect ratio are critical parameters in the reinforcing mechanism, especially because the rule of mixture does not directly stand for discontinuous-FRCs. Consequently, the reinforcement efficiency of composites reinforced with discontinuous fibers will depend on the aspect ratio rather than the fiber volume loading; discontinuous-FRCs with the same quantity of fibers will differ with respect to the provided reinforcement, and the system with higher fiber aspect ratio will provide stronger composite. In contrast, if the fiber aspect ratio is low, the fiber ends will create discontinuity in the resin matrix, act as stress concentration sides and weaken the composite (Shouha et al, 2014).

Table 2. Classification of discontinuous-FRCs according to the fiber aspect ratio.

Type of Discontinuous-FRC		l_f	d_f	l/d	Wt/Vol %	Manufacturer
I. Low aspect ratio discontinuous-FRC *i.e.* micrometer-scale discontinuous-FRCs	Alert*	60-80 µm	6-10 µm	6-13	84/62	Jeneric/Pentron, Wallingford, CT, USA
	Nulite F*	150-200 µm	<9 µm	16-22	83/71	Nulite System International PTY Ltd, Hornsby, Australia
	Restolux*	80-120 µm	10-15 µm	5-12	85wt%	Lee Pharmaceutical, South El Monthem CA, USA
II. High aspect ratio discontinuous-FRC *i.e.* millimeter-scale discontinuous-FRCs	everX Posterior*	0.3-2.0 mm	16-17 µm	18-125 most of the fibers within 59-94	74.4/53.6	GC Corporation, Tokio, Japan

Wt/Vol% is the total fraction of fibers and particulate-fillers.
Alert* Ref: Manhart J et al, 2001; (no declaration on the portion of fibers versus particulate fillers). Contains crushed and chopped glass fibers.
Nulite F* Ref: van Dijken JW et al, 2006; (no declaration on the portion of fibers versus particulate fillers). Contains micro-rod glass fibers.
Restolux* Ref: Drummond JL et al, 2009; (54 wt_f% are fibers; no data on the vol%). Contained chopped glass fibers.
everX Posterior * Ref: Garoushi S et al 2013; Abouelleil H et al, 2015; Lassila et al, 2016; (~ 9 wt_f% are E-glass millimeter-scale fibers, which is Vf=7.2%, Study IV; Bijelic-Donova et al, 2016).

An attempt to establish a high aspect ratio discontinuous-FRC was made in 2007 (Garoushi et al, 2007a). A restorative composite with a semi-interpenetrating network (semi-IPN) polymer matrix and short E-glass fiber was introduced. It contained 22.5 Wt_f% of short fiber fillers with a length of 3 mm embedded in 22.5 Wt% of a dimethacrylate-polymethylmethacrylate resin matrix and 55 Wt% of silane treated $BaAlSiO_2$ inorganic filler particles. Although it showed excellent in vitro performance (Garoushi et al 2007a; Garoushi et al, 2008), there were challenges related to the handling properties of the composite. Experimental versions of this millimeter-scale discontinuous-FRC indicated that fibers with lengths from 2 mm to 5 mm provide almost equal reinforcement capacity. In addition, it was demonstrated that although 22 Vf% provided the best increase in strength (flexural and compressive) and flexural modulus, this was not significantly different from 14.7 Vf% for compressive

strength, from 10 Vf% for flexural strength or from 8.5 Vf% for both flexural strength and flexural modulus (Garoushi et al, 2006b). These findings governed the idea that if handling of the experimental discontinuous-FRC is difficult due to the short fibers of 3 mm in length, but the properties are not significantly reduced by using shorter millimeter-scale fibers, then the upper limit for the fiber length could be 2 mm and the acceptable fiber load could be 8.5 to 10 Vf%. Similar findings with regards to the fiber load were also presented in other studies; fiber concentration of 10 Vf% was optimal in terms of enhancing the properties and still being independent of the fiber orientation, whereas properties of composite formulations with higher fiber amounts were dependent on the fiber orientation (Norman et al, 2003). Comparably, 10 Wt_f% fiber inclusion into filled composite resin allowed good wetting of the fibers with the resin and gained mechanical properties similar to material combinations with higher fiber amounts (Fonseca et al, 2014). Now is also known that the lower limit for the fiber aspect ratio in the discontinuous-FRC systems is 5.2 (Shouha et al, 2014). Based on earlier findings, the experimental millimeter-scale discontinuous-FRC was modified and launched on the market in 2011 under the brand name Xenius Base, which was later changed to everX Posterior. The length of the E-glass fiber in this formulation varies between 1.0 mm and 2.0 mm (Table 2) (Garoushi et al, 2013b; Abouelleil et al, 2015), which makes its aspect ratio as high as 59 -118 (58.8-117.6). For the same material, however, Lassila et al. have reported a range value between 0.3 mm and 1.5 mm (Lassila et al, 2016).

By way of a summary, the upper limit for short fibers' length within discontinuous-FRC systems could be considered 2 mm and 10 Vf% for fiber load. The lower limit for the fibers aspect ratio is 5.2. The discontinuous-FRC provides isotropic or anisotropic reinforcement. The reinforcing capacity of these systems could be affected firstly by the low aspect ratio and secondly due to misorientation of the very short fibers. They decrease the orientation factor (Krenchel) and also limit the insertion of fibers by reducing fiber packing *i.e.* the closeness of the fiber arrangement (Harris, 1999).

On the other hand, fiber arrangement has a clinical impact. Changes in fiber orientation would most likely occur during the placement of the composite into the cavity. The application (filling) technique could cause alignment of the fibers from an initially random orientation to in-one-plane orientation, attaining in practice an anisotropic reinforcement. In the case of millimeter-scale discontinuous-FRC this would be influenced by gradual fiber length and cavity size. For example, in cavities with smaller width than the fiber length, the short

fibers will orient in the plane of the cavity length during placement, obtaining in this case an anisotropic reinforcement. Obviously, shorter millimeter-scale fibers could offer a possibility for multidirectional orientation and isotropic reinforcement, whereas longer millimeter-scale fibers would align in one direction and provide an anisotropic reinforcement. Some of the investigated properties of the dental discontinuous-FRCs are reported in Table 3.

Table 3. Some mechanical properties of different types of dental discontinuous-FRCs.

	FS (MPa)	FM (GPa)	FT (MPa $m^{1/2}$)	VH (N/mm^2)	Depth of cure (mm)
experimental discontinuous-FRC	180‘ 210‡	11‘	**14~!**	84ø	4 ø
everX Posterior	124* 111# 101§ 201^ 153†	9.5* 12.2# 8.3§ 14.6†	2.2# 3.1†	52§ 68†	4.6* 5.3^
Alert	119* 125+ 125°	9.9* 12.5+ 12.5°	2.9* 1.2∂ 2.3° 12.5~	75.2~	2.3*
Restolux			1.6¨		

VH: Vicker’s microhardness.
There is no data available for the Nulite composite.
‡ Ref: Garoushi et al, 2007a (specimens stored dry at room temperature for 48 hours).
~ Ref: Garoushi et al, 2011 (specimens stored dry at 37°C for 30 days). **! Unit in $MNm^{-1.5}$**
ø Ref: Garoushi S, Vallittu PK, Lassila LVJ. (2008) Depth of cure and surface microhardness of experimental short fiber-reinforced composite. Acta Odontol Scand 66(1):38-42. (specimens stored in water at 37°C for 24 hours).
‘ Ref: Garoushi et al, 2012 (specimens stored dry at room temperature for 24 hours).
* Ref: Garoushi et al, 2013b (specimens stored dry at room temperature for 48 hours).
# Ref: Belli et al, 2014 (FT evaluated in 4-point bending; specimens stored in water at 37°C for 24 hours).
§ Ref: Leprince et al, 2014 (specimens stored dry at room temperature for 24 hours).
^ Ref: Goracci et al, 2014 (specimens stored in water at 37°C for 24 hours).
† Ref: Abouelleil et al, 2015 (specimens stored in water at 37°C for 48 hours).
+ Ref: Ilie et al, 2009 (specimens store in water at 37°C for 24 hours).
∂ Ref: Bonilla et al, 2001 (specimes stored dry at room temperature for 24 hours).
° Ref: Manhart et al, 2000 (specimens stored in sodium chloride solution at 37°C for 24 hours).
~ Ref: Manhart et al, 2001 (spesimens stored in sodium chloride solution at 37°C for 24 hours).
¨ Ref: Drummond et al, 2009 (specimens stored dry at 37°C for 6 months).

Structural tests with millimeter-scale discontinuous-FRC have been conducted in several studies, either on premolars (Baretto et al, 2015: Kemaloglu et al, 2015) or on molars (Frater et al, 2014; Rocca et al, 2015; Yasa et al, 2015; Ozsevik et al, 2015). These studies have shown that the use of millimeter-scale discontinuous-FRC in reinforcing the remaining tooth structure and the restoration is either advantageous (Frater et al, 2014; Kemaloglu et al, 2015; Yasa et al, 2015; Ozsevik et al, 2015) or insignificant (Baretto et al, 2015;

Rocca et al, 2015). These studies, however, have employed non-uniformed designs. Similar to the fixed partial FRCs, which were shown to have enhanced durability when shaped anatomically (Behr et al, 2005), the millimeter-scale discontinuous-FRC could provide sufficient reinforcement if it is shape-optimized, which means it is layered following the anatomic shape of the tooth. The space needed for the veneering composite covering the fibers would optimally be 1.5 mm (1-2 mm) (Garoushi et al, 2006a), and has been shown *in vitro* that a substructure made of an anatomically shaped discontinuous-FRC veneered with 1 mm of PFC strengthens the restoration and changes the failure pattern from splitting to chipping (Garoushi et al, 2013a).

The properties of discontinuous-FRCs deteriorate in water, similarly to PFCs. Water diffuses via the resin matrix and leaches the fibers' surface (Valittu et al, 1998). Regions with poorly impregnated fibers and void spaces will be obviously most prone to water absorption (Vallittu, 1995). This will weaken the fiber-matrix bond and lower the mechanical properties of the FRC. Water absorption is influenced by the total amount of the inorganic phase comprising the fibers and the particulate filler phase, the hydrophilicity of the resin composition and the degree of silanization (Vallittu, 1995; Valittu et al, 1998; Miettinen et al, 1999).

2.4.3.3 Clinical performance of dental discontinuous-FRC restorations

Behr et al. were the first to suggest that an anatomically shaped FRC framework improves the load-bearing capacity of the FRC restoration (Behr et al, 2005), and Xie et al. showed that bucolingual support is important (Xie et al, 2007). Furthermore, Keulemans et al. tested if using a discontinuous-FRC could enable an anatomically shaped FRC appliance and observed that a veneered millimeter-scale discontinuous-FRC framework design is both supportive and clinically feasible (Keulemans et al, 2009). Another *in vitro* study also suggested that bi- or multidirectional FRC could enable a sufficient reinforcement for the restoration in multiple directions and that, from a biomechanical point of view, could mimic the tooth structure better than the unidirectional FRC (Turkaslan et al, 2009).

The millimeter-scale discontinuous-FRC is intended to replace the missing dentin structure and needs to be protected with a layer of PFC in order to attain a wear resistant surface and polishability, but also in order to prevent bacterial adhesion (Lassila et al, 2009). The millimeter-scale discontinuous-FRC layer as a substructure and the surface *i.e.* protective PFC layer form a bilayered composite structure (Vallittu, 2015). One advantage of having dental fillings

reinforced with discontinuous fibers is the preservation of the dental tissue and minimizing catastrophic tooth fractures, as well as providing a possibility for successfully replacing missing tooth tissue by utilizing a minimally invasive and adhesive technique. In addition, under high stresses, the fiber reinforcement allows retaining of the fractured fragments (Ozcan et al, 2005; Dyer et al. 2005). These conveniences provided by the fibers are important because they have the ability to prolong the service life and functionality of the restoration.

Clinically, wear due to surface roughness, fiber exposure and non-uniform fiber distribution have been observed for some low aspect ratio discontinuous-FRCs. Fiber exposure could lead to discoloration and secondary caries. Moreover, material fracture and cusp fractures were reported as the main reasons for micrometer-scale discontinuous-FRCs failure (van Dijken et al, 2006), which was not the case with the millimeter-scale discontinuous-FRC (Garoushi et al, 2012). Consequently, it could be concluded that owing to their insufficient fiber length, micrometer fibers act as microfiller particles instead of fiber fillers, which yields properties comparable with PFCs (van Dijken et al, 2006).

2.5 Physicomechanical properties of direct restorative materials: testing and biomechanics

Attempts have been made to link the materials performance *in vitro* with their clinical performance and a list of material tests, which may predict relevant clinical factors, has been proposed (Sarret, 2005). An *in vitro* test should be designed to closely simulate the clinical conditions (Kelly et al, 2012), because ISO standard tests are criticized for employing standardized specimens instead of simulating a clinical situation by using natural teeth (Heintze et al, 2011).

ISO tests are, however, important for analyzing the materials' properties and thus increasing patients' safety (Heintze et al, 2011). The importance of designing *in vitro* experiments in accordance with clinically relevant geometries and loading conditions stems from the review article of Lohbauer et al. (Lohbauer et al, 2013). The subsequent paragraphs of this thesis review selected tests and related properties. Their clinical implementation is schematically presented in Figures 1 and 6.

2.5.1 Flexural strength (FS) and flexural modulus (FM)

The three-point bending test on rectangular specimens simultaneously measures compressive, tensile and shear stresses. Compressive stresses develop on the upper side of the specimen, tensile stresses on the lower side of the specimen and shear stresses at the ends of the specimen. Three-point bending test measures the material's maximum stress *i.e.* the flexural strength of the material, and is known as transverse strength or as modulus of rupture (Anusavice et al, 2012; Sakaguchi et al, 2012).

The flexural modulus (modulus of elasticity or Young's modulus) describes the material's stiffness within the range of its elastic portion (Anusavice et al, 2012; Sakaguchi et al, 2012). In other words, the flexural modulus characterizes the ability of the material to withstand non-permanent changes under tension or compression. A material with low flexural modulus would be resilient (flexible) and would undergo reversible elastic deformation. Practically this means, that such a material would deform under pressure (as masticatory stresses), and return to its original size upon release of the stress, whereas a material with high modulus would be rigid (fragile) and will not deform, but most likely brake. Some dependency of the flexural modulus on the thickness of the material has been discussed. Stiffer material in small thicknesses is said to be more fragile, than if applied in a thicker layer; stiff material becomes stronger if applied in a thicker layer (Hamburger et al, 2014). A high elastic modulus is not desirable for a restorative material, because it would not tolerate any deformation even under slight stress and consequently, it would fracture easily. Instead, the restorative material should permit small deformations and therefore, should have a moderately high modulus *i.e.* some flexibility, like dentin (Anusavice et al, 2012). Closely matching moduli between the restorative material and dentin, which flexural modulus is 17 MPa (Sakaguchi et al, 2012), could enable an even distribution of the stresses at the dentin-composite interface.

2.5.2 Diametral tensile strength (DTS) and compressive strength (CS)

The diametral tensile and compressive strengths are considered to be good indicators for simulating the masticatory forces encountered in the mouth. In both diametral and compressive tests, specimens are loaded in compression in different planes, either perpendicularly to the specimen's vertical plane (diametral test) or axially (compression test). It is common for the both test designs that the fracture occurs due to the tensile and complex shear stresses within the material. Tensile stresses generated during diametrical compression

in the diametral test set-up determines tensile, not compressive strength. Therefore, this test gives a measure of the material's tensile strength and is designed for brittle materials (Anusavice et al, 2012; Sakaguchi et al, 2012). Medeiros reported that the diametral test evaluates the resistance of a material to the lateral forces generated during function (Medeiros et al, 2007), whereas the compressive test aims to evaluate the material's resistance to vertical stresses (Willem et al, 1993), as are the occlusal forces during function. Hence, the diametral tensile strength would be beneficial in describing the tensile stresses encountered in anterior restorations (Mota et al, 2006), which are subjected to tensile stresses from oblique or transverse loading due to their position and anatomical form (Schwartz et al, 2004). The compressive strength would be a more important property for understanding the durability of posterior restorations, which encounter higher masticatory loads or parafunctional forces. A restorative material having high diametral tensile, compressive and flexural strength would withstand the occlusal forces encountered in high stress bearing areas.

2.5.3 Apparent horizontal shear strength (AHSS)

The method used for testing the apparent horizontal shear strength (AHSS) is the short-beam shear test. It measures the average interfacial shear stresses, which develop at the interface. The apparent horizontal shear strength should be differentiated from the interlaminar shear strength (ILSS), which is applicable to composites reinforced with uni- and bidirectional fibers, but not discontinuous-FRCs. The AHSS test method is suitable for calculating the shear stresses occurring in the core, because the typical mode of failure for short-beam specimens is the shear failure in the core. It is a macroscopic test which measures the interfacial shear stresses between the fibers and the matrix (Murphy, 1998). Specimen geometry, thickness, test type (3- or 4-point bending) and failure type all need to be described when reporting AHSS results (Whitney, 1985).

2.5.4 Fracture toughness (FT, K_{IC}) and work of fracture (Wf)

Fracture toughness is probably the most important material's property since it describes the ability of the material to resist the propagation of a pre-existing crack inside the material under stress. It is evaluated on rectangular specimens with centrally located crack. Fracture toughness characterizes the mechanism of fracture of a material with embodied flaws and cracks. This is important for two reasons: first, flaws in the material may exist naturally or could be introduced or nucleated during service, and second, their presence might

reduce the fracture toughness particularly if subjected to tensile stresses (Anusavice et al, 2012). In addition, the microstructure of the material is detrimental to its fracture toughness, which in turn is proportional to the material's strength and ductility (Anusavice et al, 2012). If, when stressed, the material does not have the capacity for even slight plastic deformation, the final fracture might appear as sudden and catastrophic, although pre-existing flaws (superficial or internal) weaken the material, due to the localized high stresses around them. Consequently, fracture toughness has been also defined as the "*ability of a material to plastically deform"* or alternatively as "*the energy required for fracture*" (Sakaguchi et al, 2012). Fracture toughness correlates with the energy involved in the crack propagation, that is, the energy stored in the crack surface and the energy that is consumed in plastic deformation (G_{IC}). This energy rate associates with the inherent flaw size (a_0). The toughness, also referred to as the modulus of toughness, is equal to the entire area under the stress-strain curve including both the area under the elastic and plastic portions (Sakaguchi et al, 2012). When this energy required to break the specimen (*i.e.* fracture toughness) is measured as the total area under the load-displacement curve, and is divided by twice the fractured area, the total fracture work is obtained (W_f). The toughening mechanisms of the restorative material versus the toughening mechanisms of the biological materials (enamel, dentin) may influence the work of fracture (Baudin et al, 2009). In addition, the fracture work of dental filling could be substantially improved by including fiber reinforcement into the restoration, that is by layering the fiber preform to the cavity floor before applying the composite material (Xu et al, 2003).

2.5.5 Fatigue strength

The material in service is subjected to slow and repetitive cycling loading, rather than to single-load or only a few cycles. The resistance of the material to the repetitive cycles is usually tested by fatigue tests. Fatigue is defined as a "*progressive fracture under repeated loading*", whereas fatigue strength is *"the stress level at which material fails under repeated loading"* (Sakaguchi et al, 2012). Fatigue failure occurs after a flaw has progressed into a critical crack or cracks have coalesced over many cycles. This results in premature failure (Anusavice et al, 2012). Fatigue failures can occur although the static strength of the material is high and withstands stresses. If a material sustains some stress level without failure under an infinite number of cycles, then at that stress level the material could provide maximum service *i.e.* endurance limit (Anusavice et al, 2012).

Surface flaws and defects are crucial for the fatigue properties of the restorative material, because any kind of defects, notches or surface irregularities can initiate cracks, which, over time, progress into macroscopic cracks and lead to fracture. Consequently, any factors that affect the handling properties of the composite or any degradation processes (water media, humidity and elevated temperatures) that generate or increase the pre-existing flaw within the material may compromise the fatigue properties of the material (Sakaguchi et al, 2012). Characterizing the fatigue resistance of a material provides an understanding into how the material behaves, how it would possibly respond to a clinical environment and what will cause its failure.

2.5.6 Aspects of flaws: influence of stresses on them and their influence on the interlayer adhesion

A material could be naturally porous, where inherent flaws naturally exist in the material, or flaws could be introduced into the material during the manufacturing or manipulation process (placement and layering technique, grinding and polishing). The importance of flaws becomes significant because of the: 1. location (superficial vs. internal) and subsequent distribution of stresses around them; 2. material behaviour and response to their presence (brittle versus ductile material); and 3. oxygen entrapment and the consequent effect on the polymerization and interlayer bonding.

Superficial flaws may occur as a consequence of polishing and finishing procedures, while internal flaws are the result of poor handling. Superficial flaws and flaws orientated perpendicularly to tensile stresses are subjected to higher stresses than same sized interior flaws and flaws subjected to compressive loads (Anusavice et al, 2012). To avoid failures induced by superficial flaws, the material should be highly polished. Examples of the second type of flaws, internal flaws, are pores and bubbles. These are critical types of defects as they increase the stresses ability to initiate a failure and reduce material strength. Thus, the strength of a restored cavity is likely to be strongly affected by the placement technique and packing of the composite (Baudin et al, 2009). To avoid internal flaws, the composite material should be handled with care.

The resilience of the material is also important in the response to the flaws. Ductile materials could relieve localized stresses around a flaw because of their ability for plastic deformation, which allows for blunting of the crack tip. In contrast, brittle materials cannot reduce the stress by plastic deformation, but

instead permit concentration of the stresses around the flaw and may initiate a crack (Anusavice et al, 2012).

Pores or voids are known to provide pathways for oxygen passage to greater depths within the composite structure. This was observed in some FRCs (Vallittu 1997; Miettinen et al, 1999; Karacaer et al, 2003), but is possible for both particulate- and fiber-reinforced composites (Baudin et al, 2009; Vallittu 1997; Miettinen et al, 1999; Karacaer et al, 2003). Voids play a role as oxygen reserves (Vallittu 1997), trapping the oxygen inside the composite and allowing diffusion along their surface. Consequently, voids allow internal inhibition (Vallittu 1997; Miettinen et al, 1999). Normally, an air inhibited layer is formed and located in the top surface of each resin layer, when composite increments are superimposed, for example when the layering technique is implemented for direct composite restorations. However, inclusion of voids might change this course. In addition to the fillers, other factors that are reported to affect the inhibition depth are the monomer composition and its viscosity (Lee et al 2004; Gauthier et al, 2005), polymerization temperature (Gauthier et al, 2005), light-curing time (Kim et al, 2006), the rate of oxygen consumption (Lee et al, 2004) and the resin-filler interaction (Shawkat et al, 2009).

Interestingly, among the other factors that can induce the formation of flaws within a material are cavity shape and the presence of sharp edges in the preparation, as well as the layering *i.e.* bonding materials with relatively different elastic moduli (Anusavice et al, 2012). It thus follows from the above that flaws in direct composite restorations are both manifold and multifactorial, and all their aspect should be born on mind when restoring a cavity.

2.6 Tooth tissue characteristics

2.6.1 Fracture resistance properties and toughening mechanisms in dentin

Dental tissues are also composites, namely they are biologic composites (Bayne et al, 2013). Teeth are, however, heterogeneous hard tissue with a graded organization of enamel, dentin and cementum, and the interface junctions such as dentinoenamel junction (DEJ) and cementoenamel junction (CEJ). These multiple tissues account for the variation in tooth tissue properties (Giannini et al, 2004).

With respect to the fracture properties, both enamel and dentin are anistotropic materials *i.e.* their properties are orientation dependent. Particularly enamel is distinctively a highly anisotropic material, being strongest when stressed in tension in the direction of the enamel rods (Rassmussen et al, 1976; Giannini et al, 2004). Dentin, on the other hand, is less anisotropic (Rassmussen et al, 1976; Kinney et al, 1999). It has been thought that dentin is weaker in the direction perpendicular to the dentinal tubules, as easier fractures accompanied with less fracture work were obtained in that direction (Rassmussen et al, 1976). In contrast to this earlier knowledge, however, it is now known that dentin is stiffest in the direction of the collagen fibrils, which are orientated perpendicularly to the dentinal tubules (Kinney et al, 1999; Kinney et al, 2003). In other words, dentin is stiffest in the direction perpendicular to the dentinal tubules. This could be explained by the isotropic structure of dentin at the microstructural level. Indeed, dentin is comprised of dentinal tubules surrounded with peritubular dentin (*cylindrical inclusion*) and an intertubular dentinal matrix (*matrix phase*) (Kinney et al, 1999). The tubules, with their adjacent peritubuluar cuffs, are microscopic cylindrical channels orientated radially between the DEJ or CEJ and the pulp, whereas the intertubular dentin encloses mineralized collagen fibrils, 50 to 100 nm in diameter, forming felt-like structure named as the intertubular dentin matrix. In relation to the dentinal tubules, this intertubular collagen fibril matrix is orientated perpendicularly. This results in the orthogonal arrangement of the structural components of dentin (Kinney et al, 2003), which likely reduces its structural anisotropicity. Namely, it has been suggested that dentin shows isotropic symmetry (Kinney et al, 2003), and that the properties of dentin are strongly determined by the mineralized collagen fibrils, not dentin tubules (Kinney et al, 1999; Kinney et al, 2003). The orthogonal orientation between the tubules and collagen fibrils substantially affects the toughening mechanisms in the dentin. These have been described to be slight deflections and microcracking in perpendicular orientation (crack extension perpendicular to the dentin tubules) and bridging by collagen fibrils and uncracked ligaments in parallel orientation (crack extension parallel to the dentin tubules) (Nalla et al, 2003a; Nalla et al, 2003b). Consequently, the optimal toughness is not perpendicular to the dentin tubules, but parallel to them. In the latter case, the toughness is provided by the collagen fibrils (Nalla et al, 2003a). Likewise, the internal orientation of the tubules and collagen fibrils affects other dentin properties too (Kinnely 1999; Giannini et al, 2004). Owing to the negligible effect of the tubule orientation on the elastic characteristics, dentin has been thought of as an isotropic material (Kinnely 1999). Some tooth tissue properties are presented in Table 4.

Table 4. Some mechanical properties of enamel and dentin.

	FT **(MPa ·m$^{1/2}$)**	**FM** **(GPa)**	**UTS** **(MPa)**	**SS** **(MPa)**	**CS** **(MPa)**	**W_f** **(J/m^2)**
Enamel	0.4-1.5* 0.7-1.3†	84†	10†	90†	384*†	13 and 200 for fracture parallel and perpendicular to the enamel rod respectively#
Dentin	3.08 *^ 3.13 at 37°C ^ post-fatigue:1.80√	17†	106†	138†	297*†	270 and 550 for fracture perpendicular and parallel to dentin tubules respectively#

UTS: ultimate tensile strength (micro-tensile test); **SS:** shear strength (push-out test).
*Willems G, Lambrechts P, Braem M, Vanherle G. (1993) Composite resins in the 21st century. Quintessence Int; 24(9): 641-658.
^El Mowafy OM, Watts DC. (1986) Fracture toughness of human dentin. J Dent Res; 65(5):677-681.
Rasmussen ST, Patchin RE, Scott DB, Heuer AH. (1976) Fracture properties of human enamel and dentin. J Dent Res; 55(1): 154-164.
√ Imbeni V, Nalla RK, Bosi C, Kinney JH, Ritchie RO. (2003) In vitro fracture toughness of human dentin. J Biomed Mater Res; 66A (1):1-9.
†Sakaguchi et al, 2012; pp.41,43,84,86.

3. AIMS OF THE THESIS

The series of studies included within the current thesis were conducted with the aim to investigate various physicomechanical properties of the millimetre-scale discontinuous-FRC and to evaluate the intrinsic properties of the material, which are important for optimizing its application technique. The presence of millimetre-scale discontinuous fibers makes the structure of the composite fibrous, which closely resembles dentin. Hence, special emphasis was set on its possible use as a direct, dentin replacing material. The working hypothesis was that this fibrous composite material could improve the fracture resistance of direct restorations as well as change the fracture pattern of the restored tooth unit, and minimize the incidence of catastrophic fractures, thus possibly improving the longevity of the restoration. The working hypothesis was tested by conducting structural and behavioral tests.

The subsequent specific aims were established to:

1. Evaluate the static-load bearing capacity of direct composite restorations made on endodontically treated maxillary central incisors, including individually formed FRC posts only or with millimetre-scale discontinuous-FRC cores, as well as millimetre-scale discontinuous-FRC post-core units. Additionally, the effect of millimetre-scale discontinuous-FRC on the failure mode of the restorations was assessed.

2. Determine the bond strength between two successive increments of millimetre-scale discontinuous-FRC, and to investigate the role of the oxygen inhibition layer on the bond strength.

3. Investigate the fatigue versus fracture load behaviour of millimetre-scale discontinuous-FRC anterior crown restorations and to correlate this finding with the fracture resistance of the plain material.

4. Assess the clinically relevant mechanical properties of the millimetre-scale discontinuous-FRC through various test set-ups including three-point bending, single-edge-notched-beam (SENB) three-point bending, apparent horizontal shear strength evaluated by short-beam method and mechanical properties in compression and tension (diametral tensile strength). Some fiber- and matirx related properties were also evaluated. These included measurements of the fiber length as well as the critical fiber length, then the fiber volume fraction, the fiber diameter and the fiber orientation distribution.

4. MATERIALS AND METHODS

The materials used to fabricate the specimens in studies I-IV are listed in Table 5.

Table 5. Materials used in studies I-IV.

Brand	Manufacturer	Composition	Study
Experimental discontinuous-FRC	Turku Clinical Biomaterials Centre (TCBC)	Filler: 22.5wt% short E-glass, 55wt% silane treated silica ($BaAlSiO_2$) Monomer: PMMA, bis-GMA, TEGDMA	I
everX Posterior	GC	Filler: E-glass fiber, barium glass and silicon dioxide Monomer: bis-GMA, TEGDMA, PMMA	II, III, IV
Supreme XTE	3M ESPE	Filler: zirconia/silica cluster and a non-agglomerated/non-aggregated silica filler Monomer: bis-GMA, UDMA, TEGDMA, bis-EMA	I, II, IV
Filtek Z250	3M ESPE	Filler:Zirconia/silica Monomer: bis-GMA, bis-EMA, UDMA	II
Filtek Silorane	3M ESPE	Filler: Quartz and yttrium fluoride Monomer: TEGDMA, ECHCPMS	II
Filtek Bulk Fill	3M ESPE	Filler:zirconia/silica and ytterbium trifluoride Monomer: bis-GMA, bis-EMA, UDMA, Procrylat	IV
G-ænial anterior	GC	Filler: pre-polymerized: silica and strontium; inorganic filler: silica >100 nm and fumed silica <100 nm. Monomer: UDMA, dimethacrylate co-monomers	III, IV
EverStick C&B	Stick Tech-GC	E-glass fibers, PMMA, bis-GMA	I
Scotch Bond multi-purpose etchant, primer and adhesive	3M ESPE	Etchant: 35% phosphoric acid; Primer: HEMA, water, vitrebond copolymer; Adhesive: HEMA, bisGMA.	I
Stick Resin	Stick Tech-GC	Monomer: bis-GMA, TEGDMA	I
ParaCem®Catalyst	Coltène Whaledent	Fillers: Silanized barium glass, amorphous silica Monomers: bis-GMA, bis-EMA, TEGDMA, Benzoyl peroxide	I
ParaCem® Base	Coltène Whaledent	Barium glass silanized, Amorphous silica Monomers: bis-GMA, bis-EMA, TEGDMA, Initiators	I

4.1 Study I

4.1.1 Fabrication of the direct restorations reinforced with FRC and/or millimeter-scale discontinuous-FRC

Direct anterior composite restorations were made on human endodontically treated maxillary central incisors replicating a situation where only one-third of the coronal structure of the tooth remained. Direct composite restorations were prepared on both non-reinforced and reinforced endodontically treated incisors (ETI).

Non-reinforced ETI received direct PFC or experimental millimeter-scale discontinuous-FRC coronal restorations. Reinforced ETI were restored with direct pre-impregnated E-glass FRC posts or experimental millimeter-scale discontinuous-FRC posts, and coronal restorations were made either of PFC or experimental millimeter-scale discontinuous-FRC. The experimental composite blend was prepared as described earlier by Garoushi (Garoushi et al, 2007a). The groups are schematically presented in original publication I, Bijelic et al, 2013.

Prior to the restoration procedure, the post space and the remaining dentin surface were first etched for 20 s using a 35% phosphoric acid (Scotchbond™ Etchant, 3M Espe, MN, USA) and then cleaned with a water spray and gentle air-dried. Subsequently dentin primer and dentin adhesive (Scotchbond Multi-Purpose Primer and Adhesive, 3M, Espe, MN, USA) were applied according to the manufacturer's instructions.

The FRC root canal posts fabricated in this study were individually formed FRC posts. The pre-impregnated fiber bundle was first cut to a length of 14 mm, and then immediately inserted into the root canal post space. Both ends (apical and coronal end) were fitted in leaving 4 mm of the fiber bundle above the coronal opening (Figure 3), and then light-polymerized (Demi L.E.D., Kerr, Middleton, USA) *in situ* for 20 s. The individually formed FRC post was then removed from the canal and cured for 40 s outside the canal. Next, the surface of the FRC post was wetted with light-polymerizable dimethacrylate resin (Stick Resin, Stick Tech, Turku, Finland) for 5 min and protected from any light source by a lightproof box until cementation. The individually formed FRC posts were cemented with a dual-curing composite resin luting cement (ParaCem® Universal DC, Coltène/Whaledent, Altstätten, Switzerland) according to the manufacturer's instructions.

Discontinuous-FRC posts were prepared by incrementally condensing and polymerizing the experimental short fiber composite resin into the root canals. Each layer was polymerized for 40 s.

Crown contour and dimensions were standardized utilizing a transparent mold fabricated of (transparent) polyvinyl siloxane impression material (Memosil 2, Heraeus Kulzer, Germany). The PFC (Supreme XTE, Shade A3, 3M Espe, St.Paul, MN, USA) and experimental discontinuous-FRC were applied to the transparent mold, which was then placed on the tooth surface with slight pressure. After removing the excess material, the crown was light- polymerized for 40 s (20 s on each side) first outside the mold and then for another 40 s (20 s per side) upon removal of the mold (Figure 4). The light source was placed in close contact with the crown surface. All crowns were built-up in three increments and, upon fabrication, were finished and polished with diamond burrs, white stones and diamond polishing cups under water cooling.

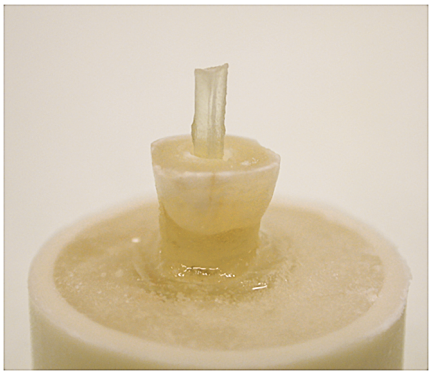

Figure 3. Individually formed FRC post inserted into the post space (fitting step).

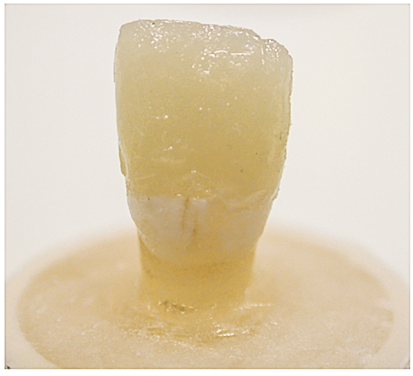

Figure 4. Coronal restoration made of discontinuous-FRC (non-finished, non-polished specimen).

4.1.2 Mechanical testing

The acrylic block containing the restored tooth was fixed to the inclined metal base, providing a 45 degree angle between the palatal surface of the tooth and the loading tip. A static load until fracture was applied on the palatal side of the crowns, approximately 2 mm below the incisal edge. A universal testing machine (Lloyd LRX, Lloyd Instruments Ltd, Fareham, UK) was used to test the fracture resistance of the restored teeth, with a cross head speed of 1.0 mm/min. The specimens were loaded until fracture and the load values were measured in N. The load

deflections curves were recorded and analyzed after testing. The beginning of the specimen damage was classified as the initial fracture (IF) and the maximal load at which the final fracture appeared, was classified as the final fracture (FF).

4.1.3 Visual examination

Differences regarding the fracture pattern among the groups were visually analyzed by two operators and divided into two groups: 1. Favorable *i.e.* restorable type, which is reparable crown fracture that occurred above the preparation line and above or at the simulated bone level; and 2. Unfavorable *i.e.* non-restorable type, which is a non-repairable root fracture that occurred below the simulated bone level.

4.2 Study II

4.2.1 Fabrication of the specimens for determining the thickness of the oxygen inhibition layer and for evaluation of its effect on the interlayer shear bond strength

Specimens for measuring the thickness of the oxygen inhibition layer (OIL) were prepared according to the microscopic technique previously suggested by several authors (Ruyter 1981; Rueggeberg et al, 1990; Vallittu, 1997). The groups and the protocol are described in Table 6, whereas the microscope technique is schematically presented in Figure 5. Additionally, the interlayer shear bond strength with present, treated or removed OIL was also investigated. The same restorative material was used for both the substrate and adherent material depending on the group to which they belonged (Table 6). The corresponding unpolymerized composite material was inserted into the retentive cavity with a diameter of 5 mm and a depth of 3 mm, which was previously prepared in an acrylic resin block, and light-cured for 40 s (Elipar S10, 3M Espe, St Paul, MN, USA). Following the polymerization, the adherent material was applied to the substrate in approximately 2 mm increments using a translucent polyethylene mold with an inner diameter of 3.6 mm and polymerized for 40 s.

Two aging methods were used, dry storage at 37˚C for five days and thermocycling (TC) (between 5°C and 55°C) for 6 000 cycles before testing. TC specimens were pre-stored in distilled water at room temperature (23±1°C) for 48 hours prior to the thermal aging procedure.

Table 6. Overview of the protocols used in study II.

Groups 1-3 were prepared for OIL thickness evaluation (n=3). Groups 1-4 were prepared for the shear bond strength test (n=12). Materials investigated were EverX Posterior, Z250, Supreme XTE and Silorane.	
Group 1 Intact OIL	The OIL was not removed. The **OIL thickness** measurements were performed as soon as the specimens were prepared. For **the shear bond test**, the adherent composite was applied to an untreated surface of the polymerized composite *i.e.* with present (intact) OIL.
Group 2 Alcohol treatment	The OIL was removed by wiping it from the surface of the cured specimen using alcohol sponges soaked in 99 wt% ethanol (Etax Aa, Altia Corporation, Rajamäki, Finland) for 20 s and the gently air dried for another 20 s.
Group 3 Water spray treatment	The OIL was removed with water applied as a water spray for 20 s from a distance of ~ 5 mm perpendicular to the specimen surface and then gently air dried for another 20 s.
Group 4 Removed OIL	The OIL was removed by mechanically polishing the surface with 1000 grit silicon carbide abrasive grinding paper (SiC, Struers, Copenhagen, Denmark) at 250 rpm under water cooling using an automatic grinding machine (LaboPol-25, Struers A/S, Copenhagen, Denmark). After grinding, the surface of the first composite increment was gently dried with an air-spray for 20 s.

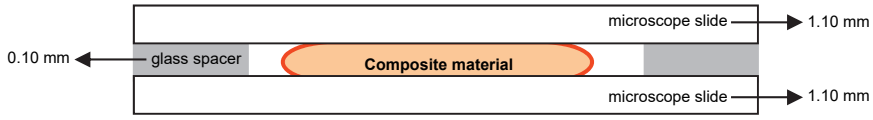

Figure 5. Schematically presented assembly for measuring the OIL thickness, which develops only at the sides of air-composite contact *i.e.* at the outer (red) boundaries between the spacers and the polymerized composite.

4.2.2 Measuring the thickness of the oxygen inhibition layer and the interlayer shear bond strength

A stereomicroscope (Heerbrugg, Switzerland) was used to measure the thickness of the OIL. Ten locations around the periphery of the polymerized specimen were measured at a magnification of x40. The thickness values in μm were measured between the outer boundary of the specimen and the polymerized-unpolymerized resin interface. Micrographs of each specimen were taken in order to visually examine the OIL.

The debonding shear bond strength test until fracture was conducted on a universal testing machine (Lloyd, Lloyd Instruments, Fareham, UK) at a crosshead speed of 1.0 mm/min and at room temperature (23±1°C). Following testing, with the aim to analyze the failure mode of the broken specimens, all

fractured surfaces were visually examined with a light microscope at a magnification of x40.

4.2.3 Visual examination

Failure mode examination among the groups was conducted by two operators. Three types of failures were observed: adhesive, cohesive and mixed.

4.3 Study III

Study III was designed to evaluate the correlation between selected mechanical properties measured by standardized ISO specimens and the fatigue resistance of a simulated case replicating clinical scenario of an anterior crown restoration. The hypothesized correlation is shown in Figure 6.

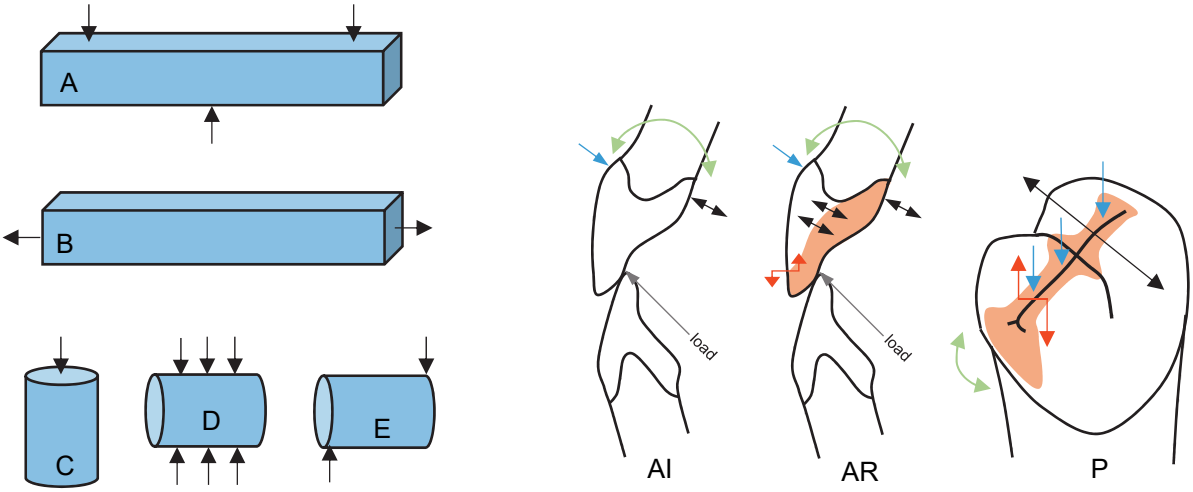

Figure 6. Schematic representation of the hypothesized correlation of some mechanical properties between standardized ISO specimens (A-E) and restorations on anterior (AI and AR) and posterior teeth (P). A: flexure; B: tension; C: compression; D: diametral compression, diametral tension; E: shear; AI: load and stresses encountered in intact anterior tooth; AR: load and stresses encountered in restored anterior tooth (class IV); and P: stresses encountered in restored posterior tooth (class II). Black arrows in A-E: stress direction. In AI, AR and P, blue arrows: compression; Black arrows: tension; Red: arrows shear; Green arrows: flexure; Gray arrows: load direction. (Scheme modified from Bayne, 2013 p.e8). Stress distribution in anterior intact and restored teeth collected from de Castro Albuquerque et al, 2003 and Garbin et al, 2010.

Two composite materials were assessed in Study III: a millimeter-scale discontinuous-FRC (everX Posterior) and a microfilled hybrid composite material (G-ænial anterior).

4.3.1 Fabrication of the standardized (ISO) specimens

Specimens were prepared according to standardized protocols described in corresponding ISO specifications. In study III, flexural strength (FS), flexural modulus (FM), fracture toughness (FT), diametral tensile strength (DTS) and compressive strength (CS) were evaluated.

Specimens for assessing the FS and FM were prepared in a stainless steel mold with dimensions 2x2x25 mm according to ISO 4049. The composite material was placed into the mold in one layer and then the specimens were polymerized on both sides in five overlapping portions (20 s each), with a light-polymerizing unit (Elipar™ S10, 3M Espe, St.Paul, MN, USA) with an output intensity of 1600 mW/cm^2 and a wavelength range between 430-480 nm.

Cylindrical specimens, 4 mm in diameter and 6 mm in height, were prepared for evaluating the DTS and CS, following the procedure given in ISO 4104. The composite material was placed in two increments (2 mm each) and light-polymerized on four sides (top, bottom and two lateral sides) for 20 s per side.

FT specimens were fabricated according to the adapted ISO 20795-1 method. Single-edge-notched-beam (SENB) specimens (2.5x5x25 mm) were prepared using a custom-made stainless steel split mold. A precisely designed slot was fabricated centrally in the mold extending to its mid-height. This enabled a central location of the notch and accurate crack length (a). The composite material was placed in two increments (2.5 mm each). The centrally located, sharp crack was produced by inserting a straight edged razor blade into the prefabricated slot prior to polymerization of the second layer. A scalpel blade was finally used to make a sharp notch in the specimen. Upon removal from the mold, each specimen was also light-polymerized on the opposite side (five overlapping portions (20 s each) per side).

4.3.2 Fabrication of the direct composite crown restorations

The direct composite crowns in this study were fabricated on a zirconia model resembling an abutment model of a maxillary central incisor with a chamfer finish line. Hence, a situation of anterior crown preparation was replicated. An anatomical shape of the upper central incisor was waxed onto the zirconia model and a flat incisal edge surface was secured in this stage, in order to better adapt the flat surface of the loading tip during the test setup. A transparent polyvinyl siloxane impression (Memosil 2, Heraeus Kulzer, Hanau, Germany) was then taken in order to standardize the crown contour and

dimensions. Utilizing the transparent mold, the direct composite restorations were fabricated as described in paragraph 4.1.1, either from a discontinuous-FRC (everX Posterior) or a microfilled hybrid composite material (G-ænial anterior). Fracture resistance determined by static load (n=10/composite material) and compressive fatigue limits (n=20/composite material) were evaluated.

4.3.3 Mechanical testing of the standardized (ISO) specimens

All specimens were dry stored at 37°C for 48 hours and tested in a universal testing machine (Lloyd model LRX, Lloyd Instruments, Fareham, UK) at a crosshead speed of 1.0 mm/min.

A three-point bending test was conducted for testing the FS, FM and FT. The FS values in MPa and the FM in GPa were calculated automatically by the software and were then rechecked using equations 1 and 2 according to ISO 4049: **Equation 1:** $FM = F_1 l^3 / 4 b h^3 d$ where: FM is the flexural modulus, F_1 is the load at the highest point in the straight line portion of the load-deflection curve in N, l is the distance between the supports in mm, b is the width of the specimen measured prior to testing in mm, h is the height of the specimen measured prior to testing in mm and d is the deflection at load F_1. **Equation 2:** $FS = 3 F l / 2 b h^2$ where: FS is the flexural strength, F is the maximum load exerted on the specimen in N, whereas l, b and h are as defined in equation 1.

For the DTS, each specimen was placed with its longitudinal side between the platens of the testing machine, whereas for the CS, each specimen was placed with the flat end on the supporting plate. In relation to the specimens' longitudinal axis, the compressive type of load was applied perpendicularly (in DTS setup) or parallel *i.e.* axially (in CS setup) until failure. The diameter and the length of each specimen were recorded prior to testing with a digital caliper. Both DTS and CS were calculated in MPa using equations 3 and 4: **Equation 3:** $DTS=2 F /\pi l D$, where: DTS is the diametral tensile strength, F is the maximum applied load in N, l is the length of the specimen in mm and D is the diameter of the specimens in mm. **Equation 4:** $CS = 4 F / \pi D^2$, where: CS is the compressive strength, F is the maximum applied load in N and D is the diameter of the specimen in mm.

The FT was calculated accordingly to equation 5: **Equation 5:** $K_{IC} = [P L / B W^{3/2}] f(x)$, where: $f(x)=3/2x^{1/2} [1.99-x (1-x) (2.15-3.93x+2.7x^2)] / (1+2x) (1-x)^{3/2}$ and $0 < x < 1$ with x=a/W. K_{IC} is the fracture toughness, P is the load in kilo newton (kN), L is the span length (2 cm), B is the specimen thickness in

centimeters (cm), W is the specimen depth (height) in cm, x is a geometrical function dependent on a/W and a is the crack length in cm.

4.3.4 Static and fatigue compression test conducted on the direct composite crown restorations

Fracture resistance tested by the static load test, and fatigue resistance by the staircase approach were conducted immediately upon fabrication of the specimens. In both setups, the load cell was applied to the crowns on the palatal side at a 45 degree angle using a universal testing machine (Lloyd LRX, Lloyd Instruments Ltd, Fareham, UK). The static load test was performed with a cross head speed of 1 mm/min, at room temperature (23±1°C) and values measured in N. The fatigue resistance was determined by compressive fatigue limits (CFL) at 10 000 cycles in a water bath and a frequency of 1 Hz. The staircase test, known as the “up and down” method, was used for determining the CFL, as described by Draughn (Draughn, 1979). The specimens in this test were consecutively tested, but the initial level at which the first specimen was tested, was previously determined from preliminary data. The loading level for every subsequent specimen, on the other hand, was depended on the survival or the failure of the previous specimen; in the case of failure, the load level for the next specimen was decreased, whereas in the case of survival, the load level for the next specimen was increased. In the present study, the magnitude of this level was fixed at 20 N. The procedure of increasing the maximum load by 20 N following a survival and decreasing the load by 20 N following a failure was continued for each subsequent crown specimen. Equations 6 and 7 were consequently used to calculate the CFL and its standard deviation (S): **Equation 6:** $CFL = Xo + d\ (A/N \pm 1/2)$ and **Equation 7:** $S = 1.62 \times d\ (NB - A^2 / N^2 + 0.029)$ (Draughn, 1979). In equations 6 and 7 the CFL is the compressive fatigue limit, Xo is the lowest load level considered in the analysis, d is the fixed load increment (20 N) used in the sequential test and S is the standard deviation. A, N and B are computed taking into consideration the load value in N at which the restoration was tested, the stress level (*i*) starting from the lowest designated as 0 (i=0) or 1,2 etc. for every next stress level (i=1; i=2 etc.) and the number of failures at the given stress level (n_i). Consequently, A is the sum of all $i \cdot n_i$ ($A=\Sigma i \cdot n_i$); B is the sum of all $i^2 \cdot n_i$ ($B= i^2 \cdot n_i$) and N is the sum of all failures for all stress levels together ($N=\Sigma n_i$). A positive sign (+) in equation 6 was used in the case of non-failures and a negative sign (-) in the case of failures. The crowns that survived the 10 000 cycles during the fatigue test (eleven SFC and twelve PFC crowns), were immediately loaded statically in order to evaluate the fracture resistance after the fatigue, also known as the post-fatigue (PF) fracture resistance.

4.3.5 Visual examination

Fracture pattern was visually examined by two operators. Two failure types were distinguished, brittle seen as splitting of the crown, and ductile defined as cracking of the crown.

4.4 Study IV

4.4.1 Fabrication of the standardized (ISO) specimens

The methodology used in study IV concurs partly with the methodology used in study III. Therefore, for details regarding the preparation of the standardized specimens, the reader is referred to paragraph 4.3.1. In addition to FS, FM, FT, DTS and CS, apparent horizontal shear strength (AHSS) was also evaluated. Four materials were evaluated in study IV: millimeter-scale discontinuous-FRC (everX Posterior), nanofilled (Supreme XTE), microfilled hybrid (G-ænial anterior) and flowable bulk-fill (Filtek Bulk Fill).

AHSS was determined for rod shaped specimens (3.6 mm in diameter and 14.5±0.2 mm in length) by the short-beam method, according to ASTM D 4475 – 96. The composite material was packed into the transparent mold and the specimen was then light-polymerized on both sides for 20 s in five overlapping irradiations (Elipar S10, 3M ESPE, St. Paul, MN, USA). Once it was removed from the mold, each longitudinal side of the specimen was further polymerized for 20 s in five overlapping places.

4.4.2 Evaluation of the fiber volume fraction, fiber length and critical fiber length

Fiber volume fraction (V_f %) was calculated using **Equation 8** (Hull et al, 1996):

$$V_f\ \% = \frac{Wt_f / \rho_f}{Wt_f / \rho_f + Wt_m / \rho_m} \times 100$$

where Wt is the weight fraction (Wt%), ρ is the density, f represents the fiber and m the matrix. Wt_f = 8.6 wt% (Wt_f of the short E- glass fibers in everX Posterior) and ρ_f = 2.56 (2.56-2.58) g/cm^3 (Hull et al, 1996; Harris, 1999). The matrix is comprised of resin and particulate fillers where $\rho_{(resin)}$ = 1.23 g/cm^3 (Hull et al, 1996; Obukuro et al, 2008), $Wt_{(resin)}$ = 23.7 wt%, $\rho_{(particulate\ filler)}$ = 2.8 g/cm^3 and $Wt_{(particulate\ filler)}$ = 67.7 wt%

The fiber length (l_f) was measured using the direct technique, by separating the fibers from the matrix, following the technique previously described by Garoushi (Garoushi et al, 2013b). Eight batches of discontinuous-FRC (everX Posterior) were evaluated. Fibers were deposited onto glassware and examined with light microscopy (Leica; Leica Mycrosystems, Wild, Heerbrugg, Switzerland). The average fiber length was then defined as $\mathbf{L_N = \Sigma\ Ni\ Li\ /\ \Sigma\ Ni}$, where L_N is the number average of the fiber length and Ni is the number of fibers with length Li (Hull et al, 1996). Four thousand fibers were measured in total (500/batch).

If the fiber diameter (d_f), ultimate tensile strength (σ_{fu}) of the glass fiber and interfacial shear strength (τ_i) of the glass FRC are known, the critical fiber length (l_{fc}) can be calculated as $\boldsymbol{l_{fc} = \sigma_{fu}\ d_f\ /\ 2\ \tau_i}$ (Norman et al, 2003). The diameter of the individual glass fiber in our study was 17 µm and the tensile strength of the E-glass fiber was estimated at 2.0 GPa (Hull et al, 1996; Harris, 1999). Furthermore, the shear-lag model assumes that the shear stress at the fiber-matrix interphase is constant and is 20 MPa for a typical glass-FRC (Hull et al, 1996). The interfacial shear stress evaluated by a macroscopic short-beam test in our study was 15.6 MPa. Consequently, experimentally obtained result was compared with the typical values presented in the literature (Hull et al, 1996).

4.4.3 Scanning electron microscopy (SEM) evaluation of the fiber diameter (d_f) and fiber orientation distribution (FOD)

The d_f was determined from SEM images, which were processed with the Image J program (National Institutes of Health, USA). A cross section of a fiber bundle was examined with SEM for this purpose. The specimens were wet ground (Stuers LabPol-21, Stuers A/S, Copenhagen, Denmark) with silicon carbide papers of decreasing abrasiveness (1000-, 1200-, 4000-grit) and gold sputter coated before examination with a scanning electron microscopy (SEM, JSM 5500, Jeol Ltd., Tokyo, Japan). The d_f was determined as the mean value calculated from one hundred measurements per specimen (n=6).

In the present investigation the FOD was visually studied by sectioning the SENB specimens (12 slices obtained from n=6) along their long-axis plane with a high performance precision cut-off saw at 300 rpm (Struers Secotom 50, Struers, Ballerup, Denmark) and analyzing their images by SEM. The specimens were wet ground (Stuers LabPol-21, Stuers A/S, Copenhagen, Denmark) with silicon carbide papers of decreasing abrasiveness (1000-,

1200-, 4000-grit) and gold sputter coated before the SEM examination. After testing the specimens, their fracture surfaces were examined with SEM.

4.4.4 Mechanical testing

FS, FM, FT, DTS and CS were measured as described in 4.3.3. For computing the AHSS, the rod shaped specimen was placed with its long axis perpendicular to the loading nose and its midpoint centered to the loading nose. The side supports were adjusted to a span length of 11±0.2 mm and specimens were loaded by a universal material testing machine (Lloyd model LRX, Lloyd Instruments Ltd., Fareham, UK) at a crosshead speed of 1.0 mm/min until failure. The diameter of each specimen was measured prior to testing with a digital caliper and the AHSS in MPa was calculated using equation 9: **Equation 9:** $AHSS = 0.849\ P / d^2$, where AHSS is the apparent shear strength; P is the breaking load in N and d is the specimen diameter in meters (m).

In this study, the SENB specimens were additionally utilized to measure the work of fracture. This fracture work (Wf) was calculated in joules per square meter (J/m^2), by using equation 10: **Equation 10:** $Wf = U / [2B (H - a)] \times 1000,$ where *Wf* is the fracture work, U is the recorded area under the load-deflection curve and represents the energy required to break the whole specimen. $U = \int P d\Delta$ in newton millimeters (Nmm), where **Δ** is the measured deflection for load P in N; B is the specimen width (thickness) in mm, H is the specimen height in mm and a is the crack length in mm.

4.5 Statistical analysis

Data from studies I-IV were analyzed with SPSS version 19 (Study I-III) and 23 (Study IV) (Statistical Package for Social Science, SPSS Inc, Chicago, IL, USA). An analysis of variance (ANOVA) test at the significance level of p=0.05 (Study I, II and IV) or p=0.001 (Study III) was used. In all studies this was followed by Tukey's *post hoc* analysis and with the Pearson correlation in Studies III and IV. Additionally, in study III and study IV, equality of variance was validated by the Levene test (p=0.05).

A two-way ANOVA was used in study I to define if the initial fracture load and final fracture load were different for the investigated materials.

A two-way ANOVA was used in Study II to determine if the material type and the surface treatment had an effect on the OIL thickness, and a three-way ANOVA was conducted to reveal if the material type, surface treatment and storage condition affected the interlayer shear bond strength between the composite layers.

In study III, a one-way ANOVA was used to investigate the dependency between the material type and the mechanical properties. A two-way ANOVA was also used to analyze if the material and the fracture load type (static or fatigue) affected the fracture resistance of the investigated materials. The correlation among the ISO mechanical properties, and the clinical scenario (static fracture resistance and fatigue performance of anterior crowns), was assessed by means of Pearson correlation.

In study IV, a two-way ANOVA was used to define if the material type and storage condition had an influence on the mechanical properties. Properties, fiber volume fraction, fiber length, critical fiber length, fiber diameter and fiber orientation distribution were not statistically analyzed as only one discontinuous-FRC was used; there was no counterpart for comparison.

In addition, crowns and specimens were visually expected in all studies and fracture patterns were assessed. Failure modes were not statistically analysed.

5. RESULTS

5.1 Fracture behavior of the direct restorations reinforced with FRC and/or millimeter-scale discontinuous-FRC (Study I)

Initial and final fracture load values were recorded for the direct anterior composite restorations made on severely structurally compromised central maxillary incisors. Their fracture behavior was also analyzed (Table 7). There was no difference between the initial (IF) and final (FF) fracture load values observed for the restorations made of PFC ($p>0.05$). However, the restorations made of millimeter-scale discontinuous-FRC exhibited differences with regards to the IF and FF; the IF values in all millimeter-scale discontinuous-FRC groups were lower than the FF values. Although the fracture resistance of the millimeter-scale discontinuous-FRC restorations made on non-reinforced teeth was highest, it also resulted in the highest frequency of unfavorable fractures (63%). FRC- or millimeter-scale discontinuous-FRC posts provided as good reinforcement, but the latter resulted in less unfavorable fractures (37%). The use of FRC-posts for reinforcing direct PFC restorations insignificantly improved the failure pattern (51% favorable fractures).

Table 7. Fracture resistance of the direct composite restorations reinforced with FRC and/or discontinuous-FRC, with the standard deviation in brackets (SD), and their failure mode distribution (Study I).

GROUPS	Fracture Load (N)		Fracture types (%)	
	IF (SD)	FF (SD)	Favorable	Unfavorable
PFC non-reinforced teeth	164.8[a] (95.1)	164.8[a] (95.1)	49	51
FRC-post reinforced PFC	296.0[ab] (184.5)	296.0[ab] (184.5)	51	49
Discontinuous-FRC non-reinforced teeth	469.8[b] (249.0)	515.8[b] (241.6)	37	63
FRC-post reinforced discontinuous-FRC	442.3[ab] (169.3)	467.2[ab] (156.8)	50	50
Discontinuous-FRC post-core-crown	441.1[ab] (245.1)	490.5[b] (288.6)	63	37

Same superscript letter above the values represents groups that were not statistically different ($p > 0.05$).

5.2 Thickness of the oxygen inhibition layer (OIL) (Study II)

All investigated materials, regardless of OIL surface treatment, demonstrated measurable thickness (Figure 7; Table 8). This indicated that none of the investigated treatments (ethanol wiping and water-spray) was able to remove the OIL. The only treatment that was anticipated to remove the OIL completely was the grinding procedure, which was employed in the debonding *i.e.* shear bond investigation (paragraph 5.3).

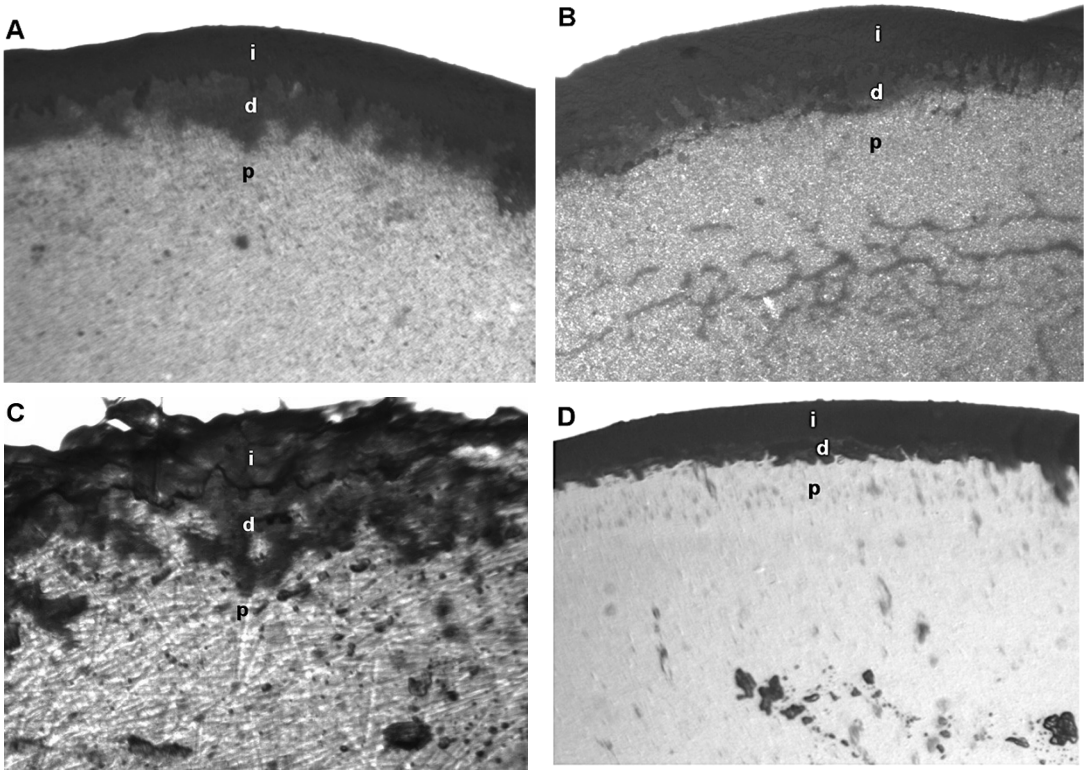

Figure 7. The OIL is showed on a stereomicroscope micrograph x40. A: nanofilled (Supreme XTE); B: microhybrid (z250); C: discontinuous-FRC (everX Posterior); and D: silorane-based composite (Silorane) after alcohol treatment. OIL thickness values are given in Table 8. i: inhibited layer; d: diffusion zone and p: polymerized composite. Modified from original publication II (Bijelic-Donova et al, 2015).

Table 8. Thickness of the oxygen inhibition layer (OIL) of the tested materials, with the standard deviation in brackets (SD). Modified from original publication II (Bijelic-Donova et al, 2015).

Material	Surface treatment of the OIL	Thickness of the OIL in µm.
EverX Posterior	Intact OIL	20.1 (5.5)*
	Alcohol-treated OIL	20.8 (5.7)*
	Water-spray treated OIL	22.9 (4.7)*
Filtek Z250	Intact OIL	14.5 (2.6)[a]
	Alcohol-treated OIL	15.2 (4.2) [a]
	Water-spray treated OIL	18.8 (3.0) [b]
Filtek Supreme XTE	Intact OIL	17.1 (3.0)^
	Alcohol-treated OIL	19.2 (3.1)^
	Water-spray treated OIL	18.5 (2.6)^
Filtek Silorane	Intact OIL	13.8 (3.4)†
	Alcohol-treated OIL	12.0 (2.2)†
	Water-spray treated OIL	11.6 (2.4)†

Same superscript letter above the values represents groups that were not statistically different ($p > 0.05$). ANOVA was performed for each material separately.

The inhibition depth was greatest for the millimeter-scale discontinuous-FRC material, irrespectively of whether the OIL was intact or treated with alcohol or water-spray. Thin OIL was also measured on the surface of the silorane-based composite. Both intact and treated OIL gave measurable values for this type of composite.

5.3 Interlayer shear bond strength between superimposed layers of similar composite and failure mode assessment (Study II)

The interlayer shear bond strength of incrementally placed layers of dimethacrylate composites (millimeter-scale discontinuous-FRC and PFCs) was not affected by the alcohol or water-spray treatment of the OIL. Indeed, these OIL surface treatments revealed no difference in comparison to the intact OIL ($p>0.05$), which suggests that they did not improve nor weaken the debonding. This was not the case for the silorane-based composite, which interlayer shear bond strength decreased significantly after wiping the OIL with alcohol ($p<0.05$) (Figure 8). This finding correlated with the failure mode analysis which revealed a high percentage of adhesive failures for the alcohol treated OIL of the polymerized surface of silorane-based composite (Figure 9). This was observed for both dry and thermally aged specimens. Removal of the OIL resulted in a significant reduction of the interlayer shear bond strength

irrespective of the material and aging type, however (Figure 8). It could thus be concluded that the absence of the OIL impaired the interlayer connection. In addition, complete OIL removal by grinding was related to a high occurrence of adhesive failures identified for all, except the millimeter-scale discontinuous-FRC, where mainly cohesive breaks were observed (indicated by the black arrows in Figure 9). Cohesive and mixed types of failures were also observed for alcohol and water-spray treatments for the other dimetharcylate composite materials and the water-spray treated OIL surface of silorane-based composite material (Figure 9).

Interestingly, the interlayer shear bond strength was insignificantly improved following the TC, which could be due to the post-curing allowed by the pre-storage of the specimens in distilled water for 48 hours in room temperature (23±1°C) before subjecting them to thermal cycling.

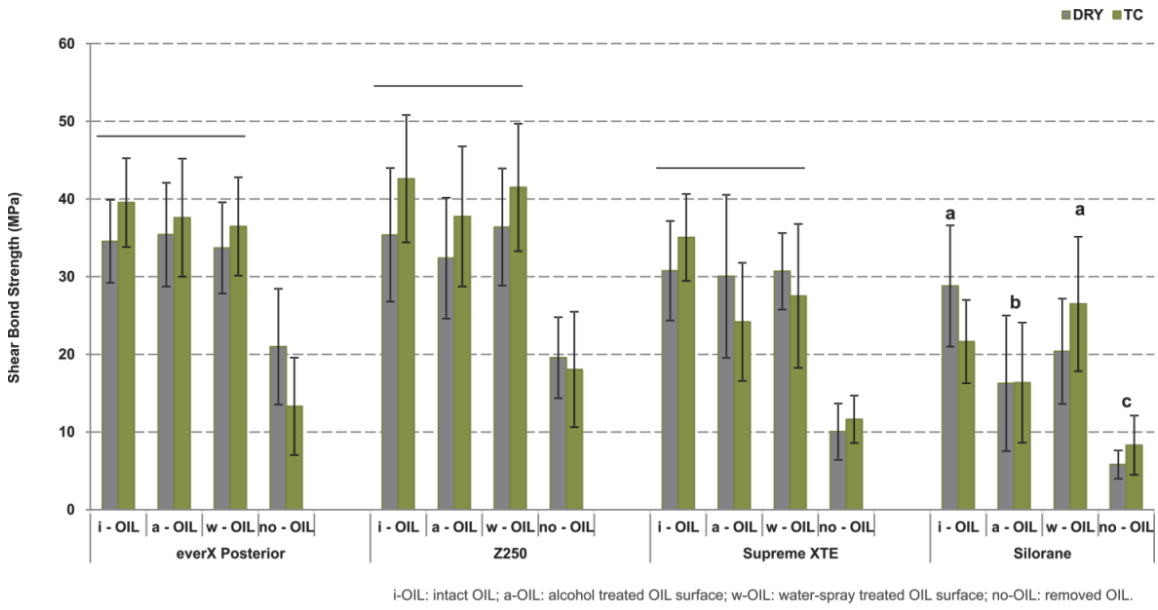

Figure 8. The figure represents the interlayer shear bond strength (MPa) of superimposed composite layers of the investigated materials, with present OIL (i-OIL), treated OIL surface (a-OIL and w-OIL) and absent OIL (no-OIL). The line above the columns and the same superscript letters indicate groups that were not statistically different ($p>0.05$). Modified from original publication II (Bijelic-Donova et al, 2015).

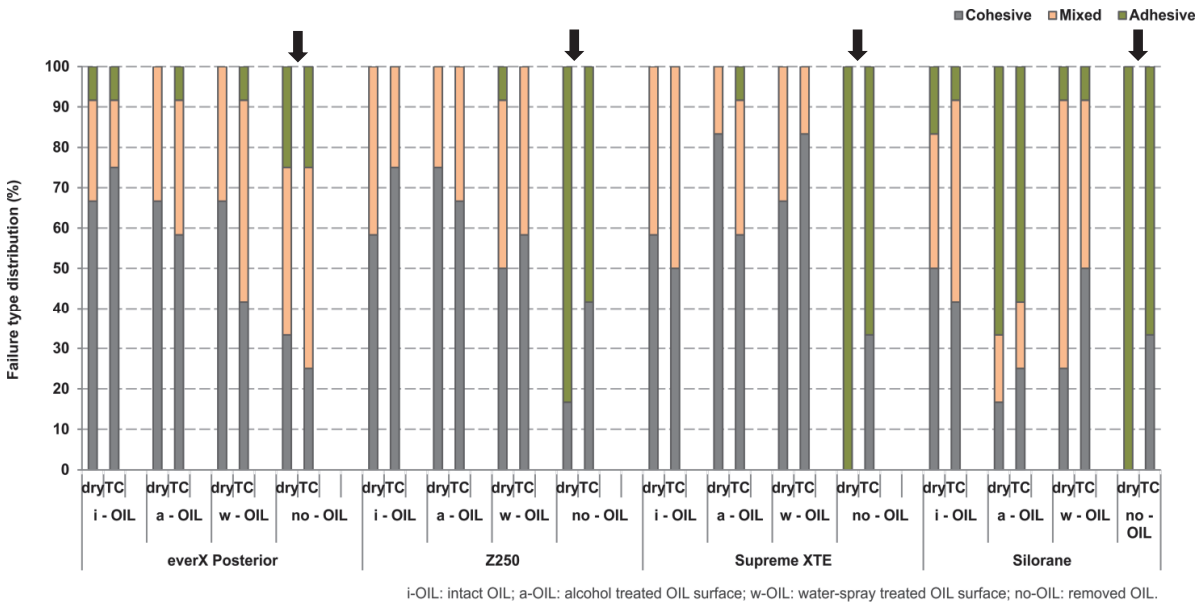

Figure 9. Failure mode evaluation (%) of tested shear bond specimens. Modified from original publication II (Bijelic-Donova et al, 2015).

5.4 Physicomechanical properties (Study III and IV)

The difference between the properties investigated in Study III and Study IV was the aging method. Figures 10 and 11 summarize the results from Study III and Study IV, respectively.

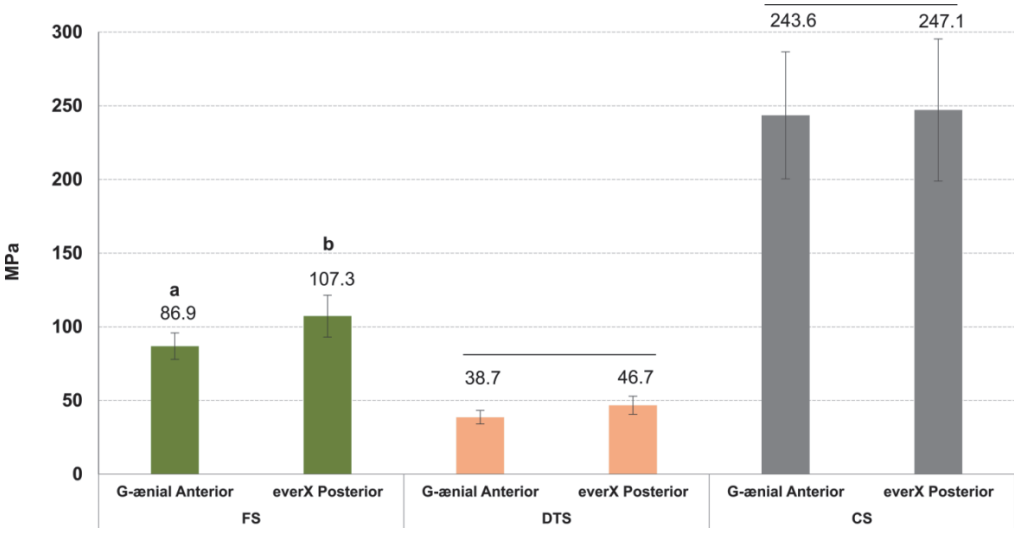

Figure 10. Presented are the results from Study III (in MPa). Specimen (n=10/group) were stored dry at 37°C for 48 hours before testing. The lines above the columns indicate groups that were not statistically different (p>0.05).

The difference between the dry aging methods, 2 days (Study III) and 7 days (Study IV), was not statistically different ($p>0.05$). FM values for the PFC (G-ænial Anterior) were 15.4 GPa and 15.0 GPa at 2 days and 7 days dry aging, respectively. For the millimeter-scale discontinuous-FRC (everX Posterior), these values were 10.1 GPa and 12.6 GPa. With the same dry aging periods used, FT values were 1.0 MPa•m^{½} (2 d) and 0.9 MPa•m^{½} (7 d) for the PFC, and 2.6 MPa•m^{½} (2 d) and 2.4 MPa•m^{½} (7 d) for the millimeter-scale discontinuous-FRC. Statistically insignificant differences could be prescribed to the group size variances, n=10/group in Study III and n=8/group in Study IV.

The water storage caused a reduction of all mechanical properties regardless of the material type (Figure 11). This reduction was statistically significant only for the FS ($p<0.05$), however. In general, the material type impacted the properties and their deterioration in water. Nevertheless, this was not the case for the CS, which remained unaffected by the material type and the water.

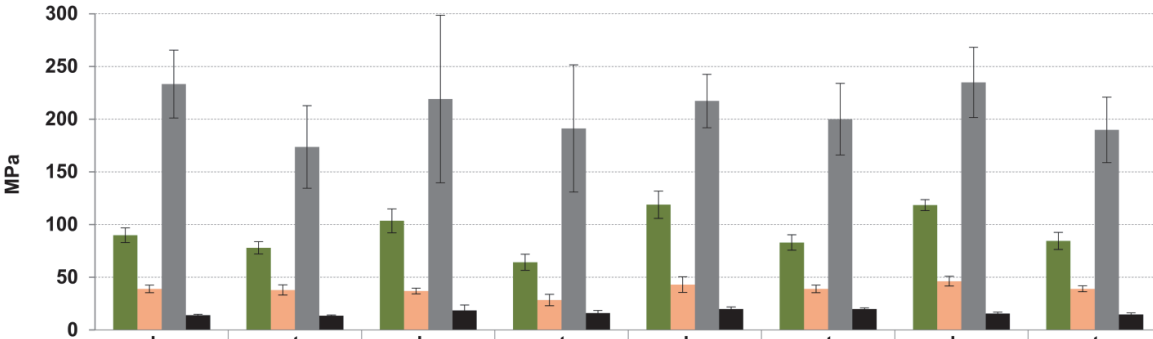

	dry	water	dry	water	dry	water	dry	water
	G-ænial Anterior		Supreme XTE		Filtek Bulk Fill		everX Posterior	
FS	89.8	78.0	103.5	64.2	118.8	83.0	118.5	84.6
DTS	39.0	38.0	36.9	28.5	43.1	39.0	46.3	39.0
CS	233.3	173.6	219.1	191.3	217.3	200.0	234.9	189.9
AHSS	14.1	13.6	18.4	16.0	19.8	19.9	15.6	14.7

Figure 11. Presented are the results from Study IV. Specimen (n=8/group) were stored at 37°C either dry for 7 days or in sterile water for 30 days before testing.

Irrespective of the aging method (dry or water), the millimeter-scale discontinuous-FRC had significantly higher K_{IC} ($p<0.05$) and Wf ($p<0.05$) compared to the others PFCs (Table 9).

Table 9. Flexural modulus (FM), fracture toughness (K_{IC}) and fracture work (Wf) for the materials investigated in Study IV, with their standard deviations in brackets (SD).

Material	Storage	FM (GPa)	K_{IC} (MPa·$m^{½}$)	Wf (J/m^2)
G-ænial Anterior	dry	15.0$^{a\#}$(1.7)	0.9$^{a\#}$(0.1)	55^{a*}(9)
	water	14.4$^{a\#}$(2.0)	0.8$^{a\#}$(0.1)	164$^{a\wedge}$(35)
Supreme XTE	dry	3.9$^{b\#}$(1.0)	1.1$^{a\#}$(0.1)	53$^{a\#}$(7)
	water	3.5$^{b\#}$(0.6)	0.9$^{a\#}$(0.1)	146$^{a\#}$(18)
Filtek Bulk Fill	dry	5.7$^{b\#}$(1.2)	1.1$^{a\#}$(0.1)	88^{a*}(14)
	water	4.7$^{b\#}$(0.9)	0.9$^{a\#}$(0.1)	203$^{a\wedge}$(9)
everX Posterior	dry	12.6^{a*}(2.8)	2.4^{b*}(0.5)	546$^{b\#}$(241)
	water	9.8$^{c\wedge}$(1.0)	1.7$^{b\wedge}$(0.2)	580$^{b\#}$(102)

Same superscript letter and sign above the values indicates groups that were not statistically different ($p>0.05$). Letter describes the statistical difference among the materials across each storage medium, whereas the signs show the statistical difference between dry and water storage mediums across each material category level.

5.5 Fracture behavior of the direct composite crown restorations (Study III)

Both the material type and the type of applied load affected the fracture resistance of the direct composite crown restorations. The static and fatigue loads were both of a compressive type. A similar trend was observed here as in Study I; the IF and FF for PFC crown restorations were same, but different for millimeter-scale discontinuous-FRC crown restorations, with the FF being higher than the IF. Irrespective of the material type, the fatigue type of load (CFL) resulted in lower fracture resistance than the static load type (IF, FF). This suggests that indeed the repetitive cycling loading leads to failures at stresses lower than the instant type of load. However, material that has been already stressed *i.e.* previously fatigued, fails at a lower instant load (PF) than unstressed material (IF, FF) (Figure 12).

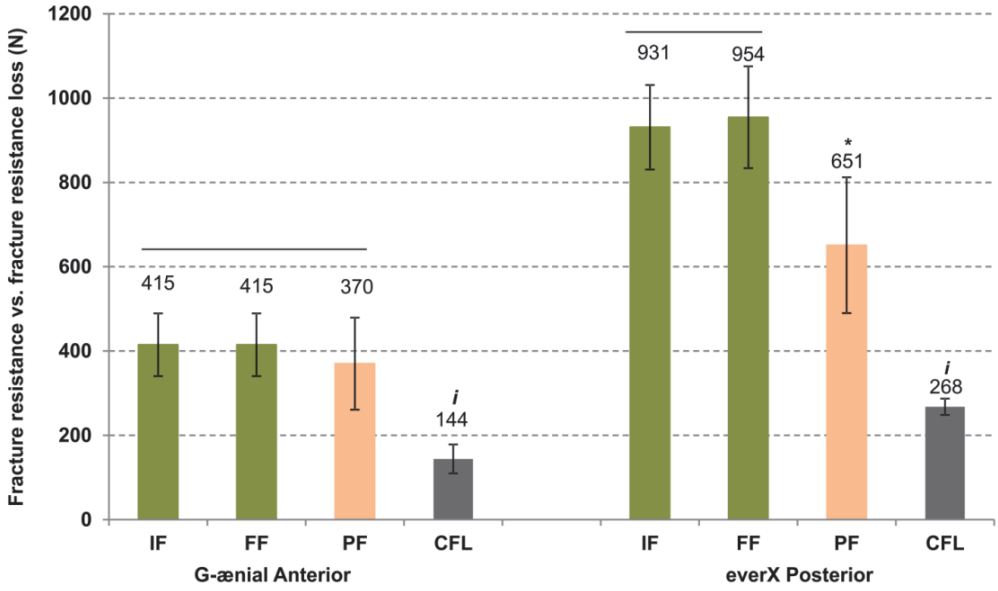

Figure 12. Fracture resistance versus fracture resistance loss (N) endured by the direct crown restorations. PF by static load was obtained from the restorations that survived the assigned fatigue life of 10 000 cylces. The CFL was the mean force used in the fatigue set up. The lines above the columns indicate groups that were not statistically different ($p>0.05$), and ***i*** indicates informative values. Modified from original study III (Bijelic-Donova et al, 2016).

The ANOVA test revealed that fatigue strength (CFL) correlated strongly with fracture toughness (FT) ($R^2=0.899$; $p<0.001$) and moderately with the diametral tensile strength (DTS) ($R^2=0.662$; $p=0.001$) of the materials. This implies that the fracture resistance of the material could be predicted based on its fracture toughness value. Pearson correlation showed a strong correlation also between the load types (static versus fatigue) ($R^2=0.821$; $p<0.001$), proposing that the static strength could be employed to predict the fatigue strength of the restoration. Hence, a combination of the two types of investigations are needed to predict the properties and behavior of a material, these being the fracture toughness of the plain material, and the static strength of simulated clinical scenario of the material (restoration). In other words, materials could be screened and fatigue investigation could be alternated with the abovementioned parameters.

Two types of fractures were visualized following the fatigue test (Figure 13). Cracking (13B) was observed for the direct millimeter-scale discontinuous-FRC crown restorations and splitting (13D) was detected for the direct PFC crown restorations. None of the millimeter-scale discontinuous-FRC crown restorations split into two segments. For the purposes of Study III, two of the

millimeter-scale discontinuous-FRC crown restorations were manually fractured (13A) in order to observe the surface where the crack initiated.

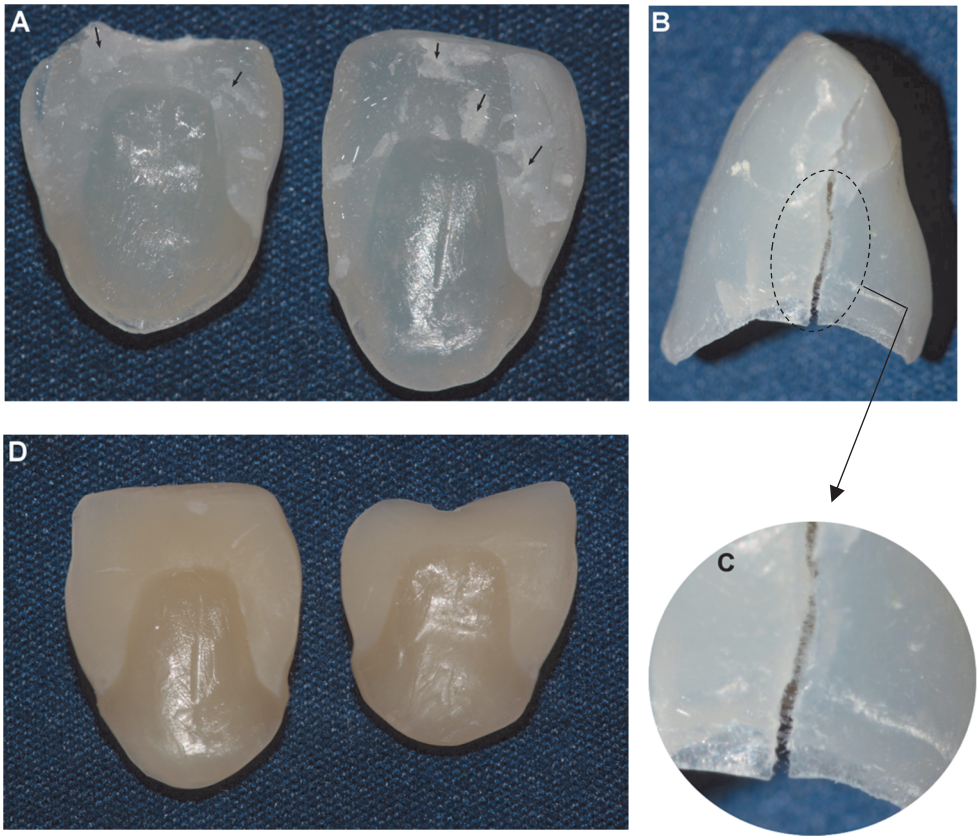

Figure 13. Splitting and cracking of the PFC (D) and millimeter-scale discontinuous-FRC (B) crown restoration, respectively. Fibers were seen to protrude at or to bridge the crack line (B). Crack line is magnified (C). After manually fracturing two millimeter-scale discontinuous-FRC restorations, a cohesive type of fracture (A) within the material was observed.

5.6 Fiber related properties of millimeter-scale discontinuous-FRC (Study IV)

Fiber volume fraction (V_f%), fiber length (l_f), critical fiber length (l_{fc}), optimal fiber length (l_{fo}) and fiber diameter (d_f) were investigated. Fiber fraction by weight (Wt_f%) was obtained from the manufacturer. Results are presented in Table 10.

Table 10. Fiber related properties of the millimeter-scale discontinuous-FRC (everX Posterior). Modified from original publication IV (Bijelic-Donova et al, 2016).

	wt_f %	V_f %	d_f (μm)	l_{fc} (mm)	l_{fc} (mm)	l_{fo} (mm)	l_f (mm)
everX Posterior	8.6	7.2	17	0.85*	1.09**	1.0-1.3#	0.3-1.9

* interfacial shear stress (τ_i) for a typical glass fiber reinforced polymer composite is 20 MPa (Hull, 1996).
** interfacial shear stress (τ_i) evaluated by the macroscopic short-beam test used in the present investigation.
# l_{fo} is the optimal fiber length measured according to $l_{fo} \approx 1.2 l_{fc}$ (Wetherhold et al, 1992).

Fiber lengths, which were measured by direct technique, were grouped by both percentage portion (%) (Table 11) and length (mm) (Table 12). Aspect ratios for the fiber groups were also computed (Table 13).

Table 11. Measured fiber lengths (l_f) grouped by percentage values (%).

Grouped by portion (%)					
Batch number	Short fibers with length: 0.1 - 0.3mm	Short fibers with length: 0.4 - 0.7mm	Short fibers with length: 0.8 - 1.0mm	Short fibers with length: 1.1 - 1.5mm	Short fibers with length: 1.6 - 2.0mm
1301232	19.0	54.8	18.2	6.6	1.4
1301252	23.4	48.6	16.8	8.8	2.4
1306101	18.8	54.2	17.6	7.8	1.6
1306262	13.8	51.8	23.4	9.0	2.0
1308261	23.8	49.8	16.0	8.4	2.0
1309191	9.8	58.0	19.2	10.2	2.8
1307082	20.0	48.8	18.2	11.4	1.6
1308292	13.0	46.6	23.0	13.0	4.4
average	**18**	**52**	**19**	**9**	**2**

The length of the short E-glass fibers measured for the millimeter-scale discontinuous-FRC, everX Posterior varied between 0.3 mm and 1.9 mm (average 1.0 mm). Most of them (71%) ranged between 0.4-1.0 mm (with average l_f in this group being 0.7 mm), whereas 11% were between 1.1-1.9 mm (with average l_f being 1.3 mm (9%) and 1.9 mm (2%)). The remaining 18% were 0.3 mm short E-glass fibers (with average l_f in this group being 0.3 mm).

Table 12. Fibers grouped according to their measured fiber length (l_f) (mm).

Grouped by length (mm)					
Batch number	Short fibers with length: 0.1 - 0.3mm	Short fibers with length: 0.4 - 0.7mm	Short fibers with length: 0.8 - 1.0mm	Short fibers with length: 1.1 - 1.5mm	Short fibers with length: 1.6 - 2.0mm
1301232	0.30	0.59	0.92	1.27	1.98
1301252	0.30	0.59	0.92	1.26	1.74
1306101	0.30	0.58	0.92	1.22	1.73
1306262	0.31	0.60	0.93	1.30	1.80
1308261	0.31	0.59	0.93	1.28	1.98
1309191	0.33	0.61	0.94	1.29	1.83
1307082	0.31	0.59	0.95	1.26	2.02
1308292	0.32	0.59	0.93	1.31	1.86
average	**0.3**	**0.6**	**0.9**	**1.3**	**1.9**

The fiber diameter measured in this study was 17 μm. Consequently, the aspect ratio for the shortest short fiber (with length 0.3 mm) is 18 and 112 for the longest short fiber (with length 1.9 mm). Table 13 summarizes the aspect ratio values according to the fiber length (l_f).

Table 13. Average aspect ratio values grouped by the fiber length (l_f).

aspect ratio l/d	Short fiber length range: l_f=0.3 mm	Short fiber length range: l_f=0.4-0.7 mm	Short fiber length range: l_f=0.8-1.0 mm	Short fiber length range: l_f=1.1-1.5 mm	Short fiber length range: l_f=1.6-2.0 mm
average	**18**	**32**	**53**	**76**	**103**

The theoretical critical fiber length was 0.85 mm. On experimental basis, using the result of our AHSS investigation, this value was 1.09 mm. The optimal fiber length was 1.02 mm and 1.31 mm, using theoretical and experimental data respectively. The differences between the types of fiber length measurements (theoretical versus experimental) were not statistically significant ($p>0.05$).

5.7 Matrix related properties of millimeter-scale discontinuous-FRC (Study IV)

Property, which was considered to be influenced by the matrix was the fiber orientation distribution (FOD). The SEM investigation (Figure 14) showed that short fibers were aligned: **a.** parallel to the crack notch, which is along the long

axis of the crack notch (perpendicular to the pressing direction) (white arrows); **b.** normal to the crack notch (red arrows); **c.** transverse (perpendicular) to the long axis of the crack notch (black arrows); and **d.** radial at the crack tip (Figure 15).

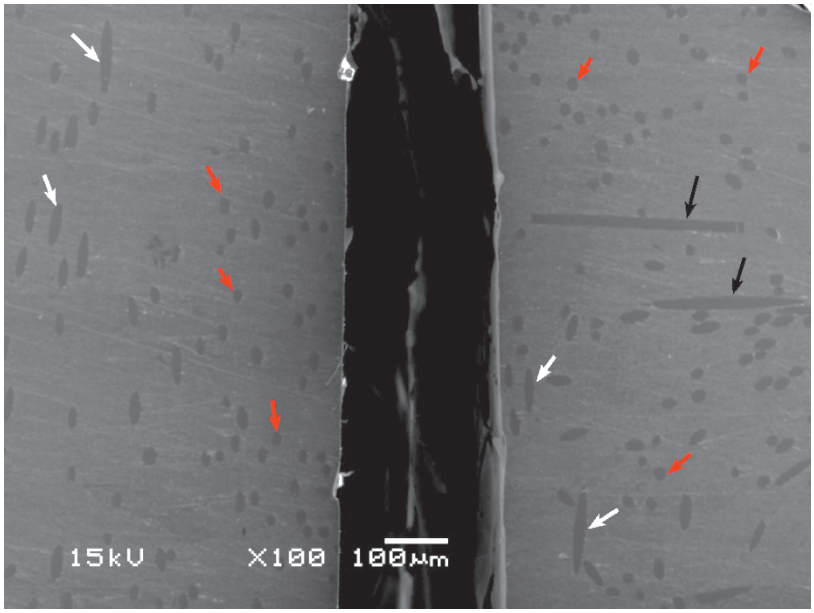

Figure 14. The FOD that was evaluated on tested, unbroken SENB specimen is shown on a SEM micrograph x100. Black arrows indicate transverse, white arrows indicate parallel and red arrows indicate fiber orientation in plane normal to the crack notch.

Radial fiber alignment was observed at the crack notch tip (Figure 15). This orientation was caused by the crossing paths of the discontinuous fibers oriented normally to the crack notch (red arrow) and transversely to the long axis of the crack notch (black arrow).

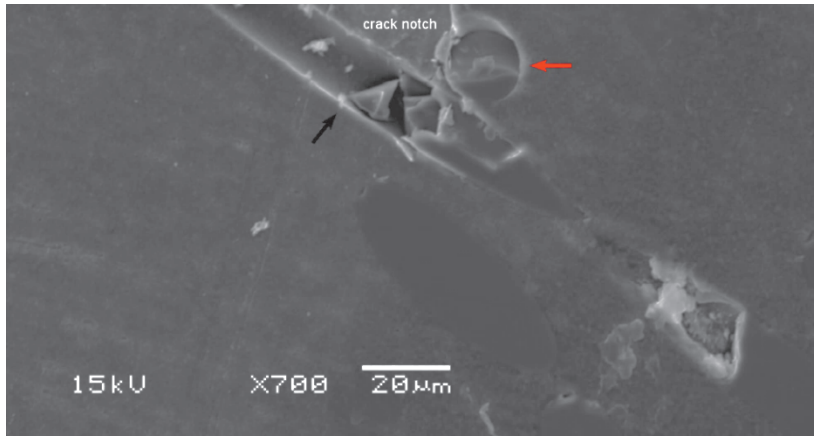

Figure 15. Shown is SEM micrograph x700 of the radial fiber alignment at the crack notch tip. Modified from original publication IV (Bijelic-Donova et al, 2016).

5.8 Fiber toughening mechanisms (Study IV)

Fracture pattern analysis by the SEM method included unbroken tested SENB specimens and fractured specimens. The SEM of the unbroken tested SENB specimens showed fiber bridging, fiber pullout and fiber breakage (Figure 16 and 17).

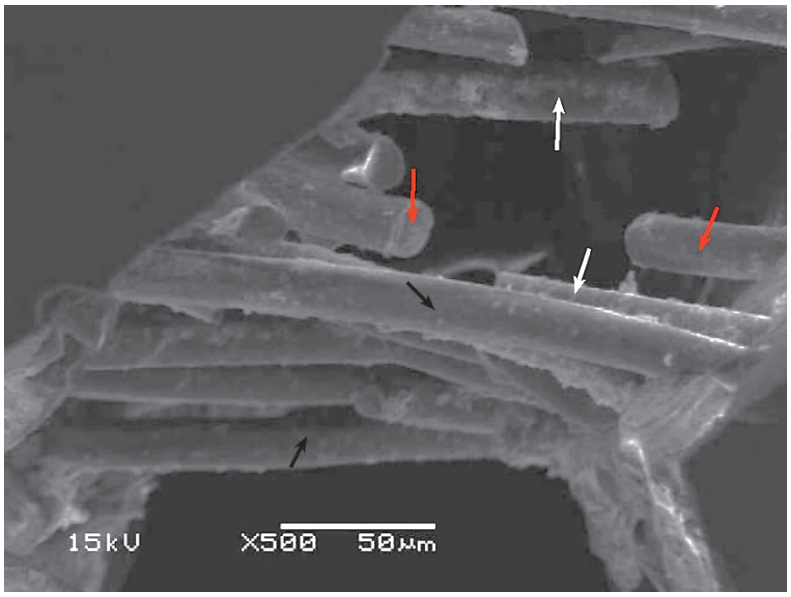

Figure 16. Shown are fiber bridging (black arrows), fiber breakage (red arrows) and fiber pull-out (white arrows) on a SEM micrograph x500.

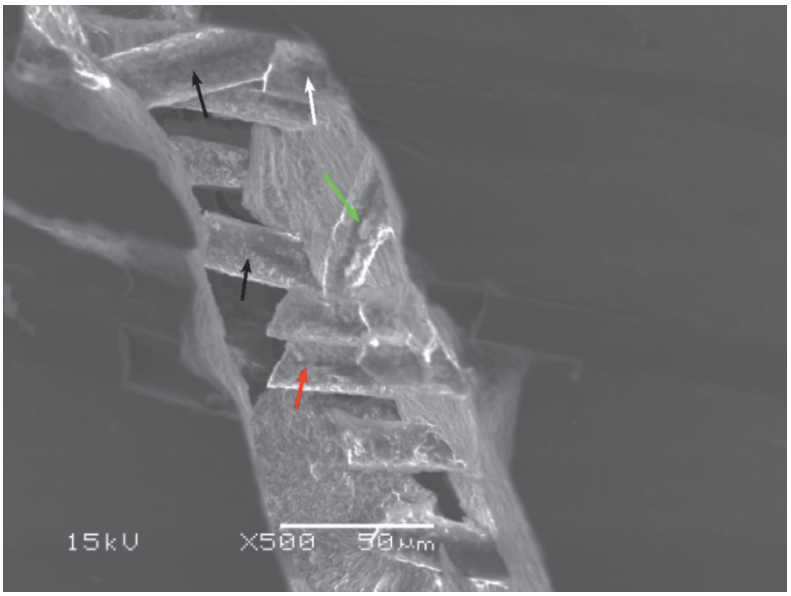

Figure 17. Shown are fiber bridging (black arrows), fiber breakage (red arrows) and fiber pull-out (white arrows) on a SEM micrograph x500. The green arrow represents fiber orientation parallel to the crack notch.

Following testing, millimeter-scale discontinuous-FRC specimens were not detached. Thus, in order to analyze the fractured surface, three specimens were manually fractured following the testing. The SEM analysis of the fractured SENB specimens (Figure 18) showed protruding fiber ends, which were covered with a thin layer of resin or, alternatively, resin clusters around the fibers ends were observed.

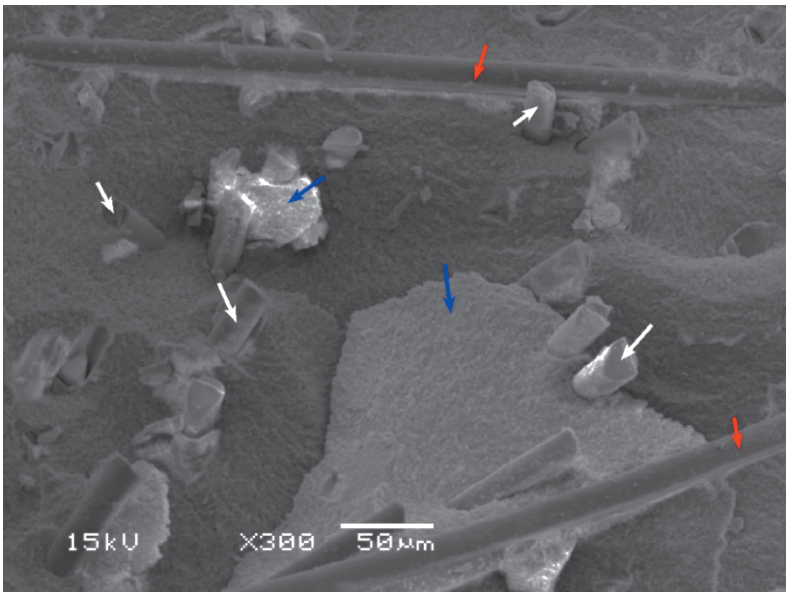

Figure 18. Shown on a SEM micrograph x300 are protruding fiber ends (white arrows). Red arrow represents fiber orientation in a plane normal to the crack notch. Resin clusters are also observed (blue arrows).

Typical load-deflection curves of the tested SENB specimens for all investigated materials are presented in Figure 19. For the millimeter-scale discontinuous-FRC, multiple cracking of the matrix occurred in the inelastic range, which is the portion between the first cracking and the peak. The brittle matrix of the conventional PFCs cracked at the first peak. This was followed by composite fracture.

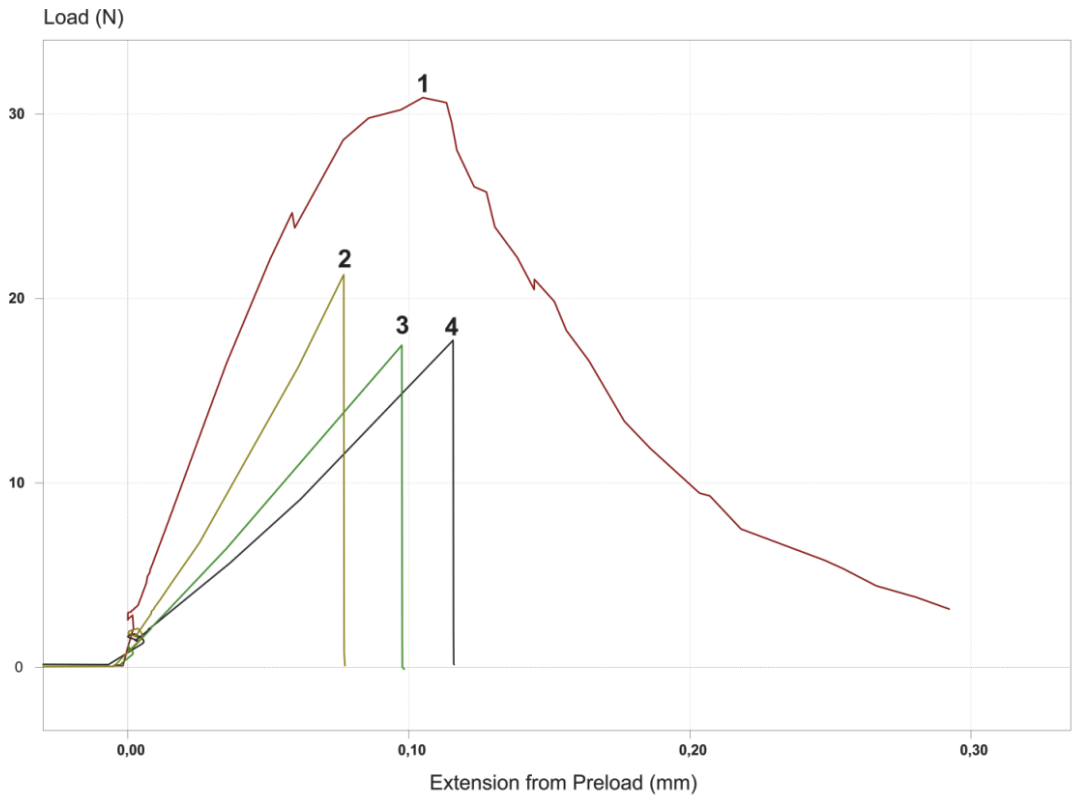

Figure 19. Presented are the load-deflection curves (SENB specimens) of the materials investigated in Study IV. 1: everX Posterior; 2: Supreme XTE; 3: G-ænial Anterior; and 4: Filtek Bulk Fill. Modified from original publication IV (Bijelic-Donova et al, 2016).

6. DISCUSSION

6.1 Discussion of the studies I - IV

This thesis is based on *in vitro* investigations and aimed to investigate the reinforcing properties of a millimeter-scale discontinuous-FRC in terms of fracture resistance and failure pattern as well as describe some bonding characteristics and physicomechanical properties of the material. Both fiber- and matrix related properties were also investigated.

Earlier developed low aspect ratio dental discontinuous-FRCs *i.e.* micrometer-scale discontinuous-FRCs (Table 2) were unsuccessful in improving the strength and the fracture toughness of the material they reinforced (van Dijken et al, 2006). Currently investigated high aspect ratio (millimeter-scale) discontinuous-FRC has two detrimental differences compared to low aspect ratio discontinuous-FRCs. First, it contains millimeter-scale discontinuous fibers, which are above the critical fiber length (Garoushi et al, 2007a; Garoushi et al, 2013b; Lassila et al, 2016), and second, the fibers are embedded into a multiphase polymer matrix (Garoushi et al, 2007a). This matrix type contains Bis-GMA based dimethacrylate monomer (cross-linked, thermoset) and PMMA linear polymer (thermoplastic). Each fiber is a silane treated E-glass type and upon polymerization, the composite blend forms a semi-IPN polymer matrix structure (Garoushi et al, 2007a). However, the semi-IPN concept is not a new development. In early 2001, preimpregnated silane treated E-glass fibers with a polymer-monomer gel were developed for some uni- and bidirectional E-glass fiber reinforcements (Vallittu, 2001). Since then, they have been used in many dental applications, one of them being root canal posts. Indeed, the semi-IPN polymer matrix based E-glass fibers have enabled the concept of individually constructed FRC posts (Le Bell-Rönnlöf, 2007; Le Bell-Rönnlöf et al, 2011). In its row form, the preimpregnated fiber bundle is non-prepolymerized, thus it is soft and easy to adjust to the anatomical shape of the root canal space. It hardens upon polymerization *in situ* in the canal, which allows the post to maintain the shape of the root canal. By contrast, the use of a prefabricated FRC post necessitates preparation of the root canal according to the post shape. This is accompanied with removal of excessive tooth tissue (radicular dentin). In other words, the canal must be designed to allow the post-space to receive the prefabricated post, whereas the individually formed FRC post is designed to fit the root canal, which consequently preserves tooth substance. Owing to this, semi-IPN polymer matrix based

individually formed FRC posts are a tissue preserving technique for restoring ETT. Preservation of the tooth structure is important because it influences the fracture resistance of the restored tooth (Schwartz et al, 2004; Torbjörner, 2013). In addition to easy handling and non-invasive post-space preparation, the semi-IPN polymer matrix based individually formed FRC posts also possess other advantages over prefabricated FRC posts. These are: 1. bonding of the post to the resin luting cement and to directly or indirectly made veneering composite (Vallittu, 2001); 2. the possibility to fill the whole post space with one or more fiber bundles (Le Bell-Rönnlöf et al, 2011); 3. the possibility to place posts out of the neutral axis of the tooth (Le Bell-Rönnlöf et al, 2011); 4. the possibility to curve the fibers to the preferred angle and to fill the coronal opening of the root canal with fibers, in order to provide more reinforcement to the cervical part (Le Bell, 2003; Le Bell-Rönnlöf et al, 2011); 5. preservation of dentin (Le Bell-Rönnlöf, 2007) and 6. reducing cement thickness (Le Bell-Rönnlöf, 2007).

Common for the individually formed FRC post and the millimeter-scale discontinuous-FRC are the matrix and the fiber type. The fiber architecture for both structures are different however; unidirectional versus discontinuous, respectively. Due to the identical composition, the materials are assumed to make a homogenous unit when used together. Consequently, **Study I** was designed to evaluate the combination of both materials in reinforcing structurally compromised anterior teeth. A few earlier findings were born in mind during the design of the first study and deciding the teeth selection.

Although the remaining coronal structure plays a significant role in selecting the restorative therapeutic choice, the post reinforcement for posterior teeth in many cases is not necessary because the pulp chamber in posterior teeth is adequately wide and deep enough (depth) to provide retention and strength (Schwartz et al, 2004). Anterior teeth, on the other hand, have an unfavorable height to width ratio; they are much longer than they are thick, and consequently, their pulp chamber does not provide retention or strength because it cannot be filled with large amounts of PFC (Schwartz et al, 2004; Le Bell-Rönnlöf, 2007). This becomes especially important in the cases when an anterior tooth is structurally compromised. In these cases the ratio of the clinical crown versus the root diameter should be considered (Le Bell-Rönnlöf, 2007). The same length to width ratio issue stands for premolars. Consequently, if anterior teeth (central and lateral incisors, and canines) and premolars are structurally compromised, post reinforcement should be

considered (Schwartz et al, 2004; Le Bell-Rönnlöf, 2007). Based on this, anterior teeth were selected in study I.

A direct restorative technique was used to restore the compromised teeth, with one third of the coronal dentin being preserved. This clinical scenario was designed because, despite the severe tooth loss, it still allows for direct restoration (Torbjörner, 2013). Fiber posts have been shown to concentrate less stresses in the cervical crown area compared to other types of posts (Garbin et al, 2010). In addition, semi-IPN E-glass fiber posts have demonstrated a similar elastic modulus to dentin (16 GPa versus 17 GPa, respectively) (Lassila et al, 2004; Le Bell-Rönnlöf, 2007). This was an additional rationale for using semi-IPN polymer based E-glass fiber posts in study I. Both non-reinforced and reinforced teeth were used and the worst case scenario was designed. Namely, the fiber bundle was placed at the middle of the root and a flat dentin surface was provided. However, leaving one third of the coronal structure does not necessitate ferrule preparation, as the remaining coronal tooth structure cervically, itself, acts as a ferrule. Thus, the fiber bundle was not cervically curved and the post was inserted with aim of providing retention. The need for the post was confirmed by the results of the control groups without post insertion, where most teeth fractured catastrophically.

Results showed that structurally compromised anterior teeth could benefit from both individually formed FRC- and millimeter-scale discontinuous-FRC posts, because the remaining tooth structure of non-reinforced teeth could not provide retention and durable restoration without posts. The non-reinforced teeth restored with millimeter-scale discontinuous-FRC provided the highest resistance to fracture, but also resulted in the highest occurrence of unfavorable fractures. This could mean that the strength of the material surpassed the strength of the remaining tooth structure. However, root fractures are not desired and post placement could be beneficial in avoiding them. Individually formed FRC posts with millimeter-scale discontinuous-FRC-core-crowns provided as good a reinforcement as the millimeter-scale discontinuous-FRC-post-core-crown structures, but the latter ones resulted in less unfavorable (root) fractures (50% and 37% respectively). Clinically this means that in most cases the millimeter-scale discontinuous-FRC restoration will favor a repair of the fractured fragments. The fracture pattern analysis suggests that millimeter-scale discontinuous-FRC reinforcement in the cervical part of the tooth could have attained a ferrule effect. A drawback of this study is that millimeter-scale discontinuous-FRC reinforced teeth were not veneered with PFC. This has downsides with regards to aesthetics, polishability,

bacterial adhesion and water sorption. Non-veneered discontinuous-FRC reinforced restorations are not suitable for clinical purposes and this poses drawback for study I. In addition, vital teeth were not included for comparison, which is also a limitation of Study I.

An incremental layering technique is normally used when directly restoring large cavities. Each increment is approximately 2 mm thick and independently cured before layering the subsequent composite layer. Void incorporation and bonding failures are some concerns related to this technique. Restoration of large cavities or ETT would necessitate placing the millimeter-scale discontinuous-FRC in several layers. Thus, **study II** was designed to evaluate the bonding properties of incrementally placed layers of millimeter-scale discontinuous-FRC and to compare it with the bonding properties of dimethacrylate- and silorane-based PFCs placed incrementally.

Oxygen inhibition is a clinically relevant subject with no obvious consensus on its effect on the interlayer adhesion. It has been suggested that the air inhibition layer functions as an adhesive layer that bonds two incrementally cured layers of composite resin with the aid of the monomer (initiator) diffusing from an overlaying composite layer (Li, 1997). Therefore, it is considered as necessary in improving the bond strength of the layered composite increments (Li, 1997; Truffier-Boutry et al, 2003; Kim et al, 2006). Conversely, it has been reported that the presence of an air inhibition layer causes inefficient interfacial curing (Eliades et al, 1989) and is not required for the initial bonding to the composite resin (Eliades et al, 1989; Shawkat et al, 2009). In order to study the OIL effect on the bonding properties of the millimeter-scale discontinuous-FRC, groups with present, treated and absent OIL were designed. The thickness of the OIL was also assessed.

The OIL was observed on the surfaces of all investigated composites, including the silorane-based composite. The thickest OIL layer, however, was measured on the surface of the millimeter-scale discontinuous-FRC. The differences in the composition, particularly in the resin matrix types, among the composite materials should be emphasized when analyzing the findings. The resin matrix types of the composite materials used in Study II could be classified into dimethacrylate and silorane-based. The latter one is an epoxy type of matrix. Dissimilar resin matrices have different initiator systems and undergo different polymerization reactions. Silorane composite contains, however, CQ (camphorquinone) as a photoinitiator (Weinmann et al, 2005) which, at the initial phase of the otherwise cationic reaction, generates radicals (Crivello,

2009; Bowen, 1956). These can explain the OIL measured on the surface of the silorane composite, which agrees with an earlier finding (Shawkat et al, 2009).

With regards to the interlayer connection of the millimeter-scale discontinuous-FRC, it should be noted that when bonding a new resin to millimeter-scale discontinuous-FRC, the substrates are the fibers, linear polymer (thermoplastic) matrix and the dimethacrylate (cross-linked) matrix. Several mechanisms are responsible for the interlayer connection. Matrix mediated bonding mechanism is the adhesion owned to its semi-IPN structure, which presumably could be enhanced by the OIL, because the unreacted radicals from the cured layer could bond covalently to the newly applied composite layer (Lastumäki et al, 2003). Fiber related bonding mechanisms are silanization and mechanical interlocking (Vallittu, 2001; Lastumäki et al, 2003; Vallittu, 2009). Silanization based adhesion is possible because E-glass fibers are silane treated with methacrylate silane (Lastumäki et al, 2003), which bond with one end (silanol group) to the hydroxyl groups (-OH) on the fiber surface and with the other end (organofunctional group) to the double bonds of the matrix monomers of the newly applied composite layer. Furthermore, surface exposed fibers make the surface texture rough. At the same time, they enlarge the surface area and consequently the bonding surface area. In addition, the areas between the exposed, protruding fibers is gap-like and promotes the interlocking mechanism of interlayer bonding between two successive composite layers. Moreover, mechanical interlocking mechanism at the nanometer level, between the adhesive or composite layer and the semi-IPN matrix composite resin, is provided by the semi-IPN itself, owing to the presence of the two polymer networks (linear and cross-linked) (Vallittu, 2009).

With regards to the interlayer connection of the dimethacrylate-base PFCs, it should be born in mind that dimethacrylates are cross-linked types of resins (thermoset), which basically bond purely based via OIL. This is because thermoset resins are not dissolvable (Lastumäki et al, 2003; Vallittu, 2009; Wolff et al, 2012). This was evident in the groups with a removed OIL, where a significant reduction of the bond strength was observed.

Consequently, the findings of study II suggests that the OIL layer should be provided, left intact and uncontaminated on the surface of the freshly cured composite layer. This finding is in agreement with other studies (Li, 1997; Truffier-Boutry et al, 2003; Kim et al, 2006). The occurrence of mainly cohesive failures with the millimeter-scale discontinuous-FRC with grinded (removed)

OIL suggests that the semi-IPN matrix type and exposed, protruding fibers could be advantageous not only for bonding indirectly fabricated structures and cementing individually formed FRC-posts, but also for adherence of a freshly applied composite layer. In other words, the presence of semi-IPN matrix based millimeter-scale discontinuous E-glass fibers were responsible for durable adhesion even though the OIL was completely removed. Somehow similar findings were shown in an earlier study, where it was found that the semi-IPN structure allowed deeper interdiffusion of the resin when the OIL was removed from the surface of the pre-impregnated fiber surface (Wolff et al, 2012).

One concern with using discontinuous-FRCs, in general, is the generation of voids, which can be either due to the manufacturing process, when for example fiber-free and matrix-rich regions might be produced, or during clinical manipulation of the composite, when for example placing it into a cavity (if not handled with care or not packed properly). Woven semi-IPN fibers have been shown to favor oxygen passage (Vallittu PK, 1997), but this is unlikely for the millimeter-scale discontinuous-FRC because further impregnation of the short fibers, as in the study of Vallittu (Vallittu PK, 1997), is not required. The voids, however, act as oxygen reservoirs (Vallittu PK, 1995) and any generation of voids must be avoided. Voids and interlayer failures are possible with the incremental technique, and therefore, composite materials should be handled with care as internal flaws (pores, voids, bubbles) have deleterious effects not only due to trapped oxygen, but also because they reduce the inherent fracture resistance of the material.

As mentioned previously, the millimeter-scale discontinuous-FRC is attempted to be veneered with the PFC protecting layer, in order to improve esthetic appearance, polishability, wear resistance, bacterial adhesion and water sorption. Thus, evaluation of the interlayer connection between millimeter-scale discontinuous-FRC and dimethacrylate-based PFC is important. The lack of this evaluation is a main limitation of study II. In addition, removal of OIL by sandblasting as used in some other studies (Wolff et al, 2012; Frese et al, 2014) was not conducted.

Evaluation of the mechanical properties that reveals the fracture properties and the fatigue sensitivity of the materials is important in order to learn what causes the material to fail. Understanding the mechanical performance of the material requires a series of *in vitro* tests, with the aim of revealing the factors that control the material's behavior. Thus, in **Study III** various physicomechanical

properties of the millimeter-scale discontinuous-FRC were investigated. The material in the oral cavity, however, fails due to fatigue loading, which is a slow and repetitive type of cycling loading. Nevertheless, most *in vitro* studies employ a static type of test (Behr et al, 2003a; Behr et al, 2005; Dyer et al, 2004; Dyer et al, 2005; Garoushi et al, 2006a; Le Bell-Rönnlöf et al, 2011). The static test is easier to conduct and is less time consuming than the fatigue type of test. In contrast to the cycling loading during fatigue, the static type of load induces linear, compressive types of loads, and is important in order to gain basic knowledge of the fracture behavior of a material. Consequently, the importance of the correlation between the two types of tests becomes obvious; a strong correlation would reveal if the fatigue performance of a material could be predicted based on its static strength values. This was evaluated in **Study III**, which in addition aimed to examine the correlation between various parameters evaluated with mechanical tests according to ISO standards and the fatigue of the composite material in simulated service (anterior crown restoration).

From a mechanical point of view, an anterior tooth behaves like a beam specimen, which is fixed only at one side during function (Garbin et al, 2010). Typical loading is at a 45 degree angle to the palatal side, which mimics the natural contact of the opposing tooth (de Castro Albuquerque et al, 2003). Based on this and with aim of obtaining as strong correlation as possible among the tested parameters, direct anterior crown restorations were selected to present the clinical scenario. Restorations were tested at 45 degree angles to the palatal side, as in study I. The results showed that the material type and the type of the applied fracture load affected the fracture resistance of the direct anterior crown restorations; the millimeter-scale discontinuous-FRC presented significantly higher fracture resistance in both static and fatigue loads. Direct crown restorations made of this fibrous material did not fracture instantly at final fracture load, but instead initial cracks were observed in the load-deflection curve. In this study, the post-fatigue strength (PF) remained below the static strength of the direct crown restorations (IF, FF in Figure 12) and might suggest that the fatigue process initiates degradation, but higher loads are required to cause the material to fail. This is supported by the fact that, regardless of the material type, the number of direct crown restorations that did survive the cycle life was higher than the number of failed ones (60% and 55% survived versus 40% and 45% failed PFC and millimeter-scale discontinuous-FRC crown restorations, respectively). The ratio between the fatigue limit and the static load was 0.3±0.03. This suggests that the endurance limit, on average, allows 30% tolerance, or in other words, a rise of the fatigue

limit by an amplitude of 30% will lead to failure at levels lower than the preassigned cycle life.

The strength of the millimeter-scale discontinuous-FRC decreased by 5% due to fatigue cycling, which is less than the PFC's strength loss of 11%. This finding reinforced earlier findings that the endurance loss better reveals the fatigue resistance of the material than the fatigue test itself (Manhart et al, 2000; Lohbauer et al, 2003). This was supported by the fracture pattern analysis, which showed a ductile fracture for the millimeter-scale discontinuous-FRC crown restorations and a brittle fracture for the PFC crown restorations (Figure 13). The brittleness of the PFC was also evident in its higher flexural modulus. A material with a higher flexural modulus might suffer more from tensile stresses than a material with lower modulus and might not be able to withstand repetitive impact forces (Braem et al, 1994). This could explain the inferior fatigue sensitivity of the PFC used in study III, manifested in the statistically insignificant differences between the initial, final and post-fatigue failure loads (Figure 12). The possibility of using the flexural modulus (Braem et al, 1994; Belli et al, 2014) or the fracture toughness (Goldman et al, 1985; Belli et al, 2014) as predictors for the material's fatigue sensitivity has been presented earlier. There is a critical filler level for both, fracture toughness and fatigue. Indeed, after surpassing the sufficient filler fraction, the effect of the filler content on the fracture toughness is negligible (Illie et al, 2012) and weak (Belli et al, 2014) or even has the opposite effect on the fatigue resistance (Htang et al, 1995). Beyond a certain level of filler content, increased filler level will not improve the fatigue resistance (Htang et al, 1995). The present study showed a strong correlation between the fracture toughness and the fatigue performance for both material types. This finding supports the suggestion made by Tyas to use the fracture toughness value as an indicator for predicting the clinical performance of the resin composites (Tyas, 1990), but contradicts the result reported by Belli, most likely due to the different methodology (4-point bending test) employed in that study (Belli et al, 2014). The existence of a strong correlation between the static and fatigue results indicates that the static load bearing capacity values can be used to predict the fatigue endurance of a material.

The millimeter-scale discontinuous-FRC demonstrated enhanced resistance capabilities to crack propagation (fracture toughness) and flexural strength, which could be explained by the fiber and matrix related properties of the material. Fibers in this fibrous composite material are longer than the critical fiber length (Garoushi et al, 2013b; Abouelleil et al, 2015; Lassila et al, 2016)

and thus, could efficiently accept the stress transferred from the matrix. The matrix type, as discussed earlier, is a semi-IPN type; the presence of thermoplastic PMMA chains reduces the stiffness of the cross-linked monomer (Bis-GMA). These characteristics might have improved the flexural properties (elasticity) of the material and its resistance to fracture propagation as well as reduce the stress distribution at the matrix-fiber interface. Our finding is in accordance with previous literature findings (Garoushi et al, 2013b; Goracci et al, 2014; Leprince et al, 2014; Abouelleil et al, 2015; Lassila et al, 2016).

The anterior crown restorations in this study were prepared and tested on a zirconia model, which might have influenced the forces endured by the restorations. This is thus a limitation of study III.

Study IV was designed in order to gain a better understanding of the properties of the millimeter-scale discontinuous-FRC and to analyze its structural characteristics. Because most mechanical properties depend on the specimen diameter, the same sized specimens were used here as in study III. The aim was to compare the physicomechanical properties after aging the material.

Short-term water storage induced deterioration of the mechanical properties irrespective of the material type. An exception was the work of fracture. Possible mechanisms for the degradative water effect are hydrolysis of the bonds between the matrix and the particulate filler, or the matrix and the fiber filler; hydrolysis of the polysiloxane bonds occurs in both PFCs and millimeter-scale discontinuous FRC (Söderholm et al, 1984; Ferracane et al, 1998; Söderholm et al, 1990; Vallittu 1995; Vallittu 1998; Miettinen 1999; Curtis et al, 2008). However, water also induces plasticization of the resin matrix, which could provide a toughening effect (Ferracane et al, 1998; Takeshige et al, 2007). Increased plasticity allows for longer bending of the specimens before fracture and a larger surface area under the load-deflection curve until the final fracture. This is crucially important for the work-of-fracture outcome, because the total area under the load-deflection curve is used in Wf calculations. This could explain the increased ability of the water stored materials to sustain crack propagation. The fracture work was especially substantially enhanced for the millimeter-scale discontinuous-FRC, which, in addition to the water related plasticization, could be owned to the semi-IPN matrix, particularly to its linear phase which improves plasticity, and to the elastic fibers properties. Namely, the elastic recovery of the fiber can be seen in its ability to bend, without fracture, and to return to its original dimensions once the tensile load is

relieved (Murphy, 1998). This allows the fiber to accumulate and release large amounts of energy, and was evident in the values for fracture work in study IV. Although, the work of fracture could be mainly controlled by the matrix properties, for the millimeter-scale discontinuous-FRC, the fibers obviously accompany this by accumulating energy.

The AHSS methodology has given rise to debate due to its sensitivity and complexity. Indeed, the short-beam test methodology is very sensitive and depends on the specimen thickness and test type (3- or 4- point bending type of test). The type of fracture pattern is important for the AHSS because the interface horizontal failure is difficult to obtain. It has been suggested that the initial damage in the form of a vertical crack must be present to allow accurate and exact propagation of the crack, and induce horizontal failure. In contrast, compressive buckling or a combination of shear and compression failures result (Whitney et al, 1985). The analysis of the stress-strain and load-deflection curves in study IV shows that there was initial damage before the final damage for the millimeter-scale discontinuous-FRC only. This suggests that the short-beam test most likely measured the AHSS properly. However, this was not the case for the other materials that were investigated, indicating that their results have to be taken with reservation. The results of the AHSS in study IV are supported by the literature (Lee, 1993; McDonough et al, 2001). However, the pull-out type of test, which measures the shear stresses caused by friction along the fiber length while it is being pulled out of the matrix, could have provided a more reliable value for the interfacial shear stresses. The fact that this was not conducted is one limitation of study IV.

The load-deflection and stress-strain curve analysis revealed some properties related to the fracture toughness, fracture work (Study IV) and fracture resistance (Study I). Typical for any FRC structure is that the forces cause a matrix to crack before the fiber fractures (Lee, 1993). Upon initiation of the first crack in the matrix, three modes of failure with FRC structures are possible: 1. immediate; 2. peak-concentrated and 3. postpeak-wise (Lee, 1993), also known as instantaneous, stepwise and statistical, respectively (Dyer et al, 2004; Dyer et al, 2005). An immediate failure will occur instantly at the first matrix crack and is typical for brittle FRCs. Peak-concentrated and postpeak-wise failures are common for ductile FRCs. In ductile FRCs, the composite continues to carry the load after the peak has occurred (matrix cracked). This is possible owing to the fibers, which improve the fracture resistance after the first peak, either by pulling-out (peakwise failure) or fiber debonding and fiber-matrix sliding (postpeak-wise failure). These events require more load for the

failure to progress, indicating increased resistance to fracture propagation, though the strength of the composite does not increase. Phenomena such as fiber pull-out, debonding or fiber-matrix sliding depend on factors such as interfacial matrix-fiber strength, the number of crack-bridging fibers, fiber diameter and length (l/d ratio) and fiber quantity (Lee, 1993). In study IV, the postpeak-wise type of load-deflection curve was observed. This was found earlier for various fiber architectures (Dyer et al, 2004; Dyer et al, 2005). In study I the matrix showed small recovering fractures, most likely because of the still intact fibers at those stages, which could also be recognized as a postpeak-wise curve type. This finding agrees with previous findings (Kim et al, 2004). The stress-strain curve analysis from Study I and the load-deflection curve analysis from Study IV show first, that discontinuous-fiber reinforcement abated instantaneous fractures and unfavorable failures, because specimens in Study IV remained in one piece, while the restorations in Study I fractured in a restorable manner (63%). Second, it also suggests that incorporation of millimeter-scale discontinuous fibers increases the resistance to crack propagation (Study IV) and to fracture (Study I). This is supported by the work of fracture values, which were significantly improved for the millimeter-scale discontinuous-FRC. As the fracture work describes the ability of a material to withstand a propagating crack, together with the fracture toughness, they specify the ability of the material to resist fractures.

Fiber- and resin matrix related properties were evaluated in an attempt to explain the observed properties for the millimeter-scale discontinuous-FRC. Mechanical properties of FRC structures are dependent on the volume fraction of the fibers embedded in the resin matrix. Therefore, it was first decided to present the fiber amount in volume fraction. Next, other fiber-related properties were also determined, as it is known that they define the properties of reinforced systems (Wetherhold et al, 1992; Lee, 1993; Vallittu, 2015). Fiber length is essentially important because in order to resist the debonding from the matrix during tension, the fiber length must be equal to or longer than the theoretical critical fiber length (Lee 1993; Hull et al, 1996; Harris, 1999; Callister, 2011; Vallittu, 2015). Nevertheless, the length of the fibers that exceed the critical fiber length is important not only for the fiber debonding effect, but also for their orientation. The fiber length - fiber orientation interaction has been observed in the greater debonding of the aligned rather than randomly orientated discontinuous fibers that undergo only limited debonding. This results in an improved load bearing capacity of the discontinuous-FRCs with randomly distributed fibers compared to aligned discontinuous-FRCs (Brighenti et al, 2012). Fiber breakage could occur,

however, if the fiber length exceeds the optimal fiber length (Wetherhold et al, 1992). Less than half (30%) of the short fibers in the millimeter-scale discontinuous-FRC were equal to or above the theoretical critical fiber length and a great portion (52%) were between 0.4 mm and 0.7 mm (Tables 10-12). Mechanical testing (Table 9), the fiber properties characterization (Table 10-12) and the SEM analysis (Figure 14-18) suggest that 1. longer discontinuous fibers (30%) would enable bridging; 2. short discontinuous fibers (18%) would behave as particulate fillers instead of fiber fillers; 3. some of the discontinuous fibers in the middle range will provide toughening by pull–out mechanisms (0.4 – 0.5 mm) and the longer ones in this range (0.6 mm – 0.7 mm) would actively carry the loading; and 4. a small portion (6%) of the fibers exceeding the optimal fiber length could break or then behave as continuous fibers. A recent study revealed, however, that dual fiber length distribution might contribute to the toughening effect and enhance the properties of discontinuous-FRCs (Lassila et al, 2016). Presumably, a similar mechanism of toughening is possible for the millimeter-scale discontinuous-FRC investigated here due to the gradual fiber length; the fibers with 0.1-0.3 mm lengths could provide isotropic reinforcement, and the longer fibers iso- or anisotropic reinforcement depending on their packing and orientation. In study IV, however, different toughening mechanisms were considered to operate simultaneously, since for example the stretching fibers would bring crack edges closer and enable the crack bridging phenomenon even for the shorter fibers (0.4-0.7 mm range). This could blunt the crack, which is initially sharp and thus, decrease its sensitivity. As a result, the crack propagation is retarded or arrested.

Furthermore, the SEM analysis of the fractured SENB specimens (Figure 18) showed pulled out and protruding fiber ends. The protruded fibers ends were covered with resin, which indicated a well-bonded system. In addition, the pulled out fibers were observed to have various lengths (Figure 16-17) possibly because of the different initial lengths (0.4-0.7 mm range). The reinforcing effects could be thus summarized to be the stretching and deflecting ability of the fibers, the bridging phenomenon (Figure 16-17), which is the ability to resist the opening and propagation of the crack by inducing a closure force on the crack, and crack blunting (Figure 15), which is the ability to reduce the stress intensity at the crack tip. The latter one was observed in the FOD SEM analysis, where the paths of the transversally and normally orientated fibers were seen to cross each other. This was named as X-orientation. The findings of this study are supported by previous literature findings (Jain et al, 1992; Wetherhold et al, 1992). The FOD was considered to be a matrix related property, because the orientation of the short fibers is dependent on the

packing of the composite and the viscosity of the matrix, which determine the flow of the fibers and hence the orientation. The FOD SEM analysis in this study was conducted on longitudinally sectioned SENB specimens. This is a two-dimensional imaging method, that itself has limitations and thus, is a limitation of study IV. Providing sections of orthogonal planes could offer a solution (Lee, 1993), although this technique too would also be two-dimensional. The fiber orientation in various dental cavities prepared on teeth, approximal box and mesial-occlusal-distal (MOD) cavity, would provide useful information on how the packing of the millimetre-scale discontinuous-FRC into a cavity would affect the FOD (random or in one plane *i.e.* transverse). The lack of this is the third limitation of study IV.

6.2 Bio-inspired FRC architectures

Natural intact teeth are biological composites composed of structural materials that generate their stiffness, strength, resilience and toughness. This balanced unit of biological structures has motivated researchers to seek for bio-inspired materials and techniques that mimic their nature (Mirkhalaf et al, 2013). Bio-inspired materials are man-made materials, which synthesis has been inspired by biological materials (Mirkhalaf et al, 2013). The biomimetic in restorative dentistry has been defined as the *"study of the structure, function, and biology of the tooth organ as a model for the design and engineering of materials, techniques, and equipment to restore or replace teeth"* (Magne, 2012a). The nature of the biological, highly mineralized tooth structure could be mimicked in at least four aspects: biomechanically (covering structural aspects in terms of composition structure, and functional aspects), structurally in terms of preservation of tooth tissue, biologically and esthetically. Biomechanically restorative materials could be divided into dentin-like, which are the composite materials, and enamel-like which are the ceramic materials (Magne, 2006). Moreover, in order to biomechanically mimic the natural tooth, various biomimetic techniques combining FRC substructure with composite material (Fennis et al, 2005; Magne et al, 2012b) or composite material overlaid with ceramic (Magne, 2006) have been employed. Results of various studies imply that these biomechanical biomimetic appliances with bidirectional-FRC does not provide satisfactory reinforcement, even though the FRC is pretreated or its inner surface is protected by a layer of composite (Behr et al, 2003a; Behr et al, 2003b; Magne et al, 2012b). To overcome the insufficient strengthening, recent studies have employed multilayered bidirectional-FRC reinforcement for single crowns by placing four or six layers of cross-linked net fibers, or by

molding them anatomically (Monaco et al, 2015; Monaco et al, 2016). The authors reported that the strength of these FRC structures depend on the number of fiber layers, and that multiple layers of bidirectional-FRC favorably distributes stresses, deflect cracks, prevent fractures in cervical direction and facilitate reparation (Fennis et al, 2005; Monaco et al, 2016). The anatomical shape resulted in the best fracture resistance, but the authors find it difficult to maintain FRC structure margins away from the cavity margins (preparation line), which led to poor marginal adaptation (Monaco et al, 2015). One of the reasons for the poor performance of the earlier biomechanical biomimetic restorations (Behr et al, 2003a; Behr et al, 2003b; Magne et al, 2012b) could be the cross-linked nature of their resin matrices.

The studies in the present thesis revealed that the semi-IPN based millimeter-scale discontinuous-FRC showed toughness values much closer to dentin than the other conventional composite materials (Tables 1 and 3). In addition, it showed microstructural characteristics similar to dentin (Study IV; Schematic Figure 2). The use of this fibrous material in combination with indirect composite materials to structurally mimic the tooth has been recently presented, but resulted in poor mechanical performance due to the thick overlay restoration (Rocca et al, 2015). Based on the investigations in the current thesis, however, durable biomechanical biomimetic restorations with the millimeter-scale discontinuous-FRC are possible. In order to achieve this, the fibrous microstructurally dentin-like material should be placed anatomically, in increments, to substitute all lost dentin tissue, whereas the thickness of the overlaying material should be equal to the enamel thickness. Practically, this means that the millimeter-scale discontinuous-FRC should be used as a reinforcing base, covered with 1.5 – 2 mm of PFC layer. Veneering material placement is important in order to achieve wear resistance and polishability, to avoid a water/saliva exposure and contamination of the fibers, and to improve the aesthetic appearance of the final restoration. This combination of millimeter-scale discontinuous-FRC and PFC forms a bilayered structure that is biomechanically biomimetic, due to the microstructural dentin-like architecture and dentin-like toughness. The bilayered structure is schematically presented in Figure 2. The advantage of this structure is that the randomly orientated discontinuous fibers are protruding at the interface side, consequently allowing the micromechanical interlocking of the composite layers and thus, reinforcing the interface of the bilayered restoration.

If, however, the cavity is large, as after MOD amalgam restoration removal or extensive Class II restoration, semi-direct or indirect techniques could be

considered in order to overcome the sensitivity of the direct technique, improve the layering, compensate the polymerization shrinkage and obtain strong proximal contacts. In this aspect as well, the millimeter-scale discontinuous-FRC possesses advantages over thermoset composite materials owing to the semi-IPN structure. The linear phase (PMMA) of the semi-IPN structure can be dissolved with monomers that have solubility parameters close to it. Examples of those would be monomer solutions containing HEMA or MMA in combination with high molecular weight dimethacrylates (Vallittu, 2001; Wolff et al, 2012). The new resin swells and diffuses into the “old” non-cross-linked (linear) polymer matrix. Upon polymerization of the newly applied material, an adhesive type of bond, namely the secondary-IPN is established (Le Bell-Rönnlöf, 2007; Vallittu, 2001; Vallittu, 2009). Mechanical bonding by means of interlocking is possible too, due to the protruding fibers. Consequently, owing to the semi-IPN promoted secondary IPN and the mechanical interlock, reliable prostho-restodontic and resto-endodontic solutions could well become a therapeutic option, with the goal of preserving maximum sound tooth tissue. This would fulfill the requirements of the structural biomimetic aspect, in terms of preservation of tooth structure.

6.3 Clinical considerations and future perspective

Methods of reactivating the millimeter-scale discontinuous-FRC base surface before cementation of an indirect overlay or before repairmen could include surface grinding with diamond burs or sandblasting before applying the semi-IPN structure dissolving monomer. The roughened surface would enlarge the bonding surface area and expose more protruding fiber ends, hence improving the adhesive type of secondary IPN bonding accompanied by mechanical interlocking. However, in this thesis only the materials’ properties were investigated and topics related to the adhesive properties of the millimeter-scale discontinuous-FRC base to indirect restorations, remain future challenges.

Furthermore, future studies should be designed towards *in vitro* and *in vivo* evaluations of biomimetic restorations made of millimeter-scale discontinuous-FRC in combination with either ceramic or indirect composite materials, and immediate dentin sealing (IDS) adhesive technique (Magne, 2005). IDS is believed to diminish the differences between the indirect composite and ceramic overlay (Magne, 2006). This research should include topics on the bonding between the millimeter-scale discontinuous-FRC base to indirect

composite restorations or ceramic restorations, techniques for improving adhesion or repair between them, and investigations on the static and fatigue endurance of properly designed structures (millimeter-scale discontinuous-FRC bases overlaid with 1.5 – 2 mm veneering materials).

Providing a retention for structurally compromised endodontically treated teeth with short millimeter-scale discontinuous-FRC posts alone or in combination with semi-IPN FRC posts, and millimeter-scale discontinuous-FRC endocrowns could also be topics of future investigations.

Another interesting topic for research is the placement technique of millimeter-scale discontinuous-FRC. Condensing the millimeter-scale discontinuous-FRC would secure maximal volume of fibers in the middle of the restoration. This could be studied by cross-sectioning millimeter-scale discontinuous-FRC restored teeth. In addition, the fiber orientation in various cavity designs, approximal or MOD, could be studied in order to determine the changes in the discontinuous fiber orientation (random or in plane) as a result of the placement technique employed.

It seems that the millimeter-scale discontinuous-FRC with its semi-IPN matrix may extend the limited reinforcement of uni- and bidirectional cross-linked and semi-IPN FRCs. It should be born in mind that dental research does not necessarily search for strong materials, but instead for a restorative material that will change the failure mode and preserve the tooth and/or restoration from fracturing. Ideally, the material should resist crack propagation and stop its progression toward the dental hard tissue. As a result, the incidence of severe tooth fractures would be diminished, repeated retreatments would be avoided and thus, a sound tooth structure would be preserved and maintained. As it nowadays becomes difficult for clinicians to select the restorative technique and even more difficult to choose the restorative material, it should be kept in mind that the semi-IPN matrix based millimeter-scale discontinuous E-glass fiber reinforced composite material could offer versatile therapeutic choices.

7. CONCLUSIONS

Within the limitations of the studies carried out in this thesis, the following findings and conclusions can be made:

1. Packing a fibrous material around the semi-IPN post, or in the root canal and the pulp chamber as post-core complex, reinforced the cervical area where normally the greatest stresses occur. Consequently, both structure types could be considered to provide a ferrule-like effect, preventing root fractures and should therefore be considered in restoring structurally compromised teeth.

2. The presence of an air inhibited layer improved bonding between the superimposed composite layers, whereas significant reduction of the bond strength was observed when this superficial layer was removed. Consequently, the oxygen inhibition layer should be preserved on the surface of freshly cured composite. Furthermore, fracture pattern analysis revealed that the presence of an oxygen inhibition layer was associated with either cohesive or mixed (cohesive and adhesive) types of fractures, while its absence led mainly to adhesive failures. An exception was the millimeter-scale discontinuous-FRC with an absent oxygen inhibition layer, which obtained mainly cohesive and mixed failures, most likely due to the protruding fibers at the interface. Based on this finding, more durable adhesion can be expected with the millimeter-scale discontinuous-FRC.

3. The presence of discontinuous, randomly orientated E-glass fibers with semi-IPN improved the physicomechanical properties of this FRC material. This was considered to be due to both E-glass fiber reinforcement and the semi-IPN matrix. Short, silanized E-glass fibers provided fiber filler reinforcement, with fibers above the critical fiber length, and particulate filler reinforcement, with fibers below the critical fiber length. The PMMA linear chains in the semi-IPN matrix type are associated with reduced brittleness, which improved the resistance to fracture propagation. This supports the idea of using the millimeter-scale discontinuous-FRC in areas where enhanced resistance to fracture propagation (toughness), and to fracture (load-bearing capacity), are needed.

4. The crack propagation in the millimeter-scale discontinuous-FRC, at the crack notch tip, appeared to initially follow the weak interfaces, but then fiber stretching, deflection and pull-out appeared to slow down the crack propagation. The additional fiber bridging mechanism impeded crack

propagation by closing the crack surfaces, blunting the crack notch and finally arresting the crack. This was observed at and behind the crack tip. Consequently, the crack was stabilized (fragments remained attached) and the toughness was increased. Similar toughening mechanisms occur in dentin. In addition, structural similarity between dentin and the millimeter-scale discontinuous-FRC seems to exist (collagen fibers versus various lengths owning discontinuous fibers). Based on these findings, the millimeter-scale discontinuous-FRC could be considered as a biomechanically biomimetic material and should be utilized in restoring teeth with severe tooth structure loss. This fibrous composite material with randomly orientated short fibers could be used as a substructure of direct and indirect restorations, and as a reinforcing base of ETT to fill the entire pulp chamber.

Advantages provided by the material could be: 1. crack obstruction, which could diminish catastrophic tooth fractures; 2. durable repairs due to the protruding fibers at the repair surface, which roughen and enlarge the bonding surface area and 3. improved reliability of the luted indirect constructions owing to the secondary IPN formation.

ACKNOWLEDGEMENTS

This work has been one of a kind journey to me, different than anything else I have done before. At some times it was filled with hopelessness and frustration, and other times with lightness and excitement. The truth is, I have made a lot of mistakes all the way till here, but each mistake has been an encouraging learning process that helped me to experience the bear of academic being. Though, I understood this just recently.

I never guessed how many people would guide me along this way. Foremost, this work would have not started without the support of Professor Pekka Vallittu, whom I thank for his inspiration, motivation, support and encouragement, and for undoubtedly sharing his invaluable academic knowledge and experience.

The spirit this work has is merely owned to the priceless belief and support of Dr. Lippo Lassila. I want to thank you Lippo for believing in me as a researcher, for patiently and laboriously leading and correcting my methodological mistakes, and for arguing with me. Indeed, arguing with you has been very educational.

The continuous encouragement of Adjunct Professor Sufyan Garoushi is very much appreciated. Our frequent debates with you Sufyan, have both inspired and encouraged me to continue my journey on learning. Thank you for your sincerity.

The incredible support of my committee member, Adjunct Professor Filip Keulemans has truly impressed me. I thank you Filip for your constructive criticism and objectivism, correcting my mistakes and for sharing your invaluable academic and clinical experience.

I am very grateful to Professor Cees Kreulen for accepting the invitation to act as an opponent to my doctoral thesis. Advices and comments given by the official reviewers Professor Alison Qualtrough and Professor Ivo Krejci are highly appreciated. My appreciation to you both is infinite. I would like to compliment Professor Emeritus Mauno Könönen for offering his help in the moments of trouble. Your expertise and support are greatly valued.

The support provided by Finnish Dental Society Apollonia, Turku University Foundation-Kosti Hämmärö dedicated fund and Turku University Foundation-

general fund and Finnish Association of Women Dentists, is highly appreciated. I thank the mentioned scholars for funding this thesis.

The care and help offered by Tarja Peltoniemi have been always very warm. Thank You Tarja very much for looking after and being there for me.

The international spirit in Turku Clinical Biomaterials Centre (TCBC) has taught me to manage and adjust my social skills, to modify my temper, to understand cultural dependent differences, to even find better comfort in some of them and to become more tolerant and flexible. I am lucky for meeting Anne-Maria Aulu (former Vuorinen) among the first people in TCBC. Thank you Anne for your sincere friendship. The TCBC crew including Adjunct Professors Mervi Puska and Niko Moritz, the lab experts Hanna Mark, Genevieve Alfront known as Sevi, Minttu Pesonen and many DDSs (general, specialists and PhDs in mixed order) Leila Perea Mosquera, Yulia Kulkova, Minori Hata, Kohji Nagata, Masahiko Kobayashi, Jingwei He, Marina Etxeberria, Qiting Huang, Aous Abdulmajeed, Tarek Omran, Khalil Shahramian are very much thanked for making the reality palatable. Every each of you has contributed to this work by simply being who you are; though Pori Jazz concert experience with Mervi, shopping trips with Hanna, conversations and dinners with Leila are all dear moments to remember. Thanks a lot to Onur Oral, Riina Mattila, Sara Nganga, Pinar Altinci, Roda Seseogullari-Dirihan, Anas Salim, Dareen Fteita, Aaro Turunen and Peter Uppstu for making our joint courses, conferences and seminars more enjoyable.

Many other colleagues have not only listening my worries, but also practically helped to carry out some experiments. Many thanks to Doctors Isil Cekis Nagas and Emre Nagas with their teams, Marija Trifunova, Elena Velkoska, Petteri Jyrkönen, Osmo Pekkala and Martat (you know how you are) for collecting, selecting and donating the teeth you extract in your daily practices. I hope you are all aware of the importance of the work you are all doing. Although we have enough teeth (for now), please keep on collecting.

My dear friend and colleague Marija Trifunova has been an amazing spiritual companion. We met in dental school, but it took us a while till we became friends at the second year (right?). You will never truly understand how important your faith has been to me. You have been asking over and over again what is it I am actually doing. I hope you have finally understood now. Nevertheless, thank you Marija for being supportive.

I would like to thank my family, particularly my mother, for her support and encouragement, and for giving me the foundation of who I am. My brother Goran, you know what you mean to me!

Finally, I would like to thank my other half, Dime, for his faith in me and for making my journey meaningful. As a thorough thinker you certainly want to know how? Despite the fact that you have always supported me no matter what I decide, and even left your comfort zone because of me, you, my dear have supported me at a few, crucially important moments for me. Indeed, when I felt down and despaired, and when my self-confidence was trying me, you returned to me faith in myself and I cannot thank you enough for that. This is how you give a meaning to all this, and please do not analyze it any deeper!

Make it simple, but not simpler.

Turku, 1 September 2016

Jasmina Bijelic-Donova

REFERENCES

Abouelleil H, Pradelle N, Villat C, Attik N, Colon P, Grosgogeat B. (2015) Comparison of mechanical properties of a new fiber reinfroced composite and bulk filling composites. Restor Dent Endod 40(4): 262-270.

Al-Turki LI, Drummond JL, Agojci M, Gosz M, Tyrus JM, Lin L. (2007) Contact versus flexure fatigue of a fiber-filled composite. Dent Mater 23(5): 648-653.

Americal Society for Testing and Materials. ASTM D4475-96. Standard test method for apparent horizontal shear strength of pultruded reinforced plastic rods by the short-beam method. ASTM, Philadelphia; 2008. Available at: http://www.astm.org/DATABASE.CART/HISTORICAL/D4475-96.htm

Anusavice KJ, Shen C, Rawls R. (2012) Phillips' science of dental materials. Saunders-Elsevier Science, St.Louis, MO. pp. 49-61.

Asmussen E, Peutzfeldt A. (1998) Influence of UEDMA, BisGMA, and TEGDMA on selected mechanical properties of experimental resin composites. Dent Mater 14 (1): 51-6.

Baldissera RA, Correa MB, Schuch HS, Collares K, Nascimento GG, Jardim PS, Moraes RR, Opdam NJM, Demarco FF. (2013) Are there universal restorative composites for anterior and posterior teeth? J Dent 41 (11): 1027-1035.

Banerji S, Mehta SB, Millar BJ. (2010) Cracked tooth syndrome. Part 2: restorative options for the management of cracked tooth syndrome. British Dental Journal 208(11): 503-514.

Baretto BC, Van Ende A, Lise DP, Noritomi PY, Jaecques S, Sloten JV, De Munck J, Van Meerbeek B. (2016) Short fibre-reinfroced composite for extensive direct restorations: a laboratory and computational assessment. Clin Oral Investig 20(5): 959-966.

Baudin C, Osorio R, Toledano M, de Aza S. (2009) Work of fracture of a composite resin: fracture-toughening mechanisms. J Biomed Mater Res A 89(3): 751-758.

Bayne SC, Thompson JY. (2013) Biomaterials. Online chapter 18; pp. e53-e69. Available at: http://www.sturdevants-operativedentistry.com/pdfs/on0018-9780323083331.pdf

Beck F, Lettner S, Graf A, Bitriol B, Dumitrescu N, Bauer P, Moritz A, Schedle A. (2015) Survival of direct resin restorations in posterior teeth within a 19-year period (1996-2015): A meta-analysis of prospective studies. Dent Mater 31(8): 958-985.

Behr M, Rosentritt M, Latzel D, Handel G. (2003a) Fracture resistance of fiber-reinforced vs. non-fiber-reinforced composite molar crowns. Clin Oral Investig 7(3): 135-139.

Behr M, Rosentritt M, Sikora MI, Karl P, Handel G. (2003b) Marginal adaptation and fracture resistance of adhesively luted glass fibre-composite reinforced molar crowns with different inner crown surfaces. J Dent 31(7): 503-508.

Behr M, Rosentritt M, Taubenhansl P, Kolbeck C, Handel G. (2005) Fracture resistance of fiber-reinforced composite restorations with different framework design. Acta Odontol Scand 63(3): 153-157.

Belli R, Petschelt A, Lohbauer U. (2014) Are linear elastic material properties relevant predictors of the cyclic fatigue resistance of dental resin composites? Dent Mater 30(4): 381-391.

Bernardo M, Luis H, Martin MD, Leroux BG, Rue T, Leitao J, DeRouen TA. (2007) Survival and reasons for failure of amalgam versus composite posterior restorations placed in a randomized clinical trial. J Am Dent Assoc 138(6): 775-783.

Beun S, Glorieux T, Devaux J, Vreven J, Leloup G. (2007) Characterization of nanofilled compared to universal and microfilled composites. Dent Mater 23(1): 51-59.

Biachhi GR, Mello B, Basting RT. (2013) The endcrown: an alternative approach for restoring extensively damaged molars. J Esthet Restor Dent 25(6): 383-390.

Bowen RI. (1956) Use of epoxy resins in restorative materials. J Dent Res 35(3): 360–369.

Braem M, Lambrechts P, Vanherle G. (1994) Clinical relevance of laboratory fatigue studies. J Dent 22(2): 97-102.

Brighenti R, Scorza D. (2012) A micro-mechanical model for statistically unidirectional and randomly distributed fibre-reinforced solids. Math Mech Solids 17(8): 876-893.

Brown D. (2000) Fiber-reinforced materials. Dent Update 27(9): 442-448.

Brunthaler A, König F, Lucas T, Sperr W, Schedle A. (2003) Longevity of direct composite restorations in posterior teeth. Clin Oral Invest 7(2): 63-70.

Butterworth C, Ellakwa AE, Shortall A. (2003) Fibre-reinforced composites in restorative dentistry. Dent Update 30(6): 300-306.

Callister WD, Rethwisch DG. (2011) Materials science and engineering. Hoboken NJ: Wiley-John Wiley & Sons Pte Ltd. p. 634-636.

Christensen RM, Waals FM. (1972) Effective stiffness of randomly orientated fiber composites. J Comp Mater 6(3): 518-535.

Conçalves F, Kawano Y, Pfeifer C, Stansbury JW, Braga RR. (2009) Influence of BisGMA, TEGDMA, and BisEMA contents on viscosity, conversion, and flexural strength of experimental resins and composites. Eur J Oral Sci 117(4): 442-446.

Crivello JV. (2009) Design of photoacid generating systems. J Photopolym Sci Tec 22(5): 575–582.

Curtis AR, Shortall AC, Marquis PM, Palin WM. (2008) Water uptake and strength characteristics of a nanofilled resin-based composite. J Dent 36(3): 186-193.

DaRosa Rodolpho PA, Donassollo TA, Cenci MS, Loguercio AD, Moraes RR, Bronkhorst EM, Opdam NJM, Demarco FF. (2011) 22-year clinical evaluation of the performance of two posterior compositees with different filler characteristics. Dent Mater 27(10): 955-963.

de Castro Albuquerque R, Polleto LT, Fontana RH, Cimini CA. (2003) Stress analysis of an upper central incisor restored with different posts. J Oral Rehabil 30(9): 936-943.

Deliperi S. (2008) Direct fiber-reinforced composite restoration in an endodontically-treated molar: a three-year case report. Oper Dent 33(2): 209-214.

Demarco FF, Correa MB, Cenci MS, Moraes RR, Opdam NJM. (2012) Longevity of posterior composite restorations: Not only matter of materials. Dent Mater 28(1): 87-101.

Demarco FF, Collares K, Coelho-de-Souza FH, Correa MB, Cenci MS, Moraes RR, Opdam NJM. (2015) Anterior composite restorations: A systematic review on long-term survival and reasons for failure. Dent Mater 31(10): 1214-1224.

Donovan TE. (2006) Longevity of the tooth/restoration complex: a review. J Calif Dent Assoc 34(2): 122-128.

Draughn RA. (1979) Compressive fatigue limits of composite restorative materials. J Dent Res 58(3): 1093-1096.

Drummond JL, Lin L, Miescke KJ. (2004) Evaluation of fracture toughness of a fiber containing composite after flexural fatigue. Dent Mater 20(6): 591-599.

Drummond JL, Lin L, Al-Turki LA, Hurley RK. (2009) Fatigue behaviour of dental composite materials. J Dent 37(5): 321-330.

Dyer SR, Lassila LV, Jokinen M, Vallittu PK. (2004) Effect of fiber position and orientation on fracture load of fiber-reinforced composite. Dent Mater 20(10): 947-955.

Dyer SR, Sorensen JA, Lassila LV, Vallittu PK. (2005) Damage mechanics and load failure of fiber-reinforced composite fixed partial dentures. Dent Mater 21(12): 1104-1110.

Eden E, Taviloglu E. (2016) Restoring crown fractures by direct composite layering using transparent strip crowns. Dent Traumatol 32(2): 156-160.

Eliades GC, Caputo AA. (1989) The strength of layering technique in visible light-cured composites. J Prosthet Dent 61(1): 31-38.

Faber KT, Evans AG. (1983) Crack deflection processes – I. Theory. Acta Metall 31(4): 565-576.

Fennis WMM, Tezvergil A, Kuijs RH, Lassila LVJ, Kreulen CM, Creugers NHJ, Vallittu PK. (2005) In vitro fracture resistance of fiber reinforced cusp-replacing composite restorations. Dent Mater 21: 565-572.

Ferracane JL, Antonio RC, Matsumoto H. (1987) Variables affecting the fracture toughness of dental composites. J Dent Res 66(6): 1140-1145.

Ferracane JL, Berge HX, Condon JR. (1998) In vitro aging of dental composites in water – effect of degree of conversion, filler volume, and filler/matrix coupling. J Biomed Mater Res 42(3): 465-472.

Ferracane J. (2005) Dental composites – which tests are useful for developing new products and predicting performcance? ADM pp. 41-52.

Ferracane JL. (2011) Resin composite – state of art. Dent Mater 27(1): 29-38.

Flores MT, Andersson l, Andreasen JO, Bakland LK, Malmgren B, Barnett F, Bourguignon C, DiAngelis A, Hicks L, Sigurdsson A, Trope M, Tsukiboshi M, von Arx T. (2007) Guidelines for the management of traumatic dental injures. I. Fractures and luxations of permanent teeth. Dent Traumatol 23(2): 66-71.

Fonseca RB, Marques AS, Bernades Kde O, Carlo HL, Naves LZ. (2014) Effect of glass fiber incorporation on flexural properties of experimental composites. Biomed Res Int 2014: 542678.

Fonseca RB, de Almeida LN, Mendes GA, Kasuya AV, Favarao IN, de Paula MS. (2016) Effect of short flass fiber/filler particle proportion on flexural and diametral tensile strength of a novel fiber-reinforced composite. J Prosthodont Res 60(1): 47-53.

Frankenberger R, Reinelt C, Kramer N. (2014) Nanohybrid vs. fine hybrid composite in extended class II cavities: 8-year results. Clin Oral Invest 18(1): 125-137.

Frater M, Forster A, Kereszturi M, Braunitzer G, Nagy K. (2014) In vitro fracture resistance of molar teeth restored with a short fibre-reinforced composite material. J Dent 42(9): 1143-1150.

Frese C, Schiller P, Staehle HJ, Wolff D. (2013) Recontouring teeth and closing diastemas with direct composite buildups: a 5-year follow-up. J Dent 41(11): 979-85.

Frese C, Decker C, Rebholz J, Stucke K, Staehle HJ, Wolff D. (2014) Original and repair bond strength of fiber-reinforced composites in vitro. Dent Mater 30(4): 456-462.

Garbin CA, Spazzin AO, Meira-Junior AD, Loretto SC, Lyra AM, Braz R. (2010) Biomechanical behavior of a fractured maxillary incisor restored with direct composite resin only or with different post system. Int Endod J 43(12): 1098-1107.

Garoushi S, Lassila LVJ, Tezvergil A, Vallittu PK. (2006a) Load bearing capacity of fibre-reinforced and particulate filler composite resin combination. J Dent 34(3): 179-184.

Garoushi SK, Lassila LV, Vallittu PK. (2006b) Short fiber reinforced composite: the effect of fiber length and volume fraction. J Contemp Dent Pract 7(5): 10- 17.

Garoushi S, Vallittu PK, Lassila LV. (2007a) Short glass fiber reinfroced restorative composite resin with semi-interpenetrating polymer network matrix. Dent Mater 23(11): 1356-1362.

Garoushi S, Lassila LV, Tezvergil A, Vallittu PK. (2007b) Static and fatigue compression test for particulate filler composite resin with fiber-reinforced composite substructure. Dent Mater 23(1): 17-23.

Garoushi S, Vallittu PK, Watts DC, Lassila LV. (2008) Polymerization shrinkage of experimental short glass fiber-reinforced composite with semi-inter penetrating polymer network matrix. Dent Mater 24(2): 211-215.

Garoushi S, Shinya A, Shinya A, Vallittu PK. (2009) Fiber-reinforced onlay composite resin restoration: a case report. J Contemp Dent Pract 10(4): 104-110.

Garoushi S, Tanner J, Vallittu PK, Lassila L. (2012) Preliminary clinical evaluation of short fiber-reinfroced composite resin in posterior teeth: 12-months report. Open Dent J 6: 41-45.

Garoushi S, Mangoush E, Vallittu P, Lassila L. (2013a) Short fiber reinforced composite: a new alternative for direct restorations. Open Dent J 30(7): 181-185.

Garoushi S, Säilynoja E, Vallittu PK, Lassila L. (2013b) Physical properties and depth of cure of a new short fiber reinforced composite. Dent Mater 29(8): 835-841.

Gauthier MA, Stangel I, Ellis TH, Zhy XX. (2005) Oxygen inhibition in dental resins. J Dent Res 84(8): 725-729.

Giannini M, Soares CJ, de Carvalho RM. (2004) Ultimate tensile strength of tooth structures. Dent Mater 20(4): 322-329.

Goldman M. (1985) Fracture properties of composite and glass ionomer dental restorative materials. J Biomed Mater Res 19(7): 771–783.

Goodacre C, Bernal G, Rungcharassaeng K, Kan JY. (2003) Clinical complications in fixed prosthodontics. J Prosthet Dent 90(1): 31-41.

Goracci C, Gadenaro M, Fontanive L, Giangrosso G, Juloski J, Vichi A, Ferrari M. (2014) Polymerization efficiency and flexural strength of low-stress restorative material. Dent Mater 30(6): 688-694.

Hamburger JT, Opdam NJ, Bronkhorst EM, Roeters JJ, Huysmans MC. (2014) Effect of thickness of bonded composite resin on compressive strength. J Mech Behav Biomed Mater 37: 42-47.

Harris B. (1999) Engineering composite materials. London, UK: IOM. pp. 9, 48-53, 75-79.

Heintze SD, Zimmerli B. (2011) Relevance of in vitro tests of adhesive and composite dental materials, a review in 3 parts. Part 1: Approval requirements and standardized testing of composite materials according to ISO specifications. Schweiz Monatsschr Zahnmed 121(9): 804-816.

Hickel R, Manhart J. (2001) Longevity of restorations in posterior teeth and reasons for failure. J Adhesive Dent 3(1): 45-64.

Hickel R, Brushaver K, Illie N. (2013) Repair of restorations – criteria for decision making and clinical recommendations. Dent Mater 29(1): 28-50.

Htang A, Ohsawa M, Matsumoto H. (1995) Fatigue resistance of composite restorations: effect of filler content. Dent Mater 11(1): 7-13.

Hull D, Clyne TW. (1996) An introduction to composite materials. Cambridge, UK: Cambridge University press. pp. 4, 11, 15, 30, 49-59, 105-132.

Ilie N, Hickel R. (2009a) Investigations on mechanical behaviour of dental composites. Clin Oral Investig 13(4): 427-438.

Ilie N, Hickel R. (2009b) Macro-, micro- and nano-mechanical investigations on silorane and methacrylate-based composites Dent Mater 25(6): 810-819.

Ilie N, Hickel R. (2011) Resin composite restorative materials. Aust Dent J 56(1): 59- 66.

Ilie N, Hickel R, Valceanu AS, Huth KC. (2012) Fracture toughness of dental restorative materials. Clin Oral Investig 16(2): 489-498.

International Organisation for Standardisation. ISO 4049 - Dentistry - polymer-based filling, restorative and luting materials, 2009.

International Organization for Standardisation. ISO 4104. Dental zinc polycarboxylate cements. ISO, Geneva; 1984.

International Organization for Standardisation. ISO 20795-1. Dentistry - - Base polymers - - Part 1: Denture base polymers. ISO, Geneva; 2013. Available at: http://www.iso.org/iso/store.htm

Jain LC, Wetherhold RC. (1992) Effect of fiber orientation on the fracture toughness of brittle matrix composites. Acta Metall Mater 40 (6): 1135-1143.

Johnson WW, Dhuru VB, Brantley WA. (1993) Composite microfiller content and its effect on fracture toughness and diametral tensile strength. Dent Mater 9(2): 95-98.

Karacaer O, Polat TN, Tezvergil A, Lassila LV, Vallittu PK. (2003) The effect of length and concentration of glass fibers on the mechanical properties of an injection- and a compression-molded denture base polymers. J Prsothet Dent 90(4): 385-393.

Kelly JR, Benetti P, Rungruanganunt P, Bona AD. (2012) The slippery slope: critical perspectives on in vitro research methodologies. Dent Mater 28(1): 47-51.

Kemaloglu H, Emin Kaval M, Turkun M, Micoogullari Kurt S. (2015) Effect of novel restoration techniques on the fracture resistance of teeth treated endodontically: An in vitro study. Dent Mater J 34(5): 618-622.

Keulemans F, Lassila LV, Garoushi S, Vallittu PK, Kleverlaan CJ, Feilzer AJ. (2009) The influence of framework design on the load-bearing capacity of laboratory-made inlay-retained fibre-reinforced composite fixed dental prosthesis. J Biomech 42(7): 844-849.

Kim KH, Park JH, Imai Y, Kishi T. (1994) Microfracture mechanisms of dental resin composites containing spherically-shaped filler particles. J Dent Res 73(2): 499-504.

Kim KH, Kim YB, Okuno O. (2000) Microfracture mechanisms of composite resin containing prepolymerized particle filers. Dent Mater J 19(1): 22-33.

Kim KH, Ong JL, Okuno O. (2002) The effect of filler loading and morphology on the mechanical properties of contemporary composites. J Prosthet Dent 87(6): 642-649.

Kim SH, Watts DC. (2004) Effect of glass-fiber reinforcement and water storage on fracture toughness (KIC) of polymer-based provisional crown and FPD material. Int J Prosthodont 17(3): 318-322.

Kim JS, Choi YH, Cho BH, Son HH, Lee IB, Um CM, Kim CK. (2006) Effect of light-cure time of adhesive resin on the thickness of the oxygen-inhibited layer and the microtensile bond strength to dentin. J Biomed Mater Res Part B: Appl Biomater 78(1): 115-123.

Kinney JH, Balooch M, Marshall GW, Marshall SJ. (1999) A micromechanics model of the elastic properties of human dentine. Arch Oral Biol 44(10): 813-822.

Kinney JH, Marshall SJ, Marshall GW. (2003) The mechanical properties of human dentin: a critical review and re-evaluation of the dental literature. Crit Rev Oral Biol Med 14(1): 13-29.

Kubo S, Kawasaki A, Hayashi Y. (2011) Factors associated with the longevity of resin composite restorations. Dent Mater J 30(3): 374-383.

Lassila LV, Tanner J, Le Bell AM, Narva K, Vallittu PK. (2004) Flexural properties of fiber reinforced root canal posts. Dent Mater 20(1): 29-36.

Lassila LV, Garoushi S, Tanner J, Vallittu PK, Söderling E. (2009) Adherence of *Streptococcus mutans* to fiber-reinforced filling composite and conventional restorative materials. Open Dent J 4(3): 227-232.

Lassila L, Garoushi S, Vallittu PK, Säilynoja E. (2016) Mechanical properties of fiber reinforced restorative composite with two distinguished fiber length distribution. J Mech Behav Biomed Mater 16(60): 331-338.

Lastumäki TM, Lassila LV, Vallittu PK. (2003) The semi-interpenetrating polymer network matrix of fiber-reinfroced composite and its effect on the surface adhesive properties. J Mater Sci Mater Med 14(9): 803-809.

Le Bell AM, Tanner J, Lassila LV, Kangasniemi I, Vallittu PK. (2003) Depth of light-initiated polymerization of glass fiber-reinfroced composite in simulated root canal. Int J Prosthodont 16(4): 403-408.

Le Bell Rönnlöf AM. (2007) Fibre-reinforced composites as root canal posts. [Doctoral thesis]. Turku: University of Turku; 2007. pp.17, 21, 28, 30.

Le Bell-Rönnlöf AM, Lassila LV, Kangasniemi I, Vallittu PK. (2011) Load-bearing capacity of human incisors restored with various fiber-reinforced composite posts. Dent Mater 27(6): e107-115.

Lee SM. (1993) Handbook of composite reinforcements. Palo Alto, CA: Wiley-VCH. pp.155-160; 217-219.

Lee TY, Guymon CA, Sonny Jönsson E, Hoyle CE. (2004) The effect of monomer structure on oxygen inhibition of (met)acrylates photopolymerization. Polymer 45(18): 6155-6162.

Leprince J, Palin WM, Mullier T, Devaux J, Vreven J, Leloup G. (2010) Investigating filler morphology and mechanical properties of new low-shrinkage resin composite types. J Oral Rehabil 37(5): 364-376.

Leprince JG, Palin WM, Vanacker J, Sabbagh J, Devaux J, Leloup G. (2014) Physico-mechanical characteristics of commercially available bulk-fill composites. J Dent 42(8): 993-1000.

Li J. (1997) Effects of surface properties on bond strength between layers of newly cured dental composites. J Oral Rehabil 24(5): 358-360.

Lien W, Vandewalle KS. (2010) Physical properties of a new silorane-based restorative system. Dent Mater 26(4): 337-344.

Lloyd CH, Iannetta RV. (1982) The fracture toughness of dental composites. I. The development of strength and fracture toughness. J Oral Rehabil 9 (1): 55-66.

Lohbauer U, von der Horst T, Frankenberger R, Kramer N, Petschelt A. (2003) Flexural fatigue behavior of resin composite dental restoratives. Dent Mater 19(5): 435–40.

Lohbauer U, Belli R, Ferracane JL. (2013) Factors involved in mechanical fatigue degradation of dental resin composites. J Dent Res 92(7): 584-591.

Lynch CD, Opdam NJ, Hickel R, Brunton PA, Gurgan S, Kakaboura A, Shearer AC, Vanherle G, Wilson NHF. (2014) Guidence on posterior resin composites: Academy of operative dentistry – European section. J Dent 42(4): 377-383.

Magne P. (2005) Immediate dental sealing: a fundamental procedure for indirect bonded restorations. J Esthet Restor Dent 17(3): 144-154.

Magne P. (2006) Composite resins and bonded porcelain: the postamalgam era? J Calif Dent Assoc 34(2): 135-147.

Magne P. (2012a) Pascal Magne:"It should not be about aesthetic but tooth-conserving dentistry". Interview by Ruth Doherty. Br Dent J 213(4): 189-191.

Magne P, Boff LL, Oderich E, Cardoso AC. (2012b) Computer-aided-design/computer-assisted-manufactured adhesive restoration of molars with a compromised cusp: effect of fiber-reinforced immediate dentin sealing and cusp overlap on fatigue strength. J Esthet Restor Dent 24(2): 135-146.

Manhart J, Kunzelmann KH, Chen HY, Hickel R. (2000) Mechanical properties of new composite restorative materials. J Biomed Mater Res 53(4): 353-361.

Manhart J, Chen HY, Hickel R (2001) The suitability of packable resin-based composite for posterior restorations. J Am Dent Assoc 132(5): 639-645.

Masouras K, Akhtar R, Watts DC, Silikas N. (2008) Effect of filler size and shape on local nanoindentation modulus of resin-composites. J Mater Sci Mater Med 19(12): 3561-3566.

Mc Donough WG, Antonucci JM, Dunkers JP. (2001) Interfacial shear strengths of dental resin-glass fibers by the microbond test. Dent Mater 17(6): 492-498.

Medeiros IS, Gomes MN, Longuercio AD, Filho LE. (2007) Diametral tensile strength and Vicker harndess of a composite after storage in different solutions. J Oral Sci 49(1): 61-66.

Miettinen VM, Narva KK, Vallittu PK. (1999) Water sorption, solubility and effect of post-curing of glass fibre reinforced polymers. Biomaterials 20(13): 1187-1194.

Mirkhalaf M, Dastjerdi AK, Barthelat F. (2013) Overcoming the brittleness of glass through bio-inspiration and micro-architecture. Nat Commun 5: 3166.

Miyasaka T. (1996) Effect of shape and size of silanated fillers on mechanical properties of experimental photo cure composite resins. Dent Mater J 15(2): 98-110.

Monaco C, Bortolotto T, Arena A, Krejci I. (2015) Restoring nonvital premolars with composite resin onlays: effect of different fiber-reinfroced composite layers on marginal adaptation and fracture load. J Adhes Dent 17(6): 567-574.

Monaco C, Arena A, Scotti R, Krejci I. (2016) Fracture strength of endodontically treated teeth restored with composite overlays with and without glass-fiber reinforcement. J Adhes Dent 18(2): 143-149.

Mota EG, Oshima HM, Burnett LH Jr, Pires LA, Rosa RS. (2006) Evaluation of diametral tensile strength and Knoop microhardness of five nanofilled composite in dentin and enamel shades. Stomatologija 8(3): 67-69.

Murphy J. (1998) The reinforced Plastics Handbook. Oxford, UK: Elsevier Advanced Technology. pp. 265, 416, 435-436.

Nalla RK, Kinney JH, Ritchie RO. (2003a) Effect of orientation on the in vitro fracture toughness of dentin: the role of toughening mechanisms. Biomaterials 24(22): 3955-3968.

Nalla RK, Kinney JH, Ritchie RO. (2003b) On the fracture of human dentin: is it stress- or strain controlled? J Biomed Mater Res 67A: 484-495.

Norman DA, Robertson RE. (2003) The effect of fiber orientation on the toughening of short fiber-reinforced polymers. J Appl Polymer Sci 90 (10): 2740-2751.

Obukuro M, Takahashi Y, Shimizu H. (2008) Effect of diameter of glass fibers on flexural properties of fiber-reinforced composites. Dent Mater J 27(4): 541-548.

Opdam NJ, Bronkhorst EM, Loomans BA, Huysmans MC. (2010) 12-year survival of composite vs. amalgam restorations. J Dent Res 89(10): 1063-1067.

Ozcan M, Breuklander MH, Vallittu PK. (2005) The effect of box preparation on the strength of glass fiber-reinforced composite inaly-retained fixed partial dentures. J Prosthet Dent 93(4): 337-345.

Ozsevik AS, Yildirim C, Aydin U, Culha E, Surmelioglu D. (2016) Effect of fibre-reinforced composite on the fracture resistance of endodontically treated teeth. Aust Endod J 42(2): 82-87.

Pallesen U, Qvist V. Composite resin fillings and inlays. (2003) An 11-year evaluation. Clin Oral Investig 7(2):71-79.

Peumans M, Van Meerbeek B, Lambrechts P, Vanherle G. (1997) The 5-year clinical performance of direct composite additions to correct tooth form and position. I. Esthetic qualities. Clin Oral Investig 1(1):12-18.

Peutzfeldt A. (1997) Resin composites in dentistry: the monomer systems. Eur J Oral Sci 105(2): 97-116.

Polesel A. (2014) Restoration of the endodontically treated posterior tooth. G Ital Endod 28(1): 2-16.

Rasmussen ST, Patchin RE, Scott DB, Heuer AH. (1976) Fracture properties of human enamel and dentin. J Dent Res 55(1): 154-164.

Rocca GT, Rizcalla M, Kjejci I. (2013) Fiber-reinforced resin coating for endocrown preparations: a technical report. Oper Dent 38(3): 242-248.

Rocca GT, Saratti CM, Cattani-Lorente M, Feilzer AJ, Scherrer S, Krejci I. (2015) The effect of a fiber reinforced cavity configuration on load bearing capacity and failure mode of endodontically treated molars restored with CAD/CAM resin composite overlay restorations. J Dent 43(9): 1106-1115.

Rodrigues SA Jr, Scherrer SS, Ferracane JL, Della Bona A. (2008) Microstructural characterization and fracture behavior of a microhybrid and a nanofill composite. Dent Mater 24(9): 1281-1288.

Rueggeberg FA, Margeson DH. (1990) The effect of oxygen inhibition on an unfilled/filled composite system. J Dent Res 69(10): 1652-1658.

Ruyter IE. (1981) Unpolymerized surface layers on sealants. Acta Odontol Scand 39(1): 27-32.

Sabbagh J, Ryelandt L, Bacherius L, Biebuyck JJ, Vreven J, Lambrechts P, Leloup G. (2004) Characterization of the inorganic fraction of resin composites. J Oral Rehabil 31(11): 1090-1101.

Sakaguchi RL, Powers JM (2012) Craig's restorative dental materials 13th ed. Philadelphia, USA: Elsevier Mosby. pp. 41,43,84,86, 161-192.

Sarrett DC. (2005) Clinical challenges and the relevance of materials testing for posterior composite restorations. Dent Mater 21(1): 9-20.

Schwartz RS, Robbins JW. (2004) Post placement and restoration of endodontically treated teeth: a literature review. J Endod 30(5): 289-301.

Shawkat ES, Shortall AC, Addison O, Palin WM. (2009) Oxygen inhibition and incremental layer bond strengths of resin composites. Dent Mater 25(11): 1338-1346.

Shouha P, Swain M, Ellakwa A. (2014) The effect of fiber aspect ratio and volume loading on the flexural properties of flowable dental composite. Dent Mater 30(11): 1234-1244.

Smales RJ, Berekally TL. (2007) Long-term survival of direct and indirect restorations placed for the treatment of advanced tooth wear. Eur J Prosthodontics Restor Dent 15(1): 2-6.

Söderholm KJ, Zigan M, Ragan M, Fischlschweiger W, Bergman M. (1984) Hydrolytic degradation of dental composites. J Dent Res 63(10): 1248-1254.

Söderholm KJ, Roberts MJ. (1990) Influence of water exposure on the tensile strength of composites. J Dent Res 69(12): 1812-1816.

Söderholm KJ (2012). Fracture of Dental Materials. In: Alexander Belov editor. Applied Fracture Mechanics. InTech, DOI: 10.5772/48354. Available from: http://www.intechopen.com/books/applied-fracture-mechanics/fracture-of-dental-materials. [chapter 4, p.112].

Takeshige F, Kawakami Y, Hayashi M, Ebisu S. (2007) Fatigue behavior of resin composites in aqueous environments. Dent Mater 23(7): 893-899.

Tayab T, Shetty A, Kayalvizhi G. (2015) The clinical applications of fiber reinforced composites in all specialties of dentistry an overview. International Journal of Composite Materials 5(1): 18-24.

Tezvergil A, Lassila LV, Vallittu PK. (2005) The shear bond strength of bidirectional and random-oriented fibre-reinforced composite to tooth structure. J Dent 33(6): 509-516.

Torbjörner A. (2013) Prosthetic treatment of the endodontically treated tooth. In: Nilner K, Karlsson S, Dahl BL editors. A textbook of Fixed Prosthodontics. The Scandinavian Approach. Stockholm: Fortbildning Gothia. [chapter 6.4].

Truffier-Boutry D, Place E, Devaux J, Leloup G. (2003) Interfacial layer characterization in dental composite. J Oral Rehab 30(1): 74-77.

Turkaslan S, Tezvergil-Mutluay A, Bagis B, Vallittu PK, Lassila LV. (2009) Effect of fiber-reinforced composites on the failure load and failure mode of composite veneers. Dent Mater J 28(5): 530-536.

Tyas M. (1990) Correlation between fracture properties and clinical performance of composite resin in class IV cavities. Aust Dent J 35(1): 46–49.

Vallittu PK. (1995) The effect of void space and polymerization time on transverse strength of acrylic-glass fibre composite. J Oral Rehabil 22(4): 257-261.

Vallittu PK. (1997) Oxygen inhibition of autopolymerization of polymethylmeth-acrylate-glass fibre composite. J Mater Sci Mater Med 8(8): 489-492.

Vallittu PK, Ruyter IE, Ekstrand K. (1998) Effect of water storage on the flexural properties of E-glass and silica fiber acrylic resin composites. Int J Prosthodont 11(4): 340-350.

Vallittu PK, Sevelius C. (2000) Resin-bonded, glass fiber-reinforced composite fixed partial dentures: a clinical study. J Prosthet Dent 84(4): 413-418.

Vallittu PK. (2001) Strength and interfacial adhesion of FRC-tooth system. In: Vallittu PK, editor. The Second International Symposium on Fibre-Reinforced Plastics in Dentistry, 13 October 2001, Nijmegen, The Netherlands. pp.2-28.

Vallittu PK (2009). Interpenetrating polymer networks (IPNs) in dental polymers and composites. J Adhes Sci Technol 23(7-8): 961-972.

Vallittu P. (2015) High-aspect ratio fillers: fiber-reinforced composites and their anisotropic properties. Dent Mater 31(1): 1-7.

van Dijken JW. (2000) Direct resin composite inlay/onalys: an 11 year follow-up. J Dentistry 28(5): 299-306.

van Dijken JW. Sunnegårdh-Grönberg K. (2006) Fiber-reinforced packable resin composites in Class II cavities. J Dent 34(10): 763-769.

van Dijken JW, Pallesen U. (2013) A six-year prospective randomized study of a nano-hybrid and a conventional hybrid resin composite in class II restorations. Dent Mater 29(2): 191-198.

van Dijken JW, Pallesen U. (2014) A randomized 10-year prospective follow-up of class II nanohybrid and conventional hybrid resin composite restorations. J Adhes Dent 16(6): 585-592.

van Heumen CC, van Dijken JW, Tanner J, Pikaar R, Lassila LV, Creugers NH, Vallittu PK, Kreulen CM. (2009) Five-year survival of 3-unit fiber-reinforced composite fixed partial dentures in anterior area. Dent Mater 25(6): 820-827.

Van Nieuwenhuysen JP, D'Hoore W, Carvalho J, Qvist V. (2003) Long-term evaluation of extensive restorations in permanen teeth. J Dentistry 31(6): 395-405.

Wagner HD, Vaia RA. (2004) Nanocomposites: issues at the interface. Mater Today 7(11): 38-42.

Weinmann W, Thalacker C, Guggenberger R. (2005) Siloranes in dental composites. Dent Mater 21(1): 68–74.

Wetherhold RC. (1989) Energy of fracture for short brittle fiber-brittle matrix composites with planar fiber orientation. Mater Sci Eng A112: 31-37.

Wetherhold RC, Jain LK. (1992) The toughness of brittle matrix composites reinforced with discontinuous fibers. Mater Sci Eng A151(2): 169-177.

Whitney JM, Browning CE. (1985) On short-beam shear tests for composite materials. Exp Mech 25(3): 294-300.

Willems G, Lambrechts P, Braem M, Celis JP, Vanherle G. (1992) A classification of dental composites according to theirs morphological and mechanical characteristics. Dent Mater 8 (5): 310-319.

Willems G, Lambrechts P, Braem M, Celis JP, Vanherle G. (1993) Composite resins in the 21st century. Quintessence Int 24 (9): 641-658.

Wolff D, Geiger S, Ding P, Staehle HJ, Frese C. (2012) Analysis of the interdiffusion of resin monomers into pre-polymerized fiber-reinforced composites. Dent Mater 28(5): 541-547.

Xie Q, Lassila LV, Vallittu PK. (2007) Comparison of load-bearing capacity of direct resin-bonded fiber-reinforced composite FPDs with four framework designs. J Dent 35(7): 578-582.

Xu HH, Schumacher GE, Eichmiller FC, Peterson RC, Antonucci JM, Mueller HJ. (2003) Continuous-fiber preform reinforcement of dental resin composite restorations. Dent Mater 19(6): 523-530.

Yasa B, Arslan H, Yasa E, Akcay M, Hatirli H. (2016) Effect of novel restorative materials and retention slots on fracture resistance of endodontically-treated teeth. Acta Odontol Scand 74(2): 96-102.

Zhu YT, Blumenthal WR, Lowe TC. (1997) Determination of non-symmetric 3-D fiber-orientation distribution and average fiber length in short-fiber composites. J Comp Mater 31(13): 1287-1301.